

ISTANBUL TECHNICAL UNIVERSITY ★ GRADUATE SCHOOL OF SCIENCE
ENGINEERING AND TECHNOLOGY

**THE INFLUENCE OF IMPERFECTLY BONDED INTERFACES ON THE
GENERALIZED RAYLEIGH WAVE DISPERSION IN PRE-STRESSED
ELASTIC STRATIFIED HALF-SPACES**

Ph.D. THESIS

Masoud NEGIN

Department of Civil Engineering

Earthquake Engineering Program

JANUARY 2015

**THE INFLUENCE OF IMPERFECTLY BONDED INTERFACES ON THE
GENERALIZED RAYLEIGH WAVE DISPERSION IN PRE-STRESSED
ELASTIC STRATIFIED HALF-SPACES**

Ph.D. THESIS

**Masoud NEGIN
(501082205)**

Department of Civil Engineering

Earthquake Engineering Program

Thesis Advisor: Prof. Dr. Ertaç ERGÜVEN

JANUARY 2015

**TAM BAĞLI OLMAYAN TEMAS KOŞULLARI ALTINDA ELASTİK VE
ÖN GERİLMELİ TABAKA İLE ÖRTÜLMÜŞ YARI DÜZLEMDE
GENELLEŞTİRİLMİŞ RAYLEIGH DALGALARININ DİSPERSİYONU**

DOKTORA TEZİ

**Masoud NEGIN
(501082205)**

İnşaat Mühendisliği Anabilim Dalı

Deprem Mühendisliği Programı

Tez Danışmanı: Prof. Dr. Ertaç ERGÜVEN

OCAK 2015

Masoud NEGIN, a Ph.D. student of ITU Graduate School of Science 501082205 successfully defended the thesis entitled “**THE INFLUENCE OF IMPERFECTLY BONDED INTERFACES ON THE GENERALIZED RAYLEIGH WAVE DISPERSION IN PRE-STRESSED ELASTIC STRATIFIED HALF-SPACES**”, which he/she prepared after fulfilling the requirements specified in the associated legislations, before the jury whose signatures are below.

Thesis Advisor : **Prof. Dr. Ertuç ERGÜVEN**
Istanbul Technical University

Jury Members : **Prof. Dr. Surkay D. AKBAROV**
Yıldız Technical University

Prof. Dr. Abdullah GEDİKLİ
Istanbul Technical University

Prof. Dr. Gülay AŞKAR
Boğazıcı University

Prof. Dr. Abdul HAYIR
Istanbul Technical University

Date of Submission : **12 November 2014**

Date of Defense : **15 January 2015**

To my family,

FOREWORD

I would like to express the deepest appreciation and thanks to Prof. Dr. Surkay Akbarov for his continuous support of my study and research, for his patience, motivation and immense knowledge. He really made a great impact on my education. Without his helps, I would not be able to finish my study at Istanbul technical university. I am very much thankful for putting me in the track of his research.

I would like to thank all of my friends who supported me and encouraged me towards my goal specially Dr. Oktay Jafarov who introduced professor Akbarov to me and completely changed my life.

I would also like to thank my advisor Prof. Dr. Ertac Erguven who provided me with his constant support, and then to my committee members for their helpful suggestions and guidance.

Finally, I would like to thank my family, for supporting me spiritually all the way through this long education and throughout my life. This work is dedicated to them.

January 2015

Masoud NEGIN

TABLE OF CONTENTS

	<u>Page</u>
FOREWORD.....	ix
TABLE OF CONTENTS.....	xi
LIST OF TABLES	xiii
LIST OF FIGURES	xv
SUMMARY	xix
ÖZET	xxi
1. INTRODUCTION	1
1.1 Scopes and Objectives	3
1.2 Literature Review	3
1.3 Organization of The Thesis	7
2. ELASTIC WAVES	9
2.1 Wave Equation.....	9
2.2 Body Waves	10
2.3 Surface Waves.....	11
2.3.1 Rayleigh waves	11
2.3.2 Love waves	12
2.3.3 Other types of surface waves	12
2.4 Dispersion of Waves	12
2.5 Boundary Conditions.....	13
2.5.1 Displacement Discontinuity Method.....	14
2.5.2 Experimental verifications.....	16
2.5.3 Engineering applications	17
2.6 Elastic Waves in Bodies with Initial Stresses	18
2.7 Generalized Rayleigh Wave in a Covered Half-Space with Initial Stresses...	19
3. GENERALIZED RAYLEIGH WAVE DISPERSION ANALYSIS IN A PRE-STRESSED ELASTIC STRATIFIED HALF-SPACE WITH IMPER- FECTLY BONDED INTERFACES	29
3.1 Formulation of The Problem	29
3.2 Solution Procedure and Obtaining The Dispersion Relation	33
3.3 Numerical Results and Discussion	34
3.4 Some Applications and Experimental Verifications	52
3.5 Conclusions	58
4. DISPERSION OF GENERALIZED RAYLEIGH WAVES IN A STRATIFIED HALF-SPACE WITH IMPERFECT INTERFACE UNDER TWO-AXIAL INITIAL STRESSES	63
4.1 Formulation of The Problem	63

4.2 Solution Procedure and Dispersion Equation	67
4.3 Numerical Results and Discussion	69
4.4 Conclusion	78
5. GENERALIZED RAYLEIGH WAVE PROPAGATION IN A STRATI- FIED HALF-SPACE WITH A LIQUID UPPER LAYER	83
5.1 Introduction	83
5.2 Formulation of The Problem	83
5.3 Method of the Solution.....	88
5.4 Numerical Results and Discussion	90
5.5 Conclusion	97
6. CONCLUSIONS AND RECOMMENDATIONS	99
REFERENCES.....	105
APPENDICES	111
APPENDIX A.1	113
APPENDIX A.2	115
APPENDIX A.3	117
CURRICULUM VITAE	120

LIST OF TABLES

	<u>Page</u>
Table 3.1 : The values of elastic constants of the selected materials (Guz ,2004).	36
Table 4.1 : The values of elastic constants of the selected materials (Guz ,2004).	70
Table 5.1 : The values of elastic constants of the selected materials (Guz ,2004).	91

LIST OF FIGURES

	<u>Page</u>
Figure 2.1 : The geometry of the considered stratified half-plane.	20
Figure 3.1 : The geometry of the considered stratified half-plane.	30
Figure 3.2 : Dispersion curves for Poisson material (Tolstoy and Usdin, 1953): First and second branches of the first (a) and the second (b) modes.	37
Figure 3.3 : Dispersion curves for the <i>I</i> pair of materials.	37
Figure 3.4 : Dispersion curves for the <i>II</i> and <i>III</i> pair of materials.	38
Figure 3.5 : Dispersion curves for the <i>IV</i> pair of materials: The first and the second branches of the first (a) and the second (b) modes.	38
Figure 3.6 : Asymptotic behavior of the dispersion curves for the <i>I</i> pair the materials as $kh \rightarrow \infty$	41
Figure 3.7 : The influence of the imperfect bonding conditions and initial stresses to the dispersion of the generalized Rayleigh wave for the <i>I</i> pair of materials in Case 1: First (a) and second (b) branches of the first mode; First (c) and second (d) branches of the second mode.	45
Figure 3.8 : The influence of the imperfect bonding conditions and initial stresses to the dispersion of the generalized Rayleigh wave for the <i>III</i> pair of materials in Case 1: First (a) and second (b) branches of the first mode; First (c) and second (d) branches of the second mode.	46
Figure 3.9 : The influence of the imperfect bonding conditions and initial stresses to the dispersion of the generalized Rayleigh wave for the <i>II</i> and <i>III</i> pair materials in Case 2: First (a) and second (b) branches of the first mode; First (c) and second (d) branches of the second mode.	47
Figure 3.10 : The influence of the imperfect bonding conditions and initial stresses to the dispersion of the generalized Rayleigh wave for the <i>IV</i> pair of materials in Case 2: First (a) and second (b) branches of the first mode; First (c) and second (d) branches of the second mode.	48
Figure 3.11 : The influence of the imperfect bonding conditions and initial stresses to the dispersion of the generalized Rayleigh wave for the <i>II</i> pair of materials in Case 3: First (a) and second (b) branches of the first mode; First (c) and second (d) branches of the second mode.	50
Figure 3.12 : The influence of the imperfect bonding conditions and initial stresses to the dispersion of the generalized Rayleigh wave for the <i>III</i> pair of materials in Case 4: First (a) and second (b) branches of the first mode; First (c) and second (d) branches of the second mode.	51
Figure 3.13 : Dispersion curves for steel half-space covered by Lucite.	53

Figure 3.14: Dispersion curves for AISI 316L stainless steel coated with vacuum plasma sprayed NiCoCrAlY.....	54
Figure 3.15: The influence of the imperfect bonding conditions and initial stresses to the dispersion of the generalized Rayleigh wave for AISI 316L steel coated with (VPS) NiCoCrAlY for the first branch of the first mode: (a) Case 1; (b) Case 2; (c) Case 3 and (d) Case 4...	55
Figure 3.16: Dispersion curves related to surface waves in the soil which is modeled as a covering layer + half-plane (Foti, 2002).	56
Figure 3.17: The influence of the imperfect bonding conditions and initial stresses to the dispersion of the generalized Rayleigh wave for AISI 316L steel coated with (VPS) NiCoCrAlY for the first branch of the first mode: (a) Case 1; (b) Case 2; (c) Case 3 and (d) Case 4...	57
Figure 4.1 : Geometry of the considered mechanical system.	64
Figure 4.2 : Dispersion curves for the <i>I</i> pair of materials: (a) Imperfection only in the transverse direction, $F_1 \neq 0, F_2 = 0$. The numbers in the figure fields show the values of the parameter F_1 ; (b) Imperfection both in the transverse and normal directions, $F_1 = F_2 \neq 0$. The numbers in the figure field show the values of the parameters $F_1 = F_2$	71
Figure 4.3 : Dispersion curves for the <i>II</i> pair of materials: (a) first branches of the first and second modes; (b) second branches of the first and second modes. The numbers in the figures fields show the values of the parameters $F_1 = F_2$	73
Figure 4.4 : The influence of the contact imperfections on the dependence between η and kh for the first branch of the first mode for the <i>I</i> pair of materials in Case 1: (a) imperfection is only in the transverse direction, $F_1 \neq 0, F_2 = 0$; (b) imperfection is in both the transverse and normal directions, $F_1 = F_2 \neq 0$	74
Figure 4.5 : The influence of the contact imperfections on the dependence between η and kh for the first branch of the first mode for the <i>II</i> pair of materials in Case 4: (a) imperfection is only in the transverse direction, $F_1 \neq 0, F_2 = 0$; (b) imperfection is in both the transverse and normal directions, $F_1 = F_2 \neq 0$	74
Figure 4.6 : The graphs of the dependence between η and kh constructed for the first branch of the first mode of the <i>I</i> pair of materials in Case 1, ($\psi^{(1)} = 0.01, \psi^{(2)} = 0$) under $\psi^{(3)} = -0.0025(a), -0.005(b)$ and $-0.01(c)$	76
Figure 4.7 : The graphs of the dependence between η and kh constructed for the first branch of the first mode of the <i>I</i> pair of materials in Case 2, ($\psi^{(1)} = 0, \psi^{(2)} = -0.01$) under $\psi^{(3)} = -0.0025(a), -0.005(b)$ and $-0.01(c)$	77
Figure 4.8 : The graphs of the dependence between η and kh constructed for the first branch of the first mode of the <i>II</i> pair of materials in Case 3, ($\psi^{(1)} = 0.01, \psi^{(2)} = -0.01$) under $\psi^{(3)} = -0.0025(a), -0.005(b)$ and $-0.01(c)$	77

Figure 4.9 : The graphs of the dependence between η and kh constructed for the first branch of the first mode of the <i>II</i> pair of materials in Case 4, ($\psi^{(1)} = 0, \psi^{(2)} = -0.01$) under $\psi^{(3)} = -0.0025(a), -0.005(b)$ and $-0.01(c)$	78
Figure 4.10: The graphs of the dependence between η and kh constructed for the second branch of the first mode (a), the first (b) and the second (c) branches of the second mode of the <i>I</i> pair of materials in Case 1, ($\psi^{(1)} = 0.01, \psi^{(2)} = 0$).....	79
Figure 4.11: The graphs of the dependence between η and kh constructed for the second branch of the first mode (a), the first (b) and the second (c) branches of the second mode of the <i>I</i> pair of materials in Case 2, ($\psi^{(1)} = 0, \psi^{(2)} = -0.01$).....	80
Figure 5.1 : Geometry of the considered mechanical system.	85
Figure 5.2 : Influence of the compressional "dead" and "following" forces to the dispersion of the generalized Rayleigh wave for the <i>I</i> pair of the materials for the first branch of the first mode when (a) $a = b = c = 0$ and (b) $a, b, c \neq 0$	92
Figure 5.3 : Influence of the compressional "dead" and "following" forces to the dispersion of the generalized Rayleigh wave for the (a) <i>II</i> pair and (b) <i>III</i> pair of the materials for the first branch of the first mode when $a, b, c \neq 0$	93
Figure 5.4 : Influence of the compressional "dead" and "following" forces to the dispersion of the generalized Rayleigh wave for the <i>IV</i> pair of the materials for the first branch of the first mode when (a) $a = b = c = 0$ and (b) $a, b, c \neq 0$	93
Figure 5.5 : The influence compressional "dead" and "following" forces to the dispersion of the generalized Rayleigh wave for the (a) <i>I</i> , (b) <i>II</i> , (c) <i>III</i> and (d) <i>IV</i> pairs of materials for the second branch of the first mode when $a, b, c \neq 0$	95
Figure 5.6 : Influence of the compressional "dead" and "following" forces to the dispersion of the generalized Rayleigh wave for the <i>IV</i> pair of the materials for the (a) first and (b) second branches of the second mode when $a = b = c = 0$	96
Figure 5.7 : Influence of the compressional "dead" and "following" forces to the dispersion of the generalized Rayleigh wave for the <i>IV</i> pair of the materials for the (a) first and (b) second branches of the second mode when $a, b, c \neq 0$	96

THE INFLUENCE OF IMPERFECTLY BONDED INTERFACES ON THE GENERALIZED RAYLEIGH WAVE DISPERSION IN PRE-STRESSED ELASTIC STRATIFIED HALF-SPACES

SUMMARY

Surface waves in an elastic layered media, which is simply modeled as a half-space covered by a layer, based on the generalized Rayleigh wave propagation play an important role in various branches of the modern engineering and natural sciences. For instance, geological studies for site characterization, determination of shear wave velocity profiles, damping ratios, fault detection and study of the earthquakes are some of the mentioned branches. These waves also have enormous applications in material sciences, electronic devices, non-destructive testing and damage detection. Therefore the theoretical study of the influence of some reference characteristics of the layered medium, such as imperfect bonding of the layers and initial stresses in constituents of the mentioned systems, on the dispersion of these waves has not only theoretical but also a practical significance. Mentioned initial stresses may arise in the elements of construction and composite materials as a result of their manufacturing or assembling processes and as a result of the temperature change of the environmental medium. Moreover, the stresses appeared under the action of the exploitation load in the members of constructions can also be taken as initial stresses with respect to the additional loading. At the same time, initial stresses might occur in the Earth's crust under the action of geostatic and geodynamic forces. Therefore, up to now there have been made many investigations on the influence of the initial stresses in the elements of constructions in the layered medium on the dispersion of waves propagated in those.

The other important issue in wave propagation process in the layered medium is the effect of the imperfect bonding of the layers to this propagation or dispersion. The investigations of these type of problems are motivated by very high sensitivity of the wave propagation characteristics to interface defects such as weak bonding between the constituents, which can be caused by interface damages or chemical actions, etc. Two classical boundary conditions, that are, perfect bonded interfaces and full slipping ones idealize real physical contact between two layers or between the covering layer and the half-space. In perfect contact condition, also known as welded interfaces all the stress and displacement components are continuous across the interface, whereas, in the case of full slipping conditions also known as non-welded interfaces there is a discontinuity in the shear component of the displacement.

It should be noted that in many cases the shear-spring type imperfectness could not be sufficient for describing the imperfect bonding of the constituents of the layered systems. In such cases, a more adequate model than the shear-spring type one must be used. For instance, normal-spring + shear-spring type imperfect interface model can be applied, according to which, not only the shear displacements, but also the normal displacements have discontinuity and the jump of the latter discontinuity depends linearly on the corresponding normal stress.

In the present study within the framework of the piecewise homogeneous body model the influence of the shear-spring + normal-spring type imperfect contact conditions on the dispersion relation of the generalized Rayleigh waves in the system consisting of the initially stressed covering layer and initially stressed half plane is investigated. The second version of the small initial deformation theory of the three-dimensional linearized theory of elastic waves in initially stressed bodies is applied and the elasticity relations of the materials of the constituents are described by the Murnaghan potential. The corresponding dispersion equation is derived and the algorithm is developed for numerical solution to this equation. The magnitude of the imperfectness of the contact conditions is estimated through the shear-spring type parameter. Consequently, the influence of the imperfectness of the contact conditions on the generalized Rayleigh wave propagation velocity is studied through the influence of the values of this parameter. Numerical results on the action of the imperfectness of the contact conditions and the influence of the initial stresses in the constituents on the wave dispersion curves are presented and discussed. In particular, it is established that the magnitude of action of the imperfectness of the contact conditions under the influence of the initial stresses on the wave propagation velocity cannot be limited with corresponding ones obtained in the case where the contact between the constituents is complete and in the case where this contact is full slipping one. The possible applications of the obtained results on geophysical and geotechnical engineering are also discussed. The results of these investigations can also be successfully used in the estimation of the degree of the bonded defects between the covering layer and half-space.

TAM BAĞLI OLMAYAN TEMAS KOŞULLARI ALTINDA ELASTİK VE ÖN GERİLMELİ TABAKA İLE ÖRTÜLMÜŞ YARI DÜZLEMDE GENELLEŞTİRİLMİŞ RAYLEIGH DALGALARININ DİSPERSİYONU

ÖZET

Yüzey dalgaları elastik katmanlı ortamda, ki genelde bir elastik tabaka ile örtülmüş elastic yarı düzlem şeklinde modellenenebilir, özellikle genelleştirilmiş Rayleigh dalgalarının yayılmasına dayanarak modern mühendislikde ve doğa bilimlerinde önemli rol oynamaktadır. Jeolojik çalışmalar kapsamında yapılan saha karakterizasyonu, kesme dalgası hız profilleri tespiti, sönüm oranları, arıza tespiti ve deprem araştırmaları için jeofizik çalışmalar söz konusu uygulamalara örnekler olarak sıralanabilir. Ayrıca, bu dalgaların malzeme bilimlerinde, elektronik cihazlarda, tahribatsız testlerde, hasar tespitinde önemli uygulamaları vardır. Bu nedenle, tabakalı ortamların referans özelliklerinin etkisini incelemek sadece bir teorik çalışma değil, aynı zamanda, pratik önemi vardır. Örneğin tam bağlı olmayan temas koşullarının ve sistemin bileşenlerinde ki oluşan ön gerilmelerin dalga dispersiyonuna verdiği etki önemli ve ciddi araştırmalar gerekmektedir. Söz konusu sistemin elemanlarında oluşan ön gerilmeler, üretim veya montaj işlemlerinin veya ortamın sıcaklık değişiminin bir sonucu olarak kompozit malzemelerde ortaya çıkabilir. Aynı zamanda, ön gerilmeleri yer kabuğunda jeostatik ve jeodinamik kuvvetlerin etkisi altında da meydana gelebilir. Bu nedenle şu ana kadar tabakalı ortamlarda yüzey dalgaların dispersiyonu hakkında ön gerilmelerin etkisi üzerinde çok araştırmalar yapılmıştır.

Yapı elemanlarında ön gerilmeler sadece sistemin statik davranışı için değil, aynı zamanda özellikle dinamik davranışları için dikkate alınması gereken faktörlerden biridir. Ön gerilmeli ortamlarda dalga yayılımına ait problemlerin incelenmesi modern formasında 20. yüzyılın ikinci yarısında başlamış ve bu güne kadar teorik ve deneysel birçok çalışma yapılmıştır. Bu araştırmalar esasen üç boyutlu lineerize edilmiş elastik dalgaların ön gerilmeli cisimlerde yayılma teorisini kullanılarak yapılmıştır. Bu teorideki ilişkiler ve denklemler, aslında, tamamı ile elastodinamik teorisinin lineer olmayan kesin ilişkileri ve denklemlerden küçük yerdeğişmelere göre lineerize edilerek elde edilmiştir. Bazi kısıtlamaları göz ardı edersek, lineerize edilmiş denklemler genellikle ön gerilmeli cisimlerin bir çok problemlerini araştırmak için imkan yaratmıştır.

Tabakalı ortamlarda yayılan dalga prosesinde diğer önemli sorun, bu yayılma veya dispersiyonuna tabakaların tam bağlı olmayan temas koşullarının etkisidir. Bu tür araştırmaların gerekli olduğu dalga yayılımının özelliklerinin arayüzeyde ki kimyasal veya mekaniksel etkilerden oluşan zayıf bağlara yüksek derecede hassas olmasından ileri gelmektedir. Ayrıca, yerin kabuk derinliklerinde de kayaların katmanları arasındaki temaslar kilometreler boyunca tam bağla olmayabilir. Üstelik kırıklar veya faylar şeklinde süreksizlikler de yer kabuğunda sık karşılaşılan özelliklerdir.

İki klasik temas koşulları, yani tam bağı ve tam açık arayüzler, aslında iki kat arasında veya örtü tabakası ve yarı-uzay arasında ki gerçek fiziksel teması idealize etmektir. Tam bağı temas koşullarında bütün gerilme ve yerdeğişme bileşenleri arayüzey boyunca süreklidir, buna karşın, tam açık temas koşullarında ise yerdeğişme bileşenlerinde bir süreksizlik vardır.

Genel olarak ele alınan problemin fiziksel özelliklerinin sayısal değerlendirilmesi için problemin hakkında yeterli bilgiye sahip olmak ve problemin doğası hakkında matematiksel anlayış gerekmektedir. Elastik dalga yayılımına arayüzey koşulları etkisini incelemek için literatürde çeşitli teorik yöntemler mevcuttur. İki tabaka arasında gerçek arayüzey koşulları matematiksel modelleme açısından daha karmaşıktır ve araştırmacılar farklı mekanik modeller ile gerçek fiziksel koşulları tanımlamak için önemli çabalar harcamışlar. Birçok araştırmacılar tarafından en sık kullanılan yöntem, yerdeğişme süreksizliği yöntemidir. Özel bir durumda, bu model, bir kesme-yaylı tam bağı olmayan arayüz modeli olarak gerçekleştirilir. Bu modele göre, sadece kesme yönündeki yerdeğişmesinde arayüz üzerinde süreksizlik var ve bu süreksizlik arayüzdeki kayma gerilmesi ile doğrusal orantılıdır. Böylece tam bağı olmayan temas koşullarının büyüklüğü kesme-yay tipi parametresi F yoluyla tahmin edilir, ki $0 \leq F \leq \infty$. $F = 0$ olması arayüzeyin her iki tarafındaki yerdeğişmelerin eşit olması anlamına gelir ki oda tam bağı temas koşullarına denk gelir. Diğer uçta da $F = \infty$ olması arayüzeyin iki tarafındaki yerdeğişmelerin birbirinden tam bağımsız olması anlamına gelir ki oda tam açık temas koşullarına karşı gelir. Böylelikle F in sıfır ve sonsuz arasında ki her hangi bir pozitif değeri de her hangi bir tam bağı olmayan temas koşullarına denk gelmesi anlamına gelir. Sonuç olarak, genelleştirilmiş Rayleigh dalgalarının yayılma hızına tam bağı olmayan temas koşullarının etkisi bu parametrenin farklı değerleri ile incelenir.

Bu çalışmada, lineer elastik parçalı homojen cisimler çerçevesinde, tam bağı olmayan temas koşullarının kesme-yaylı ve normal-yaylı modelini kullanarak genelleştirilmiş Rayleigh dalgaların dispersiyon etkisi ön gerilmeli tabaka ile örtülmüş yarı düzlemde incelenmiştir. Üç boyutlu lineerize edilmiş elastik dalgaların ön gerilmeli cisimlerde yayılma teorisinin küçük yerdeğişmelere ait ikinci versiyonu uygulanmıştır ve malzemelerin elastik ilişkileri Murnaghan potansiyeli ile verilmiştir. Bu durumda, Murnaghan potansiyelinde verilen üçüncü dereceden elastisite sabitlerinin etkileri de incelenmiştir. Sisteme uygun dispersiyon denklemi elde edilmiş ve bu denklemin sayısal çözümü için algoritma geliştirilmiştir. Ancak, dikkat etmesi gerekir ki bütün sayısal modellerde yarıdüzlem malzemesi *Çelik* olarak seçilmiştir, örtü tabaka malzemesi ise farklı olarak dört çeşit malzemeden yani *Bronze*, *Brass 59-1*, *Brass 62*, *Plexiglas*'den oluşmuştur. Tam bağı olmayan temas koşullarının büyüklüğü kesme-yay tipi parametresi yoluyla tahmin edilmiştir. Dolayısı ile, tam bağı olmayan temas koşullarının genelleştirilmiş Rayleigh dalgalarının yayılma hızına etkisi bu parametrenin farklı değerleri ile incelenmiştir. Üstelik, her iki yönde yani dalga yayılma yönünde ve dalga yayılma yönüne dik olan yönde de tam bağı olmayan temas koşullarının etkisi göz önüne alınmıştır. Buna ek olarak, tam bağı olmayan temas koşullarının farklı biçim düzeni ön gerilmelerinin, dispersiyon eğrilerine etkisinin sayısal sonuçları sunulmuş ve tartışılmıştır.

Bura da belirtilmelidir ki, bilindiği gibi genelleştirilmiş Rayleigh dalgaları adı Rayleigh dalgalarının aksine dispersivdir, yani dalga yayılma hızı dalgasayısına

bağımlıdır, hatta, genelleştirilmiş Rayleigh dalgalarının adı Rayleigh dalgalarının aksine sonsuz sayıda yayılma modları vardır. Ayrıca, her moda ait dispersiyon eğrisinin de iki dalı var. Birinci dal için, tabakanın hareketi adı Rayleigh dalgalarına benzer şekilde eliptiktir, ancak ikinci dal için bir ters hareket türü söz konusudur. Üstelik, boyutsuz dalgasayısı ilk modunun ikinci dalı, ikinci modun birinci ve ikinci dalı için kesme dalgasayı değerleri vardır. Bu çalışmada yukarıdaki sözü geçen bütün analizler ve hesaplamalarda her iki moda ait dispersiyon eğrileri elde edilmiştir ve birinci ve ikinci dallar da göz önüne alınmıştır.

Özellikle, önemli bir sonuç olarak, tam bağılı olmayan temas koşulları altında elde edilen genelleştirilmiş Rayleigh dalgalarının dispersiyon eğrileri yukarıda sözü geçen iki klasik temas modelleri, yani tam bağılı ve tam açık temas koşullarının, dispersiyon eğrileriyle sınırlı olmadığı gösterilmiştir. Bu sonuç tezdeki yapılan araştırmaların ne kadar önemli ve gerekli olduğunu tekrar göstermektedir. Ayrıca, elde edilen sonuçların jeofizik ve geoteknik mühendisliği üzerine olası uygulamaları da tartışılmıştır. Bu araştırmaların sonuçları başarılı bir şekilde tabakalar arasındaki veya tabaka ile yarıdüzlem arasında temas kusurlarının derecesinin tahmini için kullanılabilir.

Son olarak, yukarıdaki tartışmalara itibaren aşağıdaki bazı önemli sonuçlar kısaca özetlenebilir:

- Tam bağılı olmayan temas koşulları genelleştirilmiş Rayleigh dalgalarının yayılma hızının azalmasına neden olmaktadır.
- Dalga yayılma hızının düşük ve yüksek dalgasayısındaki sınır değerleri tam bağılı olmayan temas koşullarından bağımsızdır.
- Tam bağılı olmayan temas koşulları bazı malzeme çiftleri için birinci modun ikinci dalı, ikinci modun birinci ve ikinci dallarının dalgasayısı kesme değerlerini de etkilemektedir.
- Ön gerilmeler etkisi altında elde edilen dispersiyon eğrileri daha karışıktır ve dalga sayısından bağımlıdır. Bir başka deyişle ön gerilmelerin durumuna göre tam bağılı olmayan temas koşulları belirli bir dalgasayısından sonra dalga hızının azalmasına yada artılmasına neden olabilir.
- Normal yönde tam bağılı olmayan temas koşulları önemli ölçüde dalga yayılma hızını azaltmaktadır.
- Tam bağılı olmayan temas koşulları dalga yayılma hızı üzerinde ön gerilmelerin etkisinin artırmasına neden olur.
- Tam bağılı olmayan temas koşulları altında elde edilen dispersiyon eğrileri tam bağılı veya tam açık temas koşullarının dispersiyon eğrilerine sınırlı değildir. Bu sonuç yine de bu tür araştırmaların önemini ve gerekli olduğunu göstermektedir.
- Tam bağılı temas koşulları altında elde edilen sayısal sonuçlar bazı malzeme çiftleri için literatürde yayınlanan deneysel sonuçlarla karşılaştırılmış ve onaylanmıştır.

1. INTRODUCTION

The theory of elastic surface waves in layered half-spaces, though it is an old topic in classical sense, it has found highly important scientific and engineering applications through the last couple of decades. Fields of applications are vast but some notable areas might be acoustic, smart materials, Earth sciences, subsurface explorations, non-destructive testing and damage detection. Indeed, variety of mechanical, material and structural properties, presence of damages and/or cracks, different external loading, etc. make the study of these wave processes still an active and interesting field of research these days.

There are two types of the most important investigations in this regard the first of which relates to study of the effect of imperfect bonding between the covering layer and half-space on a surface wave propagation and its characteristics. But the other one is the study of influence of initial stresses which exist in the constituents of the stratified half-space on this wave.

The investigations of the first type of problems are motivated by very high sensitivity of the wave propagation characteristics to interface defects such as weak-bonding between the constituents which can be caused by interface damages or chemical actions and etc. The results of these investigations can be successfully applied to determination of various defects between the covering layer and half-space. But the investigations of the second type of problems are motivated by the non-destructive determination of mostly the residual (or initial) stresses in the elements of constructions. Currently the results of these investigations are successfully employed for determination of the mentioned residual stresses. At the same time, the foregoing investigations are also propounded the fundamental questions of the dynamics of the non-homogeneous deformable solid bodies.

It is evident from the foregoing discussions that the investigations of the generalized Rayleigh wave dispersion in a pre-stressed elastic stratified half-plane with imperfectly

bonded interfaces, which is the topic of the present thesis, lies at the junction of the above-noted two problems.

Note that propagation of the elastic waves in pre-stressed bodies is studied by utilizing the Three-dimensional Linearized Theory of Elastic Waves in Initially Stressed Bodies (TLTEWISB). The relations and equations of the TLTEWISB are obtained from the exact relations and equations of the non-linear theory of elastodynamics by linearization with respect to small dynamical perturbations. The general questions of the TLTEWISB have been elaborated in many investigations such as in works by Biot (1965), Truestell (1961), Eringen and Suhubi (1975), Guz (2004) and others. It should be noted that there are some versions of the TLTEWISB which were detailed in the monograph by Guz (2004). These versions of the TLTEWISB are distinguished from each other with respect to the magnitude of the initial strains. The version of the TLTEWISB developed for high-elastic materials, according to which the initial strains in the bodies are determined within the scope of the non-linear theory of elasticity without any restrictions on the magnitude of the initial strains, is called the large (or finite) initial deformation version. The version of the TLTEWISB, according to which, an initial stress-strain state in bodies is determined within the scope of the geometrical nonlinear theory of elasticity and changes to the elementary areas and volumes as a result of the initial deformation are not taken into account, is called the first version of the small initial deformation theory of the TLTEWISB. The second version of the small initial deformation theory of the TLTEWISB is the version, according to which, an initial stress-strain state in bodies is determined within the scope of the classical linear theory of elasticity.

It should be noted that in many cases the shear-spring type imperfectness cannot be sufficient for describing the imperfect bonding of the constituents of the layered systems. In such cases more adequate model than the shear-spring type one must be used. For instance, normal-spring + shear-spring type imperfect interface model can be applied, according to which, not only the shear displacements, but also the normal displacements have discontinuity and the jump of the latter discontinuity depends linearly on the corresponding normal stress. In connection with this, the present paper develops the investigations by Akbarov and Ipek (2010, 2012), Akbarov et al.

(2011), Akbarov (2012) and studies the influence of shear-spring + normal spring type imperfect contact conditions on the dispersion of the generalized Rayleigh waves on a system consisting of a covering layer and a half-space under two-axial initial stresses.

1.1 Scopes and Objectives

Within the framework of the piecewise homogeneous body model the influence of the shear-spring type imperfect contact conditions on the dispersion relation of the generalized Rayleigh waves in the system consisting of the initially stressed covering layer and initially stressed half plane is investigated. The second version of the small initial deformation theory of the three-dimensional linearized theory of elastic waves in initially stressed bodies is applied and the elasticity relations of the materials of the constituents are described by the Murnaghan potential. The magnitude of the imperfectness of the contact conditions is estimated through the shear-spring type parameter. Consequently, the influence of the imperfectness of the contact conditions on the generalized Rayleigh wave propagation velocity is studied through the influence of the values of this parameter. Numerical results on the action of the imperfectness of the contact conditions and the influence of the initial stresses in the constituents on the wave dispersion curves are presented and discussed. In particular, it is established that the magnitude of action of the imperfectness of the contact conditions under the influence of the initial stresses on the wave propagation velocity cannot be limited with corresponding ones obtained in the case where the contact between the constituents is complete and in the case where this contact is full slipping one. The possible application of the obtained results on the geophysical and geotechnical engineering is also discussed.

1.2 Literature Review

The review of the investigations carried out before the year 2007 on the wave propagation in pre-stressed bodies has been made in the papers by Guz (2002), Guz (2005) and Akbarov (2007). The detail consideration of the results of these investigations was made in the monographs by Biot (1965), Eringen and Suhubi (1975), Guz (2004). The review of the more recent related investigations can be

found in papers by Akbarov (2012), Akbarov and Ipek (2012), Akbarov; Agasiyev and Zamanov (2011) and etc. Amount of works related to the study of near-surface waves propagating in initially stresses layered half-spaces are enormous. Here we will present a few of those numerous studies which were carried out in the last twenty years.

Dowaikh and Ogden (1991) studied the propagation of interfacial waves (Stoneley waves) along the boundary between two half-spaces of pre-stressed incompressible isotropic elastic material and they obtained the equation for the wave speed propagation along a principal axis in respect of general strain-energy functions. In particular they showed that when an interfacial wave exists its speed is greater than that of the least of the Rayleigh wave. The propagation of elastic interfacial waves along the plane boundary separating two pre-strained compressible half-spaces has also been studied by Sotiropoulos (1998) assuming that the half-spaces were subjected to pure homogeneous finite strains. Rogerson and Fu (1995) carried out an asymptotic analysis of dispersion relations for wave propagation in a pre-strained incompressible elastic plate and obtained an asymptotic expansions for the wave speed as a function of wave number and pre-stress. Generalized Rayleigh wave propagation in a pre-stressed stratified half-plane was investigated by Akbarov and Ozisik (2003). It was assumed that complete contact conditions between the layer and half-plane were satisfied. Moreover, it was assumed that the initial strains were small and the strains and stresses corresponding to the initial state were determined within the scope of the classical linear theory of elasticity, corresponding dispersion equation was obtained and the dispersion curves which were constructed from the solution to this equation were analyzed. Wijeyewickrema et al. (2008) investigated the time-harmonic wave propagation in a pre-strained and constrained homogeneous compressible high-elastic layer and the influence of the degree of this constraint on the dispersion relations. Ogden and Singh (2011) in the presence of initial stresses derived the general constitutive equation for a transversely isotropic hyperelastic solid based on the theory of invariants to examine the propagation of both homogeneous plane waves and Rayleigh surface waves. Akbarov et al. (2011) investigated the extensional and flexural Lamb waves in a sandwich plate with finite initial strains made from compressible highly elastic materials. It is assumed that the initial strains are caused

by the uniformly distributed normal compression forces acting on the face planes of the plate and the cases where the compression forces are dead and follower are considered. Gupta et al. (2012) studied the propagation of torsional surface wave in an initially stressed non-homogeneous layer over a non-homogeneous half-space. And they showed that the inhomogeneity parameter and the initial stress play an important role for the propagation of torsional surface waves. Zhang and Yu (2013) based on the mechanics of incremental deformations investigated the guided wave propagation in unidirectional plates under gravity and initial stresses. Shams and Ogden (2014) applying the theory of the superposition of infinitesimal deformations on finite deformations in a hyperelastic material studied the propagation of Rayleigh waves in an initially stressed incompressible half-space subjected to a pure homogeneous deformation. Zhang et al. (2014) using quasistatic approximation and linearity assumption, investigated the propagation of Rayleigh waves in a magnetoelastoelectric half-space with initial stress and obtained the wave propagation velocity for four types of electromagnetic boundary. However, in considerable part of these works the interface between layers was assumed to be bonded perfectly, which it is not the real case in many applications.

Two classical boundary conditions, that are, perfect bonded interfaces and full slipping ones idealize real physical contact between two layers. In perfect contact condition also known as welded interfaces all the stress and displacement components are continuous across the interface, whereas, in the case of full slipping conditions also known as non-welded interfaces there is a discontinuity in the shear component of the displacement (Rokhlin and Wang, 1991). An actual interface conditions between two layers is much more complicated in mathematical modeling viewpoint and different investigators spent significant efforts to describe the real physical conditions by different mechanical models. To summarize some, Martin (1992) has reviewed imperfect interface models and formulated the problem mathematically. Pecorari (2001) has investigated the scattering problem of a Rayleigh wave by surface-breaking cracks with partial contact interfaces. Leungvichcharoen and Wijeyewickrema (2003) has discussed the effect of an imperfect interface on harmonic extensional wave propagation in a pre-stressed, symmetric layered composite by employing shear spring

type resistance model to simulate the imperfect interface. Melkumyan and Mai (2008) have studied the effects of imperfect bonding in piezoelectric/piezomagnetic composites and showed that imperfection of the interface bonding has significant impact on the existence of interface waves and on their velocities of propagation. Vishwakarma et al. (2014) have been considered different types of imperfect interfaces to study the propagation of a torsional surface wave in a homogeneous crustal layer over an initially stressed mantle with varying rigidities, density and initial stresses. Zhou; Lu and Chen (2012) also have tried to simulate the imperfect interface conditions by using linear spring model to study bulk wave propagation in laminated piezomagnetic and piezoelectric plates with initial stresses. Kumara and Singh (2009) have considered the propagation of plane waves at an imperfectly bonded interface of two orthotropic generalized thermoelastic rotating half-spaces with different elastic and thermal properties. Liu; Wang and Wang (2010) have analyzed SH surface waves in a piezoelectric elastic layer and an elastic half-space structure with imperfect bonding. Similar model was used by Huang and Li (2010) to study the propagation of shear waves along a weak interface of two dissimilar magnetoelectric or magnetoelectroelastic materials. Reflection and transmission problem of plane waves between piezoelectric and piezomagnetic media with imperfectly bonded interfaces has also been considered by Pang and Liu (2011). Akbarov and Ipek (2010, 2012) have studied the influence of the imperfectness of the interface conditions on the dispersion of the axisymmetric longitudinal waves in the pre-strained compound cylinder under the shear spring type model of the contact condition between layers. Kepceler (2010) has also carried out investigations of a similar type for the initially stressed bi-material compounded circular cylinder.

To the best of the authors' knowledge, up to now there has not been made any investigation related to the study of the influence of imperfectness of the contact conditions on the dispersion characteristics of the generalized Rayleigh wave not only in initially stressed stratified half-space, but also in the stratified half-spaces which has not any initial stresses. Akbarov and Ozisik (2003) have studied the influence of the third order elastic constants on the velocity of the generalized Rayleigh wave propagation in a pre-stressed stratified half-plane, but they also considered

only the perfect contact conditions in their analysis. So in the present work, within the framework of the second version of the small initial deformation theory of the TLTEWISB we attempt to study the effects of the imperfect interface conditions on the generalized Rayleigh wave propagation in a pre-stressed stratified half-plane. Piecewise homogeneous body model were applied and elasticity relations for materials of the constituents were described through the Murnaghan potential. In the classical sense (i.e. in the cases where the initial stresses in the constituents are absent), the investigations carried out in the present paper can be considered as a development of the paper by Tolstoy and Usdin (1953) (in which the generalized Rayleigh waves were studied for the perfectly bounded stratified half-plane) for the concrete selected pair of materials under imperfect contact between the layer and half-plane. At the same time, the investigations carried out in the present paper can be considered as a development of the paper by Akbarov and Ozisik (2003) also for the case where the contact between the constituents of the stratified half-plane is imperfect. Consequently, the goal of the investigations is a study of the role of imperfectness of the contact conditions on the dispersion characteristics of the pre-stressed bi-material non-linear elastic systems.

1.3 Organization of The Thesis

The thesis is divided into six chapters. The present chapter provides general introduction to the subject. Chapter 2 presents a brief review of the wave propagation theory in elastic media. Derivation of the elastodynamics equation of motion is described concisely and different types of surface waves in an elastic half-space covered by a layer is presented. Chapter 3, 4 and 5 are dedicated to the formulation of the problem and numerical analysis. And finally some conclusion and discussions about the results and some suggestions for the future works is presented in chapter 6.

2. ELASTIC WAVES

2.1 Wave Equation

In the linear theory of elasticity it is assumed that the deformations are very small and the relation between stress and strain is linear. Although this may not give an exact description of the physical problem, it provides a very useful solution which is reasonable as long as those assumptions are valid. Consider Cauchy's equations of motion:

$$\sigma_{ij,j} + \rho f_i = \rho \ddot{u}_i, \quad (2.1)$$

To derive the wave equation, we assume that a continuum is isotropic and homogeneous. Thus, the corresponding stress-strain relations can be written as follows (Hooke's law):

$$\sigma_{ij} = \lambda \varepsilon_{kk} \delta_{ij} + 2\mu \varepsilon_{ij}, \quad (2.2)$$

where λ and μ are Lamé's constants and the strain-displacement relations are:

$$\varepsilon_{ij} = \frac{1}{2}(u_{i,j} + u_{j,i}), \quad (2.3)$$

where σ is the Cauchy's stress tensor, ε is the strain tensor, ρ is the material density, δ_{ij} is the Kronecker delta function, u represent the displacement in the spatial coordinate of the system and f represent the external forces on the material particles which are assumed to be zero in our formulations. Note that the second order derivative with respect to time is represented by \ddot{u} . Combining the equations (2.1), (2.2) and (2.3) in terms of the displacement yields the equation of motion in elastodynamics for isotropic homogeneous materials:

$$(\lambda + \mu)u_{j,ji} + \mu u_{i,jj} = \rho \ddot{u}_i. \quad (2.4)$$

Note that we use the standard Einstein's index notation in all the above equations. We can also state equations (2.4) concisely using vector calculus notation. The first

summation term in the left-hand side of these equations is the divergence of \mathbf{u} , namely, $\nabla \cdot \mathbf{u}$, while the second summation term is Laplace's operator, namely, ∇^2 . Therefore, we can rewrite equations (2.4) as:

$$(\lambda + \mu)\nabla(\nabla \cdot \mathbf{u}) + \mu \nabla^2 \mathbf{u} = \rho \frac{\partial^2 \mathbf{u}}{\partial t^2}. \quad (2.5)$$

This is the equations of motion, i.e. equation (2.4), in vector representation. It can be shown using Helmholtz decomposition that the displacement field \mathbf{u} decomposes into two independent vector fields for plane-wave assumptions. These two fields represent two different kinds of waves and are solutions to the equations:

$$\nabla^2 \phi = \frac{1}{\alpha^2} \frac{\partial^2 \phi}{\partial t^2}, \quad (2.6)$$

$$\nabla^2 \psi = \frac{1}{\beta^2} \frac{\partial^2 \psi}{\partial t^2}, \quad (2.7)$$

for the longitudinal and the shear waves, respectively. Here ϕ and ψ are scalar and vector potentials of the field, and

$$\alpha = \sqrt{\frac{\lambda + 2\mu}{\rho}}, \quad (2.8)$$

$$\beta = \sqrt{\frac{\mu}{\rho}}, \quad (2.9)$$

are propagation velocities of the longitudinal and the shear waves, respectively. Indeed, it follows from these equations that two types of elastic waves can propagate in a homogeneous isotropic medium, namely longitudinal and shear or transverse waves.

2.2 Body Waves

In general, there are two principle types of elastic body waves: *Longitudinal waves* and *Transverse waves*. Longitudinal waves are called in seismology *P* or primary waves, because they represent the first arriving waves on seismograms. Transverse or shear waves, however, are called *S* or secondary waves, because they appear in seismograms after the primary waves. In longitudinal waves, the particle motion is in the direction of wave propagation, while in shear waves, the particle motion is normal to the direction of propagation. The velocities of longitudinal waves, α , and of transverse waves, β , in a homogeneous, isotropic medium are given by the equations (2.8) and (2.9) which is derived in the previous section, respectively.

2.3 Surface Waves

In addition to the body waves that propagate in all directions into the medium, there exists another type of waves which for the most part restricted to the free boundary or surface of the medium and for that reason are called *surface waves*. These waves propagate along the surface of the body and their amplitudes rapidly decrease as the distance from the boundary goes to infinity. There are two the most important types of surface waves, *Rayleigh waves* and *Love waves*, which take their names after the scientists who studied them for the first time. Rayleigh waves essentially occur by the interactions of compressional waves (P waves) and vertically polarized shear waves (S waves) with the free boundaries of the medium, however, Love waves take place in a system consisting of a layer over a half-space or in general in layered structures when the velocity of S wave increase with depth. An important characteristic of surface waves is that they are dispersive, i.e. their propagation velocity is frequency dependent. In the following chapters we will consider this feature of surface waves more precisely.

2.3.1 Rayleigh waves

As mentioned above, Rayleigh waves travel only along the free surface of an elastic bodies. The particle motion is elliptic and retrograde with respect to the direction of propagation. The components of displacement contain a vertical component and a horizontal component and the amplitude of the particle motion in these waves decreases exponentially with depth. Rayleigh waves in an elastic half-space are non-dispersive, i.e. phase and group velocities of propagation are equal and do not depend on the frequency of the waves. However, when surface waves propagate in a layered half-space, their velocities depend on the frequency of the vibrations, thickness of the layer, density and elastic properties of the constituents of the layers and the half-space. Therefore, they are dispersive and the relationships between velocity and frequency (or wavelength) with parameters of the elastic properties are plotted as dispersion curves. In this case they are called generalized Rayleigh waves. It was established by Tolstoy and Usdin (1953) that the dispersion equation of the generalized

Rayleigh waves has infinitely many modes unlike ordinary Rayleigh waves, which can propagate only in one mode.

2.3.2 Love waves

While Rayleigh waves exist at free surface of a body, Love waves require some kind of a wave guide like an elastic layer over a half-space to propagate. The particles motion in Love waves are only horizontal and perpendicular to the direction of propagation. These wave are also dispersive because their velocity obviously depends on the frequency of the propagation. Moreover, several modes of propagation exist, because of the periodic nature of their dispersion function.

2.3.3 Other types of surface waves

Elastic waves can also occur at the interface between two continua. We consider some important examples of such waves, namely, Stoneley waves, Scholte wave and slip waves at the interface between two semi-infnite solids and Scholte waves at the interface between a semi-infnite solid and a perfect fluid. Stoneley waves is a surface wave (or interface wave) that typically propagates along a solid-solid interface. In the case of a liquid-solid interface, this wave is referred to as a Scholte wave. The wave is of maximum intensity at the interface and decreases exponentially away from it. Unlike Rayleigh waves there are some restrictions for Stoneley waves to exist, which depends strongly on the values of the material parameters. Studies indicate that the possible combinations between two isotropic real solids, less than 3% of the pairings let a Stoneley wave exist. If two solids are not perfectly welded together an other type of waves so-called slip waves or interface waves propagate at the interface of two pairs.

2.4 Dispersion of Waves

If propagation velocity of waves depends on frequency we say that the waves are dispersive. In a dispersive medium a wave changes its shape during propagation, because its spectral components propagate with different velocities. This may cause some technical problems in the measurements of the velocity of propagation or in their

transmission. However this process can be used to study the properties of the medium which the waves have propagated through.

There are two types of wave dispersion: material dispersion and geometrical dispersion. The material dispersion as its name implies is due to the change in the material properties of the structure. For example, this type of dispersion is familiar from optics, since the velocity of light in media depends on its frequency. The geometrical dispersion, on the other hand, is because of the interference of waves. This type of waves dispersion occur when the waves propagate in layered structures, or along the surface of a medium. As mentioned in the previous sections we shall study this type of dispersion in our investigations.

2.5 Boundary Conditions

In general quantitative evaluation of physical properties of a considered problem requires adequate knowledge and understanding of its nature mathematically. Several theoretical methods are available in the literature for studying the influence of interfaces on elastic wave propagation depending on the character of the problem to be considered. The most frequently used method by many investigators is the *displacement discontinuity method*.

Two classical boundary conditions, that are, perfect bonded interfaces and full slipping ones idealize real physical contact between two layers. In perfect contact condition also known as *welded interfaces* all the stress and displacement components are continuous across the interface, whereas, in the case of full slipping conditions also known as *non-welded interfaces* there is a discontinuity in the shear component of the displacement (Rokhlin and Wang 1991).

Now we consider the formulation of the imperfect contact conditions on the interface plane between the covering layer and the half-space. It should be noted that, in general, the imperfectness of the contact conditions is identified by discontinuities of the displacements and forces across the mentioned interface. A review of the mathematical modeling of the various types of incomplete contact conditions for elastodynamics problems has been detailed in a paper by Martin (1992). It follows from this paper

that for most models the discontinuity of the displacement \mathbf{u}^+ and force \mathbf{f}^+ vectors on one side of the interface are assumed to be linearly related to the displacement \mathbf{u}^- and force \mathbf{f}^- vectors on the other side of the interface. This statement, as in the paper by Rokhlin and Wang (1991), can be presented as follows:

$$[\mathbf{f}] = \mathbf{C}\mathbf{u}^- + \mathbf{D}\mathbf{f}^-, \quad [\mathbf{u}] = \mathbf{G}\mathbf{u}^- + \mathbf{F}\mathbf{f}^-, \quad (2.10)$$

where \mathbf{C} , \mathbf{D} , \mathbf{G} and \mathbf{F} are three-dimensional (3×3) matrices and the square brackets indicate a jump in the corresponding quantity across the interface. Consequently, if the interface is at say $z = h$, then:

$$[\mathbf{u}] = \mathbf{u}|_{z=h^+} - \mathbf{u}|_{z=h^-}, \quad [\mathbf{f}] = \mathbf{f}|_{z=h^+} - \mathbf{f}|_{z=h^-}. \quad (2.11)$$

It follows from (2.10) that we can write incomplete contact conditions for various particular cases by selection of the matrices \mathbf{C} , \mathbf{D} , \mathbf{G} and \mathbf{F} . One such selection was made in the paper by Jones and Whitter (1967), according to which, it was assumed that $\mathbf{C} = \mathbf{D} = \mathbf{G} = \mathbf{0}$. In this case the following can be obtained from (2.10):

$$[\mathbf{f}] = \mathbf{0}, \quad [\mathbf{u}] = \mathbf{F}\mathbf{f}^-, \quad (2.12)$$

where \mathbf{F} is a constant diagonal matrix. The model (2.12) simplifies significantly the solution procedure of the corresponding problems and is adequate in many real cases. Therefore, this model is called a shear-spring type resistance model and has been used in many investigations carried out within the framework of classical elastodynamics. According to this statement, we also use the model (2.12) for the mathematical formulation of the imperfectness of the contact conditions in our investigations.

2.5.1 Displacement Discontinuity Method

Some theoretical methods are available in the literature for studying the influence of interfaces on elastic wave propagation depending on the character of the problem to be considered. These analytical models are essentially based on the following three methods: Displacement Discontinuity Method (DDM), effective moduli method and numerical methods such as distinct element method. The most frequently used method by many investigators is the displacement discontinuity method.

During past decade various investigators have studied the displacement produced by changes in normal and shear stresses across fractured medium. It is observed that the displacement in a fractured specimens are greater than those of an intact ones. This gives rise to the notion that the additional displacements associated with the fracture can be represented as displacement discontinuity in the displacement field. Experimental observations also show that is in part because of the changes in the geometry of the contact areas as the stress on the fracture increases (Pyrak-Nolte, 1987).

The displacement discontinuity method was originally suggested by Mindlin (1960) to analyze wave propagation along non-welded interfaces. Theoretically a non-welded interface is described by set of boundary conditions which require the discontinuity of displacement component along the interface while the stress components remain constant. Since that time several researchers have used those boundary conditions to investigate the characteristics of propagated waves across non-welded or imperfect interfaces. Here we represent some of those earlier works to emphasize the importance of considering the effects of interface conditions on wave propagation characteristics and to compare the results of our study with their outcomes. We will demonstrate how close they are at least qualitatively.

Schoenberg (1980) using displacement discontinuous conditions computed the reflection and transmission coefficients for harmonic plane waves on a linear slip interface for various values of interface imperfectness parameters which he calls interface compliances. His conclusions for love wave dispersion characteristics are similar to ours for generalized Rayleigh waves propagating in the layered half space, namely, limit values of the wave propagation velocity do not depend on the interface compliances or shear-spring type parameter and that the imperfectness of the contact conditions cause to decrease of the wave propagation velocity. Later, Pyrak-Nolte et al (1987) expanded Schoenberg's solution to derive two elastic interface waves travelling along a fracture by modeling the fracture as a non-welded interface. Using displacement discontinuity model they try to reproduce the effects of a fracture on wave propagation for both synthetic fractures and natural fractures in rocks for seismological investigations (Pyrak-Nolte et al, 1990,1995). It is showed that the seismic response

of a fracture is well represented by this model and the presence of fractures will result in lower seismic velocities and smaller amplitudes than if no fractures were present. Fan et al (2006) obtained analytic and numerical solutions for surface wave propagation over piezoelectric half-space with an imperfectly bonded interfaces using shear-lag model. Their results showed that the dispersion relations of the waves are sensitive to the interface property and the interface imperfection lowers the wave speed. Liu et al (2010) studied the SH surface waves propagating in a layered piezoelectric half-space with an imperfectly bonded interface and also found that the imperfect bonding lowers the propagation velocity. More recently, Zhou et al (2012) used general spring-layer model for imperfect bonding to study bulk wave propagation in initially stressed layered piezomagnetic/piezoelectric plates and they showed that the imperfection effect is more significant than the effect caused by the initial stresses. They found that the imperfections affect the wave propagation characteristic, and change the frequencies and phase velocities to a considerable extent.

2.5.2 Experimental verifications

Elastic surface waves based on Rayleigh waves propagation have played an important role in geological studies for site characterization, determination of shear wave velocity and damping ratios, fault detection and study of the earthquakes. Acoustic surface waves also have enormous applications in material sciences, electronic devices and non-destructive testing. Here we will present a few of those numerous studies in line with the purpose of our study which conform and strengthen the displacement discontinuity model numerically and or experimentally.

Myer et al (1985) laboratory experiments showed that the displacement discontinuity model predicted correctly the amplitude behavior of the waves propagated across synthetic fractures. Pyrak-Nolte et al (1990, 1992) and Roy et al (1995) derived the theoretical velocity based on the displacement discontinuity model of wave propagation across a fracture and conducted detailed laboratory measurements on intact and fractured specimens (both natural or man-made) of various material types (including steel, aluminum, quartz monzonite, dolomite) and found that the theory correctly predicted experimental measurements. Xian et al (2001) performed

experiments on the laboratory scale to image seismic wavefronts of compressional waves that are guided between parallel fractures. The resulting wavefronts showed that energy confinement between fractures is a function of fracture specific stiffness. Then by examining the change in energy among different guided-modes, fracture specific stiffness, can be predicted from laboratory as well as field data. Vlasie et al (2005) proposed a non-destructive method to test the mechanical quality of stratified aluminum/epoxy/aluminum bonds. The adhesion zone was described by a 2D material interface and surface free energy parameter was introduced to model jump conditions of the problem to compare the case with perfect contact. Such a modeling used to take into account the effect of some defects or cracks at the interface. Lai-Yu et al (2006) performed some ultrasonic detection testing using Rayleigh waves for the stratified specimens (Lucite/Steel and Aluminum /Lucite/Steel). They showed that the elastic properties of the layered media can be inferred from the Rayleigh wave information. Investigations revealed that the distributions of the surface displacement of the Rayleigh modes should be considered in the inversion of the parameters. Zerwer et al (2005) using numerical simulation based on finite element method and conducting laboratory experiments showed that by combining information from Rayleigh wave dispersion and energy dissipation it is possible to determine the location and depth of surface-breaking cracks in concrete beams.

2.5.3 Engineering applications

Surface waves have been used in geophysics and seismology for the characterization of the Earth's interior for many years. The Earth's crust however contains discontinuities such as fractures, faults and joints. These discontinuities, their location and characteristics is of great importance to study of earthquakes, mine stability, oil and gas production, etc. Thus understanding the mechanical properties of those discontinuities provides useful knowledge about that processes.

In this regard, Pyrak-Nolte et al (1987) used the displacement discontinuity model for wave propagation across a fracture to investigate its effect on seismic anisotropy in velocity and amplitudes. They conducted laboratory measurements on fractured laminated blocks of steel and by using measured P and S wave velocities they could

estimate the quantitative values of interface stiffness of the interfaces between the steel plates. Nagy (1992) by applying the similar procedure and by measuring the longitudinal and shear wave reflection coefficients showed that ratio between the normal and transverse interfacial stiffness constant of an imperfect interface can be used to identify the physical nature of the imperfection. He also used this technique to classify different types of imperfections.

Since in fractured media the energy of the interface waves concentrated mostly on the fracture, these waves can be used for remote determination of mechanical properties of the fractures. Nihei et al (1995) used this property to perform both laboratory experiments on artificial fractures and numerical simulations with dynamic boundary element method and demonstrated techniques to measure propagation velocity of these waves to extract fracture interface stiffnesses.

Extracting fracture properties from seismic data is closely related understanding of the probabilistic and spatial distributions in fracture specific stiffness. In this regard, Acosta-Colon et al (2009) studied the effects of the scale of measurement on the interpretation of fracture properties from seismic wave propagation and presented results of a laboratory study that examines the effect of field of view on the interpretation of fracture specific stiffness from seismic measurements to fully characterize the fracture.

2.6 Elastic Waves in Bodies with Initial Stresses

Problems related to the nonlinear effects of the elastic waves arise in almost all fields of modern engineering branches such as civil, mechanical, aircraft and geophysical engineering and many others. One of the most common sources of nonlinearity in such problems associated to the initial stress state in the constituents of the medium. However, problems related to study of the wave propagation in initially stressed bodies cannot be solved within the framework of the classical linear theory of elasticity. Although many attempts have been done going back to the 19th century, but it did not achieve noticeable progress until the second half of the 20th century that the general nonlinear theory of elastic waves intensively developed. Therefore, at the present time, most studies of these types of elastodynamics problems are made in the framework

of the Three-dimensional Linearized Theory of Elastic Waves in Initially Stressed Bodies (TLTEWISB). The general concepts and equations of the TLTEWISB have been presented elaborately in many classical texts such as Biot (1965), Eringen and Suhubi (1975) and others. It should be noted that, the equations of the TLTEWISB are obtained from exact relations of the nonlinear theory of elasticity in initially stressed bodies by linearization of the equations with respect to small deformation. It should be noted that there are some versions of the TLTEWISB which were developed in the monograph by Guz (2004). These versions of the TLTEWISB are distinguished from each other with respect to the magnitude of the initial strains. The version of the TLTEWISB developed for high-elastic materials, according to which the initial strains in the bodies are determined within the scope of nonlinear theory of elasticity without any restrictions on the magnitude of the initial strains, is called the large or finite initial deformation version. The version of the TLTEWISB, according to which the initial stress-strain state in bodies is determined within the scope of the geometrically nonlinear theory of elasticity and under which changes to the elementary areas and volumes as a result of initial deformation are not take into account, is called the first version of the small initial deformation theory of the TLTEWISB. The second version has an initial stress-strain state in bodies, which is determined within the scope of the classical linear theory of elasticity.

2.7 Generalized Rayleigh Wave in a Covered Half-Space with Initial Stresses

Before considering the mathematical formulation of the problem it might be useful to summarize some basic notions and concepts of the three-dimensional linearized theory of elasticity in initially stressed bodies. The stress and/or strain state of the bodies, in general, can be divided into three cases as natural state, pre-stressed state and perturbed state. In natural state it is assumed that there are no stresses and/or strains acting on the bodies. The system consists of an elastic, homogeneous and isotropic covered half-space as shown in Figure 2.1 and it is assumed that the system is under the effect of initial homogeneous normal stresses in Ox_1 direction as shown in the figure. In the following formulations the values related to the stresses, strains and displacements in the pre-stressed state are denoted by upper indices (0) as $\sigma_{ij}^{(m),0}$, $\epsilon_{ij}^{(m),0}$, and $u_i^{(m),0}$,

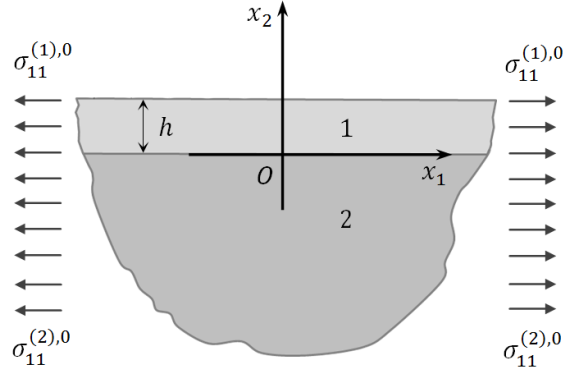


Figure 2.1: The geometry of the considered stratified half-plane.

respectively. All these quantities satisfy the system of equations of the elasticity theory in static case. These system of equations in a Lagrangian coordinate $Ox_1x_2x_3$ which in natural state coincides with Cartesian coordinates, in nonlinear form can be written as follows:

$$\frac{\partial}{\partial x_i} \left[\sigma_{in}^{(m),0} \left(\delta_n^j + \frac{\partial u_i^{(m),0}}{\partial x_n} \right) \right] = 0, \quad (2.13)$$

$$\sigma_{ij}^{(m),0} = \lambda^{(m)} e^{(m),0} \delta_i^j + 2\mu^{(m)} \varepsilon_{ij}^{(m),0}, \quad (2.14)$$

$$e^{(m),0} = \varepsilon_{11}^{(m),0} + \varepsilon_{22}^{(m),0} + \varepsilon_{33}^{(m),0}, \quad (2.15)$$

$$2\varepsilon_{ij}^{(m),0} = \frac{\partial u_i^{(m),0}}{\partial x_j} + \frac{\partial u_j^{(m),0}}{\partial x_i} + \frac{\partial u_n^{(m),0}}{\partial x_i} \frac{\partial u_n^{(m),0}}{\partial x_j}. \quad (2.16)$$

Note that the standard Einstein's index notation is used in all the above equations. In three-dimensional linearized theory of elasticity non-linear terms in equations (2.13)-(2.16) can be neglected in many cases. In this cases, equation (2.14) and (2.15) can be used in their original form, however, equations (2.13) and (2.16) are written as the following equations respectively:

$$\frac{\partial \sigma_{ij}^{(m),0}}{\partial x_i} = 0, \quad (2.17)$$

$$2\varepsilon_{ij}^{(m),0} = \frac{\partial u_i^{(m),0}}{\partial x_j} + \frac{\partial u_j^{(m),0}}{\partial x_i}. \quad (2.18)$$

It is obvious that in order to determine the pre-stresses from the equation (2.13)-(2.16) appropriate boundary conditions also will be required. These conditions for example at S_1 part of the surface of the object may be given by external force conditions and at

S_2 part of the surface of the object by displacement conditions. These conditions at S_1 part of the surface for the geometrically nonlinear systems can be written as:

$$\sigma_{in}^{(m),0} \left(\delta_n^j + \frac{\partial u_i^{(m),0}}{\partial x_n} \right) \Big|_{S_1} n_i = P_j, \quad (2.19)$$

and for the geometrically linear systems as:

$$\sigma_{ij}^{(m),0} \Big|_{S_1} n_i = P_j. \quad (2.20)$$

In S_2 part of the surface of the object in both cases (linear and nonlinear) these conditions can be written as:

$$u_i^{(m),0} \Big|_{S_2} = f_i. \quad (2.21)$$

where P_j and f_i in equations (2.20) and (2.21) are known functions. It is also required to determine appropriate contact conditions. This conditions at S_3 contact surface of two bodies may be written as follows:

$$\sigma_{in}^{(1),0} \left(\delta_n^j + \frac{\partial u_i^{(1),0}}{\partial x_n} \right) \Big|_{S_3} n_i = \sigma_{in}^{(2),0} \left(\delta_n^j + \frac{\partial u_i^{(2),0}}{\partial x_n} \right) \Big|_{S_3} n_i, \quad (2.22)$$

$$u_i^{(1),0} \Big|_{S_3} = u_i^{(2),0} \Big|_{S_3}. \quad (2.23)$$

In linear case equation (2.23) is still satisfies, however, equation (2.22) must be written in the following form:

$$\sigma_{ij}^{(1),0} \Big|_{S_3} n_i = \sigma_{ij}^{(2),0} \Big|_{S_3} n_i. \quad (2.24)$$

In equations (2.19)-(2.20)-(2.22)-(2.24), n_i indicate the components of the outward pointing unit normal vector of the corresponding surfaces.

Thus, through the above discussion stress magnitudes can be determined by given relations. Now if we add perturbations to the stresses, strains and displacements we got the following relations for $\sigma_{ij}^{(m),0}$, $\varepsilon_{ij}^{(m),0}$, and $u_i^{(m),0}$, respectively:

$$\begin{aligned} \sigma_{ij}^{(m)'} &= \sigma_{ij}^{(m),0} + \sigma_{ij}^{(m)}, \\ \varepsilon_{ij}^{(m)'} &= \varepsilon_{ij}^{(m),0} + \varepsilon_{ij}^{(m)}, \\ u_i^{(m)'} &= u_i^{(m),0} + u_i^{(m)}. \end{aligned} \quad (2.25)$$

In these relations it is assumed that:

$$\sigma_{ij}^{(m)} \ll \sigma_{ij}^{(m),0}, \quad \varepsilon_{ij}^{(m)} \ll \varepsilon_{ij}^{(m),0}, \quad u_i^{(m)} \ll u_i^{(m),0}. \quad (2.26)$$

The quantities given by equation (2.25) satisfy the equations of motion in geometrically nonlinear theory of elasticity, i.e.

$$\frac{\partial}{\partial x_i} \left[\left(\sigma_{in}^{(m),0} + \sigma_{in}^{(m)} \right) \left(\frac{\partial \left(u_i^{(m),0} + u_i^{(m)} \right)}{\partial x_n} \right) \right] = \left(\rho^{(m),0} + \rho^{(m)} \right) \frac{\partial^2 \left(u_i^{(m),0} + u_i^{(m)} \right)}{\partial t^2}, \quad (2.27)$$

$$\sigma_{ij}^{(m),0} + \sigma_{ij}^{(m)} = \lambda^{(m)} e^{(m),0} \delta_i^j + 2\mu^{(m)} \left(\varepsilon_{ij}^{(m),0} + \varepsilon_{ij}^{(m)} \right), \quad (2.28)$$

$$e^{(m),0} = \left(\varepsilon_{11}^{(m),0} + \varepsilon_{11}^{(m)} \right) + \left(\varepsilon_{22}^{(m),0} + \varepsilon_{22}^{(m)} \right) + \left(\varepsilon_{33}^{(m),0} + \varepsilon_{33}^{(m)} \right), \quad (2.29)$$

$$2 \left(\varepsilon_{ij}^{(m),0} + \varepsilon_{ij}^{(m)} \right) = \frac{\partial u_i^{(m),0} + u_i^{(m)}}{\partial x_j} + \frac{\partial u_j^{(m),0} + u_j^{(m)}}{\partial x_i} + \left(\frac{\partial u_n^{(m),0} + u_n^{(m)}}{\partial x_i} \right) \left(\frac{\partial u_n^{(m),0} + u_n^{(m)}}{\partial x_j} \right). \quad (2.30)$$

In a similar way, for perturbation case in equations (2.19), (2.21), (2.22), and (2.23) the boundary conditions can be written as follows:

$$\left(\sigma_{in}^{(m),0} + \sigma_{in}^{(m)} \right) \left(\delta_n^j + \frac{\partial u_i^{(m),0} + \partial u_i^{(m)}}{\partial x_n} \right) \Big|_{S_1} n_i = P_j, \quad (2.31)$$

$$\left(u_i^{(m),0} + u_i^{(m)} \right) \Big|_{S_2} = f_i, \quad (2.32)$$

$$\left(\sigma_{in}^{(1),0} + \sigma_{in}^{(1)} \right) \left(\delta_n^j + \frac{\partial u_i^{(1),0} + \partial u_i^{(1)}}{\partial x_n} \right) \Big|_{S_3} n_i = \left(\sigma_{in}^{(2),0} + \sigma_{in}^{(2)} \right) \left(\delta_n^j + \frac{\partial u_i^{(2),0} + \partial u_i^{(2)}}{\partial x_n} \right) \Big|_{S_3} n_i, \quad (2.33)$$

$$\left(u_i^{(1),0} + u_i^{(1)} \right) \Big|_{S_3} = \left(u_i^{(2),0} + u_i^{(2)} \right) \Big|_{S_3}. \quad (2.34)$$

If in equations (2.27)-(2.34) only the first order of perturbation are considered and the higher order terms are omitted then the linearized equations of motion, corresponding to boundary and contact conditions can be written in the following form:

$$\frac{\partial}{\partial x_i} \left[\sigma_{ij}^m + \sigma_{in}^{(m),0} \frac{\partial u_i^{(m)}}{\partial x_n} \right] = \rho^{(m)} \frac{\partial^2 u_i^{(m)}}{\partial t^2}, \quad (2.35)$$

$$\sigma_{ij}^{(m)} = \lambda^{(m)} e^{(m)} + 2\mu^{(m)} \varepsilon_{ij}^{(m)}, \quad (2.36)$$

$$e^{(m)} = \varepsilon_{11}^{(m)} + \varepsilon_{22}^{(m)} + \varepsilon_{33}^{(m)}, \quad (2.37)$$

$$2\varepsilon_{ij}^{(m)} = \frac{\partial u_i^{(m)}}{\partial x_j} + \frac{\partial u_j^{(m)}}{\partial x_i}, \quad (2.38)$$

$$\sigma_{ij}^{(m)} + \sigma_{in}^{(m),0} \frac{\partial u_i^{(m)}}{\partial x_n} \Big|_{S_1} n_i = P_j, \quad (2.39)$$

$$u_i^{(m)} \Big|_{S_2} = f_i, \quad (2.40)$$

$$\sigma_{ij}^{(1),0} + \sigma_{in}^{(1),0} \frac{\partial u_i^{(1)}}{\partial x_n} \Big|_{S_3} n_i = \sigma_{ij}^{(2),0} + \sigma_{in}^{(2),0} \frac{\partial u_i^{(2)}}{\partial x_n} \Big|_{S_3} n_i, \quad (2.41)$$

$$u_i^{(1)} \Big|_{S_3} = u_i^{(2)} \Big|_{S_3}. \quad (2.42)$$

It should be noted that in obtaining the above equations (2.35)-(2.42), it is assumed that $\frac{\partial u_i^{(m),0}}{\partial x_j} \ll 1$, then $\delta_i^j + \frac{\partial u_i^{(m),0}}{\partial x_j} \approx \delta_i^j$. This way, equations of the three-dimensional linearized theory of elasticity, (2.35)-(2.42), is obtained. Using these equations it is possible to get a mathematical formulation of the problem.

Consider pre-stressed an elastic half-space covered by an elastic layer with thickness h as shown in Figure 2.1. We consider the case where initial stresses in the layer and half-plane are determined as follows:

$$\begin{aligned} \sigma_{11}^{(1),0} &= \text{const}_1 \neq 0, \quad \sigma_{12}^{(1),0} = \sigma_{22}^{(1),0} = 0, \\ \sigma_{11}^{(2),0} &= \text{const}_2 \neq 0, \quad \sigma_{12}^{(2),0} = \sigma_{22}^{(2),0} = 0. \end{aligned} \quad (2.43)$$

Finally, equations of the motion for the case given by these equations and boundary conditions, (2.35)-(2.42), can be written as follows:

$$\begin{aligned} \frac{\partial \sigma_{11}^{(m)}}{\partial x_1} + \frac{\partial \sigma_{12}^{(m)}}{\partial x_2} + \sigma_{11}^{(m),0} \frac{\partial^2 u_1^{(m)}}{\partial x_1^2} &= \rho^{(m)} \frac{\partial^2 u_1^{(m)}}{\partial t^2}, \\ \frac{\partial \sigma_{12}^{(m)}}{\partial x_1} + \frac{\partial \sigma_{22}^{(m)}}{\partial x_2} + \sigma_{11}^{(m),0} \frac{\partial^2 u_2^{(m)}}{\partial x_1^2} &= \rho^{(m)} \frac{\partial^2 u_2^{(m)}}{\partial t^2}. \end{aligned} \quad (2.44)$$

Note that, constitutive relations for a linear isotropic elastic solid are given by:

$$\sigma_{ij}^{(m)} = \lambda^{(m)} \theta^{(m)} \delta_{ij} + 2\mu^{(m)} \varepsilon_{ij}^{(m)}, \quad \theta^{(m)} = \varepsilon_{11}^{(m)} + \varepsilon_{22}^{(m)}, \quad i, j = 1, 2. \quad (2.45)$$

where $\lambda^{(m)}$ and $\mu^{(m)}$ are Lamé's parameters or constants. The strain components in equation (2.45) can be calculated through the following formula:

$$\varepsilon_{ij}^{(m)} = \frac{1}{2} \left(\frac{\partial u_i^{(m)}}{\partial x_j} + \frac{\partial u_j^{(m)}}{\partial x_i} \right), \quad i, j = 1, 2. \quad (2.46)$$

On the free face plane of the covering layer the following boundary conditions satisfy:

$$\sigma_{12}^{(1)} \Big|_{x_2=h} = 0, \quad \sigma_{22}^{(1)} \Big|_{x_2=h} = 0. \quad (2.47)$$

It should be noted that at the interface of the layer and the half-space boundary conditions for the two classical types of interfaces, i.e. full contact interfaces and full slipping interfaces are considered separately. These boundary conditions for the full contact interfaces:

$$u_i^{(1)} \Big|_{x_2=0} = u_i^{(2)} \Big|_{x_2=0}, \quad \sigma_{i2}^{(1)} \Big|_{x_2=0} = \sigma_{i2}^{(2)} \Big|_{x_2=0}, \quad i, j = 1, 2. \quad (2.48)$$

and for full slipping interfaces can be written as follows:

$$\begin{aligned} u_2^{(1)} \Big|_{x_2=0} &= u_2^{(2)} \Big|_{x_2=0}, \\ \sigma_{22}^{(1)} \Big|_{x_2=0} &= \sigma_{22}^{(2)} \Big|_{x_2=0}, \\ \sigma_{12}^{(1)} \Big|_{x_2=0} &= 0, \quad \sigma_{12}^{(2)} \Big|_{x_2=0} = 0. \end{aligned} \quad (2.49)$$

Moreover, we assume that the following decay conditions are satisfied:

$$\sigma_{ij}^{(2)} \Big|_{x_2 \rightarrow -\infty} \rightarrow 0, \quad u_i^{(2)} \Big|_{x_2 \rightarrow -\infty} \rightarrow 0, \quad i = 1, 2. \quad (2.50)$$

Now if we substitute equation (2.46) into (2.45) and (2.45) into (2.44) the equations of the motion can be written in the following forms:

$$\begin{aligned} \lambda^{(m)} \left(\frac{\partial^2 u_1^{(m)}}{\partial x_1^2} + \frac{\partial^2 u_2^{(m)}}{\partial x_1 \partial x_2} \right) + 2\mu^{(m)} \frac{\partial^2 u_1^{(m)}}{\partial x_1^2} + \mu^{(m)} \left(\frac{\partial^2 u_1^{(m)}}{\partial x_2^2} + \frac{\partial^2 u_2^{(m)}}{\partial x_1 \partial x_2} \right) \\ + \sigma_{11}^{(m),0} \frac{\partial^2 u_1^{(m)}}{\partial x_1^2} = \rho^{(m),0} \frac{\partial^2 u_1^{(m)}}{\partial t^2}, \\ \lambda^{(m)} \left(\frac{\partial^2 u_2^{(m)}}{\partial x_2^2} + \frac{\partial^2 u_1^{(m)}}{\partial x_1 \partial x_2} \right) + 2\mu^{(m)} \frac{\partial^2 u_2^{(m)}}{\partial x_2^2} + \mu^{(m)} \left(\frac{\partial^2 u_2^{(m)}}{\partial x_1^2} + \frac{\partial^2 u_1^{(m)}}{\partial x_1 \partial x_2} \right) \\ + \sigma_{11}^{(m),0} \frac{\partial^2 u_2^{(m)}}{\partial x_1^2} = \rho^{(m),0} \frac{\partial^2 u_2^{(m)}}{\partial t^2}. \end{aligned} \quad (2.51)$$

According to Helmholtz decomposition rule, these displacement fields can be described by the potentials for the longitudinal waves, ϕ , and transverse waves, ψ , in the following form:

$$u_1^{(m)} = \frac{\partial \phi^{(m)}}{\partial x_1} + \frac{\partial \psi^{(m)}}{\partial x_2},$$

$$u_2^{(m)} = \frac{\partial \phi^{(m)}}{\partial x_2} - \frac{\partial \psi^{(m)}}{\partial x_1}. \quad (2.52)$$

Substituting these relations into (2.51) we obtain:

$$\begin{aligned} & \left(\lambda^{(m)} + 2\mu^{(m)} + \sigma_{11}^{(m),0} \right) \left(\frac{\partial^3 \phi^{(m)}}{\partial x_1^3} + \frac{\partial^3 \psi^{(m)}}{\partial x_2 \partial x_1^2} \right) + \mu^{(m)} \left(\frac{\partial^3 \phi^{(m)}}{\partial x_1 \partial x_2^2} + \frac{\partial^3 \psi^{(m)}}{\partial x_2^3} \right) \\ & + \left(\lambda^{(m)} + \mu^{(m)} \right) + \left(\frac{\partial^3 \phi^{(m)}}{\partial x_2^2 \partial x_1} - \frac{\partial^3 \psi^{(m)}}{\partial x_1^2 \partial x_2} \right) + \rho^{(m),0} \frac{\partial^2}{\partial t^2} \left(\frac{\partial \phi^{(m)}}{\partial x_1} + \frac{\partial \psi^{(m)}}{\partial x_2} \right) = 0, \end{aligned} \quad (2.53)$$

$$\begin{aligned} & \left(\lambda^{(m)} + 2\mu^{(m)} \right) \left(\frac{\partial^3 \phi^{(m)}}{\partial x_1^2 \partial x_2} + \frac{\partial^3 \psi^{(m)}}{\partial x_2^2 \partial x_1} \right) + \left(\mu^{(m)} + \sigma_{11}^{(m),0} \right) \left(\frac{\partial^3 \phi^{(m)}}{\partial x_2 \partial x_1^2} - \frac{\partial^3 \psi^{(m)}}{\partial x_1^3} \right) \\ & + \left(\lambda^{(m)} + 2\mu^{(m)} \right) + \left(\frac{\partial^3 \phi^{(m)}}{\partial x_2 \partial x_1^2} - \frac{\partial^3 \psi^{(m)}}{\partial x_1 \partial x_2^2} \right) + \rho^{(m),0} \frac{\partial^2}{\partial t^2} \left(\frac{\partial \phi^{(m)}}{\partial x_2} - \frac{\partial \psi^{(m)}}{\partial x_1} \right) = 0. \end{aligned} \quad (2.54)$$

Equation (2.53) can also be written in the following form:

$$\begin{aligned} & \frac{\partial}{\partial x_1} \left(\nabla \phi^{(m)} + \frac{\sigma_{11}^{(m),0}}{\lambda^{(m)} + 2\mu^{(m)}} \frac{\partial^2 \phi^{(m)}}{\partial x_1^2} - \frac{1}{\left(c_1^{(m)} \right)^2} \frac{\partial^2 \phi^{(m)}}{\partial t^2} \right) \\ & + \frac{\partial}{\partial x_2} \left(\nabla \psi^{(m)} + \frac{\sigma_{11}^{(m),0}}{\mu^{(m)}} \frac{\partial^2 \psi^{(m)}}{\partial x_1^2} - \frac{1}{\left(c_1^{(m)} \right)^2} \frac{\partial^2 \psi^{(m)}}{\partial t^2} \right) = 0. \end{aligned} \quad (2.55)$$

Similarly, equation (2.54) can also be written as:

$$\begin{aligned} & \frac{\partial}{\partial x_2} \left(\nabla \phi^{(m)} + \frac{\sigma_{11}^{(m),0}}{\lambda^{(m)} + 2\mu^{(m)}} \frac{\partial^2 \phi^{(m)}}{\partial x_1^2} - \frac{1}{\left(c_1^{(m)} \right)^2} \frac{\partial^2 \phi^{(m)}}{\partial t^2} \right) \\ & + \frac{\partial}{\partial x_1} \left(\nabla \psi^{(m)} + \frac{\sigma_{11}^{(m),0}}{\mu^{(m)}} \frac{\partial^2 \psi^{(m)}}{\partial x_1^2} - \frac{1}{\left(c_2^{(m)} \right)^2} \frac{\partial^2 \psi^{(m)}}{\partial t^2} \right) = 0. \end{aligned} \quad (2.56)$$

As can be seen from equations (2.55) and (2.56), $\phi^{(m)}$ and $\psi^{(m)}$ potentials must satisfy the following wave equations:

$$\nabla^2 \phi^{(m)} + \frac{\sigma_{11}^{(m),0}}{\lambda^{(m)} + 2\mu^{(m)}} \frac{\partial^2 \phi^{(m)}}{\partial x_1^2} = \frac{1}{\left(c_1^{(m)} \right)^2} \frac{\partial^2 \phi^{(m)}}{\partial t^2}, \quad (2.57)$$

$$\nabla^2 \psi^{(m)} + \frac{\sigma_{11}^{(m),0}}{\mu^{(m)}} \frac{\partial^2 \psi^{(m)}}{\partial x_1^2} = \frac{1}{(c_2^{(m)})^2} \frac{\partial^2 \psi^{(m)}}{\partial t^2}. \quad (2.58)$$

In equations (2.55) and (2.56), $\nabla^2 = \frac{\partial^2}{\partial x_1^2} + \frac{\partial^2}{\partial x_2^2}$ is Laplace operator and,

$$c_1^{(m)} = \sqrt{\frac{\lambda^{(m)} + 2\mu^{(m)}}{\rho^{(m)}}}, \quad c_2^{(m)} = \sqrt{\frac{\mu^{(m)}}{\rho^{(m)}}}.$$

In the case where $\sigma_{11}^{(1),0} = \sigma_{11}^{(2),0} = \sigma_{22}^{(1),0} = \sigma_{22}^{(2),0} = 0$, this formulation transforms to the corresponding one made within the scope of the classical linear theory of elastodynamics. We assume that $\phi^{(m)}$ and $\psi^{(m)}$ functions are represent as follows:

$$\begin{aligned} \phi^{(m)} &= \phi_0^{(m)}(x_2) \cos(kx_1 - \omega t), \\ \psi^{(m)} &= \psi_0^{(m)}(x_2) \sin(kx_1 - \omega t). \end{aligned} \quad (2.59)$$

Substituting presentation (2.59) into the relations (2.57) and (2.58) we obtain the following differential equations for the $\phi_0^{(m)}(x_2)$ and $\psi_0^{(m)}(x_2)$ as follows:

$$\frac{d^2 \phi_0^{(m)}}{dx_2^2} - \frac{k^2 \sigma_{11}^{(m),0}}{\lambda^{(m)} + 2\mu^{(m)}} \phi_0^{(m)} = - \left(\frac{c}{c_1^{(m)}} \right)^2 \phi_0^{(m)}, \quad (2.60)$$

$$\frac{d^2 \psi_0^{(m)}}{dx_2^2} - \frac{k^2 \sigma_{11}^{(m),0}}{\mu^{(m)}} \psi_0^{(m)} = - \left(\frac{c}{c_2^{(m)}} \right)^2 \psi_0^{(m)}. \quad (2.61)$$

We determine the solution to these differential equations as follows:

$$\begin{aligned} \phi_0^{(1)} &= A_1^{(1)} \exp(ikp_1^{(1)}x_2) + A_2^{(1)} \exp(-ikp_1^{(1)}x_2), \\ \psi_0^{(1)} &= B_1^{(1)} \exp(ikp_2^{(1)}x_2) + B_2^{(1)} \exp(-ikp_2^{(1)}x_2), \\ \phi_0^{(2)} &= C_1^{(2)} \exp(kq_1^{(2)}x_2), \\ \psi_0^{(2)} &= D_1^{(2)} \exp(kq_2^{(2)}x_2), \end{aligned} \quad (2.62)$$

where

$$\begin{aligned} p_1^{(1)} &= \left(\frac{c^2}{(c_1^{(1)})^2} - \left(1 + \frac{\sigma_{11}^{(1),0}}{\lambda^{(1)} + 2\mu^{(1)}} \right) \right)^{1/2}, \quad p_2^{(1)} = \left(\frac{c^2}{(c_2^{(1)})^2} - \left(1 + \frac{\sigma_{11}^{(1),0}}{\mu^{(1)}} \right) \right)^{1/2}, \\ q_1^{(2)} &= \left(1 + \frac{\sigma_{11}^{(2),0}}{\lambda^{(2)} + 2\mu^{(2)}} - \frac{c^2}{(c_1^{(2)})^2} \right)^{1/2}, \quad q_2^{(2)} = \left(1 + \frac{\sigma_{11}^{(2),0}}{\mu^{(2)}} - \frac{c^2}{(c_2^{(2)})^2} \right)^{1/2}. \end{aligned} \quad (2.63)$$

Finally, the dispersion equation after some mathematical manipulations can be expressed formally as follows:

$$\det \left\| \alpha_{ij} \left(kh, c, \lambda^{(1)}, \lambda^{(2)}, \mu^{(1)}, \mu^{(2)}, \rho^{(1)}, \rho^{(2)}, \sigma_{11}^{(1),0}, \sigma_{11}^{(2),0} \right) \right\| = 0. \quad (2.64)$$

where $i, j = 1, 2, \dots, 6$. This completes the solution method of the problem under consideration.

3. GENERALIZED RAYLEIGH WAVE DISPERSION ANALYSIS IN A PRE-STRESSED ELASTIC STRATIFIED HALF-SPACE WITH IMPERFECTLY BONDED INTERFACES

3.1 Formulation of The Problem

The geometry of the problem is shown in Figure 3.1. It is assumed that the half-plane covered by the layer with thickness h . In the natural state we determine the positions of the points by the Lagrangian coordinates which coincide with the Cartesian system of coordinates $Ox_1x_2x_3$. The layer and the half-plane occupy the regions $\{-\infty < x_1 < +\infty, 0 \leq x_2 \leq h, -\infty < x_3 < +\infty\}$ and $\{-\infty < x_1 < +\infty, -\infty < x_2 \leq 0, -\infty < x_3 < +\infty\}$, respectively. Note that the following notation will be used through the formulations: the values related to the layer and half-plane are denoted by upper indices (1) and (2) respectively and the values related to the initial (or residual stresses) are denoted by upper indices (m) , 0 where $m = 1, 2$. We consider the case where initial stresses in the layer and half-plane are determined as follows:

$$\sigma_{11}^{(m),0} = \text{const}_m \neq 0, \quad m = 1, 2, \quad \sigma_{ij}^{(m),0} = 0, \quad \text{for } i = j \neq 1. \quad (3.1)$$

All investigations in the present paper are made in the framework of the second version of the small initial deformation theory of the TLTEWISB in the plane strain state in the plane.

According to Guz (2004), the equations of motion for the considered case are written as:

$$\begin{aligned} \frac{\partial \sigma_{11}^{(m)}}{\partial x_1} + \frac{\partial \sigma_{12}^{(m)}}{\partial x_2} + \sigma_{11}^{(m),0} \frac{\partial^2 u_1^{(m)}}{\partial x_1^2} &= \rho^{(m)} \frac{\partial^2 u_1^{(m)}}{\partial t^2}, \\ \frac{\partial \sigma_{12}^{(m)}}{\partial x_1} + \frac{\partial \sigma_{22}^{(m)}}{\partial x_2} + \sigma_{11}^{(m),0} \frac{\partial^2 u_2^{(m)}}{\partial x_1^2} &= \rho^{(m)} \frac{\partial^2 u_2^{(m)}}{\partial t^2}. \end{aligned} \quad (3.2)$$

In (3.2) the conventional notation is used. We assume that the following boundary conditions on the free face plane of the covering layer satisfy:

$$\sigma_{12}^{(1)} \Big|_{x_2=h} = 0, \quad \sigma_{22}^{(1)} \Big|_{x_2=h} = 0. \quad (3.3)$$

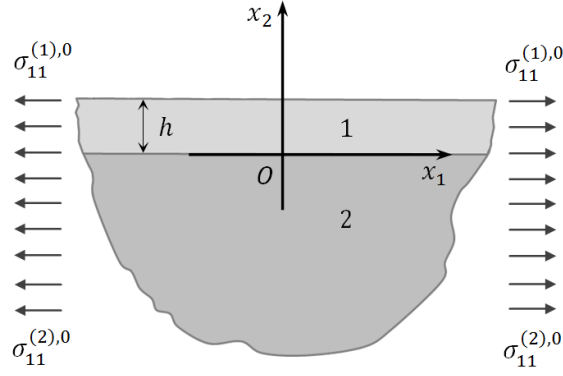


Figure 3.1: The geometry of the considered stratified half-plane.

Now we consider the formulation of the imperfect contact conditions on the interface plane between the covering layer and half-plane. It should be noted that, in general, the imperfectness of the contact conditions is identified by discontinuities of the displacements and forces across the mentioned interface. A review of the mathematical modeling of the various types of incomplete contact conditions for elastodynamics problems has been detailed in a paper by Martin (1992). It follows from this paper that for most models the discontinuity of the displacement \mathbf{u}^+ and force \mathbf{f}^+ vectors on one side of the interface are assumed to be linearly related to the displacement \mathbf{u}^- and force \mathbf{f}^- vectors on the other side of the interface. This statement, as in the paper by Rokhlin and Wang (1991), can be presented as follows:

$$[\mathbf{f}] = \mathbf{C}\mathbf{u}^- + \mathbf{D}\mathbf{f}^-, \quad [\mathbf{u}] = \mathbf{G}\mathbf{u}^- + \mathbf{F}\mathbf{f}^-, \quad (3.4)$$

where \mathbf{C} , \mathbf{D} , \mathbf{G} and \mathbf{F} are three-dimensional (3×3) matrices and the square brackets indicate a jump in the corresponding quantity across the interface. Consequently, if the interface is at say $x_2 = 0$, then:

$$[\mathbf{u}] = \mathbf{u}|_{x_2=0^+} - \mathbf{u}|_{x_2=0^-}, \quad [\mathbf{f}] = \mathbf{f}|_{x_2=0^+} - \mathbf{f}|_{x_2=0^-}.$$

It follows from (3.4) that we can write incomplete contact conditions for various particular cases by selection of the matrices \mathbf{C} , \mathbf{D} , \mathbf{G} and \mathbf{F} . One such selection was made in the paper by Jones and Whitter (1967), according to which, it was assumed that $\mathbf{C} = \mathbf{D} = \mathbf{G} = \mathbf{0}$. In this case the following can be obtained from (3.4):

$$[\mathbf{f}] = \mathbf{0}, \quad [\mathbf{u}] = \mathbf{F}\mathbf{f}^-, \quad (3.5)$$

where \mathbf{F} is a constant diagonal matrix. The model (3.5) simplifies significantly the solution procedure of the corresponding problems and is adequate in many real cases. Therefore, this model i.e. the model (3.5) is called a shear-spring type resistance model and has been used in many investigations carried out within the framework of classical elastodynamics by Jones and Whitter (1967), Berger; Martin and McCaffery (2000), and within the framework of the TLTEWISB by Kepceler (2010) and by Akbarov and Ipek (2010, 2012). According to this statement, we also use the model (3.5) for the mathematical formulation of the imperfectness of the contact conditions and these conditions are written as follows:

$$\begin{aligned}\sigma_{i2}^{(1)}|_{x_2=0} &= \sigma_{i2}^{(2)}|_{x_2=0}, \quad i = 1, 2, \\ u_2^{(1)}|_{x_2=0} &= u_2^{(2)}|_{x_2=0}, \\ u_1^{(1)}|_{x_2=0} - u_1^{(2)}|_{x_2=0} &= F \frac{h}{\mu^{(1)}} \sigma_{12}^{(1)}|_{x_2=0}, \quad F > 0,\end{aligned}\tag{3.6}$$

where F is the non-dimensional shear spring parameter and $0 \leq F \leq \infty$. Note that the case where $F = 0$ means that the displacement component across the interface is continuous and therefore the half-space and covering layer are perfectly bonded together or to say that they are in welded contact condition. At the other extreme, $F = \infty$ implies that the half-space and covering layer are completely unbounded together and the full slipping condition is satisfied. Thus, any other finite positive values of F expresses different imperfect interface conditions in the problem.

Moreover, we assume that the following decay conditions are satisfied:

$$\sigma_{ij}^{(2)} \Big|_{x_2 \rightarrow -\infty} \rightarrow 0, \quad u_i^{(2)} \Big|_{x_2 \rightarrow -\infty} \rightarrow 0, \quad i = 1, 2.\tag{3.7}$$

As stated above, we assume that the constitutive relations of the materials of the constituents are given by the Murnaghan potential which is given as follows Guz (2004):

$$\Phi^{(m)} = \frac{1}{2} \lambda^{(m)} \left(A_1^{(m)} \right)^2 + \mu^{(m)} A_2^{(m)} + \frac{a^{(m)}}{3} \left(A_1^{(m)} \right)^3 + b^{(m)} A_1^{(m)} A_2^{(m)} + \frac{c^{(m)}}{3} A_3^{(m)}, \tag{3.8}$$

where $\lambda^{(m)}$ and $\mu^{(m)}$ are Lamé's and $a^{(m)}$, $b^{(m)}$ and $c^{(m)}$ are the third order elasticity constants. Here $A_1^{(m)}$, $A_2^{(m)}$ and $A_3^{(m)}$ are the first, second and the third algebraic

invariants of Green's strain tensor respectively. For the case under consideration, the expressions of these invariants are:

$$\begin{aligned} A_1^{(m)} &= \varepsilon_{11}^{(m)} + \varepsilon_{22}^{(m)}, \\ A_2^{(m)} &= \left(\varepsilon_{11}^{(m)}\right)^2 + 2\left(\varepsilon_{12}^{(m)}\right)^2 + \left(\varepsilon_{22}^{(m)}\right)^2, \\ A_3^{(m)} &= \left(\varepsilon_{11}^{(m)}\right)^3 + 3\left(\varepsilon_{12}^{(m)}\right)^2 \left(\varepsilon_{11}^{(m)} + \varepsilon_{22}^{(m)}\right) + \left(\varepsilon_{22}^{(m)}\right)^3, \end{aligned} \quad (3.9)$$

where

$$\varepsilon_{ij}^{(m)} = \frac{1}{2} \left(\frac{\partial u_i^{(m)}}{\partial x_j} + \frac{\partial u_j^{(m)}}{\partial x_i} \right). \quad (3.10)$$

According to Guz (2004), linearized constitutive relations for the layer and half-plane materials are obtained in the following form:

$$\begin{aligned} \sigma_{11}^{(m)} &= A_{11}^{(m)} \varepsilon_{11}^{(m)} + A_{12}^{(m)} \varepsilon_{22}^{(m)}, \\ \sigma_{22}^{(m)} &= A_{12}^{(m)} \varepsilon_{11}^{(m)} + A_{22}^{(m)} \varepsilon_{22}^{(m)}, \\ \sigma_{12}^{(m)} &= 2\mu_{12}^{(m)} \varepsilon_{12}^{(m)}, \end{aligned} \quad (3.11)$$

where

$$\begin{aligned} A_{11}^{(m)} &= \lambda^{(m)} + 2\mu^{(m)} + \frac{\sigma_{11}^{(m),0}}{\mu^{(m)}} \left(2b^{(m)} + c^{(m)} \right) \\ &\quad + \frac{2\sigma_{11}^{(m),0}}{3K_0^{(m)}} \left[\left(a^{(m)} + b^{(m)} \right) - \left(2b^{(m)} + c^{(m)} \right) \frac{\lambda^{(m)}}{2\mu^{(m)}} \right], \\ A_{22}^{(m)} &= \lambda^{(m)} + 2\mu^{(m)} + \frac{2\sigma_{11}^{(m),0}}{3K_0^{(m)}} \left[\left(a^{(m)} + b^{(m)} \right) - \left(2b^{(m)} + c^{(m)} \right) \frac{\lambda^{(m)}}{2\mu^{(m)}} \right], \\ A_{12}^{(m)} &= \lambda^{(m)} + \frac{b^{(m)}}{\mu^{(m)}} \sigma_{11}^{(m),0} + \frac{2\sigma_{11}^{(m),0}}{3K_0^{(m)}} \left[a^{(m)} - b^{(m)} \frac{\lambda^{(m)}}{\mu^{(m)}} \right], \\ \mu_{12}^{(m)} &= \mu^{(m)} + \frac{b^{(m)}}{3K_0^{(m)}} \sigma_{11}^{(m),0} + \frac{c^{(m)} \sigma_{11}^{(m),0}}{4\mu^{(m)}} \left[\frac{\lambda^{(m)} + 2\mu^{(m)}}{3K_0^{(m)}} \right], \\ K_0^{(m)} &= \lambda^{(m)} + \frac{2\mu^{(m)}}{3}. \end{aligned} \quad (3.12)$$

This completes the formulation of the problem and in the case where $\sigma_{11}^{(1),0} = \sigma_{11}^{(2),0} = 0$ this formulation transforms to the corresponding one made within the scope of the classical linear theory of elastodynamics.

3.2 Solution Procedure and Obtaining The Dispersion Relation

Each displacements component of the considered system are represent as follows:

$$\begin{aligned} u_1^{(m)} &= \varphi_1^{(m)}(x_2) \sin(kx_1 - \omega t), \\ u_2^{(m)} &= \varphi_2^{(m)}(x_2) \cos(kx_1 - \omega t). \end{aligned} \quad (3.13)$$

This way we obtain the following equations for the $\varphi_1^{(m)}(x_2)$ and $\varphi_2^{(m)}(x_2)$ from the equations (3.1), (3.2), (3.11)–(3.13),

$$\begin{aligned} \frac{d^2 \varphi_1^{(m)}}{d(kx_2)^2} + b_{21}^{(m)} \varphi_1^{(m)} + c_{21}^{(m)} \frac{d \varphi_2^{(m)}}{d(kx_2)} &= 0, \\ \frac{d^2 \varphi_2^{(m)}}{d(kx_2)^2} + b_{22}^{(m)} \varphi_2^{(m)} + c_{22}^{(m)} \frac{d \varphi_1^{(m)}}{d(kx_2)} &= 0, \end{aligned} \quad (3.14)$$

where

$$\begin{aligned} b_{21}^{(m)} &= -\frac{A_{11}^{(m)}}{\mu_{12}^{(m)}} - \frac{\sigma_{11}^{(m),0}}{\mu_{12}^{(m)}} + \frac{\rho^{(m)} \omega^2}{\mu_{12}^{(m)} k^2}, \quad c_{21}^{(m)} = \frac{-A_{12}^{(m)} - \mu_{12}^{(m)}}{\mu_{12}^{(m)}}, \\ b_{22}^{(m)} &= -\frac{\mu_{12}^{(m)}}{A_{22}^{(m)}} - \frac{\sigma_{11}^{(m),0}}{A_{22}^{(m)}} + \frac{\rho^{(m)} \omega^2}{A_{22}^{(m)} k^2}, \quad c_{22}^{(m)} = \frac{\mu_{12}^{(m)} + A_{12}^{(m)}}{A_{22}^{(m)}}. \end{aligned} \quad (3.15)$$

We can solve the system (3.14) using linear operator method as follows:

$$\begin{aligned} \left(D^2 + b_{21}^{(m)} \right) \varphi_1^{(m)} + c_{21}^{(m)} D \varphi_2^{(m)} &= 0, \\ c_{22}^{(m)} D \varphi_1^{(m)} + \left(D^2 + b_{22}^{(m)} \right) \varphi_2^{(m)} &= 0, \end{aligned} \quad (3.16)$$

or in matrix form as:

$$\begin{bmatrix} D^2 + b_{21}^{(m)} & c_{21}^{(m)} D \\ c_{22}^{(m)} D & D^2 + b_{22}^{(m)} \end{bmatrix} \begin{bmatrix} \varphi_1^{(m)} \\ \varphi_2^{(m)} \end{bmatrix} = \begin{bmatrix} 0 \\ 0 \end{bmatrix}, \quad (3.17)$$

where D is the differentiation operator: $D = d/d(kx_2)$. This homogeneous system (3.17) has non-trivial solution only when the determinant of operational matrix be zero, that is:

$$\left(D^2 + b_{21}^{(m)} \right) \left(D^2 + b_{22}^{(m)} \right) - c_{21}^{(m)} c_{22}^{(m)} D^2 = 0,$$

or

$$D^4 + B_2^{(m)} D^2 + C_2^{(m)} = 0, \quad (3.18)$$

where

$$B_2^{(m)} = b_{22}^{(m)} + b_{21}^{(m)} - c_{21}^{(m)} c_{22}^{(m)}, \quad C_2^{(m)} = b_{21}^{(m)} b_{22}^{(m)}. \quad (3.19)$$

Therefore we derive the following differential equation for $\phi_2^{(m)}(x_2)$:

$$\left(D^4 + B_2^{(m)}D^2 + C_2^{(m)}\right)\phi_2^{(m)}(x_2) = 0. \quad (3.20)$$

We determine the solution of (3.20) as follows:

$$\begin{aligned} \phi_2^{(1)}(x_2) &= Z_1^{(1)}\exp\left(R_1^{(1)}kx_2\right) + Z_2^{(1)}\exp\left(-R_1^{(1)}kx_2\right) \\ &\quad + Z_3^{(1)}\exp\left(R_2^{(1)}kx_2\right) + Z_4^{(1)}\exp\left(-R_2^{(1)}kx_2\right), \\ \phi_2^{(2)}(x_2) &= Z_1^{(2)}\exp\left(R_1^{(2)}kx_2\right) + Z_3^{(2)}\exp\left(R_2^{(2)}kx_2\right), \end{aligned} \quad (3.21)$$

where

$$R_1^{(m)} = \sqrt{-\frac{B_2^{(m)}}{2} + \sqrt{\frac{(B_2^{(m)})^2}{4} - C_2^{(m)}}}, \quad R_2^{(m)} = \sqrt{-\frac{B_2^{(m)}}{2} - \sqrt{\frac{(B_2^{(m)})^2}{4} - C_2^{(m)}}}. \quad (3.22)$$

In a similar way using (3.22) we can also determine the function $\phi_1^{(m)}(x_2)$ from (3.16).

Finally, we obtain the dispersion equation considering the conditions (3.3)–(3.7). This dispersion equation after some mathematical manipulations can be expressed formally as follows:

$$\det\left\|\alpha_{ij}\left(c, kh, F, \sigma_{11}^{(1),0}, \sigma_{11}^{(2),0}, a^{(1)}, b^{(1)}, c^{(1)}, a^{(2)}, b^{(2)}, c^{(2)}\right)\right\| = 0, \quad (3.23)$$

where $i, j = 1, 2, \dots, 6$ and

$$c = \frac{\omega}{k}, \quad c_1^{(m)} = \sqrt{\frac{\lambda^{(m)} + 2\mu^{(m)}}{\rho^{(m)}}}, \quad c_2^{(m)} = \sqrt{\frac{\mu^{(m)}}{\rho^{(m)}}}. \quad (3.24)$$

The explicit expressions of the α_{ij} ($i, j = 1, 2, \dots, 6$) in the dispersion equation (3.23) are given in Appendix A.1. This completes the solution method of the problem under consideration.

3.3 Numerical Results and Discussion

We will assume that,

$$\operatorname{Re}R_1^{(1)} = \operatorname{Re}R_2^{(1)} = 0, \quad R_1^{(2)} > 0, \quad R_2^{(2)} > 0. \quad (3.25)$$

In this case, the solution (3.21) corresponds to such a wave propagation in the layered half-plane that the layer undergoes an oscillatory motion in the Ox_2 direction

propagating in the Ox_1 direction with velocity c . The disturbances in the layer decay exponentially with depth in the half-plane and therefore the wave can be considered as a generalized Rayleigh wave confined to the pre-stressed covered layer (Tolstoy and Usdin, 1953).

First we consider the numerical results for the case where $\sigma_{11}^{(1),0} = \sigma_{11}^{(2),0} = 0$, i.e. for the case where initial stresses in the constituents are absent. We recall that this case for the Poisson material has been discussed by Tolstoy and Usdin (1953) and also discussed in the monograph by Eringen and Suhubi (1975). It was established by Tolstoy and Usdin (1953) that the dispersion equation (3.23) has infinitely many modes unlike ordinary Rayleigh waves, which can propagate only in one mode. Moreover, the dispersion curves related to each mode has two branches which were denoted by M_{1n} and M_{2n} respectively for the n -th mode. For the first M_{1n} branch the displacement of the layer circumscribes the ellipse similar to the ordinary Rayleigh waves, but for the second M_{2n} branch leads to an opposite type of motion. As noted above, numerical results are given by Tolstoy and Usdin (1953) for the Poisson materials, i.e. for the case where $\lambda^{(1)} = \mu^{(1)}$, $\lambda^{(2)} = \mu^{(2)}$ (it is assumed that $\nu^{(1)} = \nu^{(2)} = 0.25$, where $\nu^{(m)}$ is Poisson's coefficient), under $c_1^{(1)}/c_2^{(1)} = c_1^{(2)}/c_2^{(2)} = \sqrt{3}$, $c_2^{(2)}/c_2^{(1)} = 3.147$, $\rho^{(2)}/\rho^{(1)} = 1.374$ (where $\rho^{(m)}$ is the density of the m -th material). After programming of (3.23), the above mentioned case (Poisson materials) was considered first in our numerical studies. Figure 3.2 shows the dependencies (dispersion curves) between $\bar{c}(= 3.147c/c_2^{(2)})$ and kh for different values of shear spring parameter F . In this figure the graphs denoted by M_{11} and M_{12} (Figure 3.2a) correspond respectively to the first and second branch of the first mode, whereas the graphs denoted by M_{21} and M_{22} (Figure 3.2b) correspond to the first and second branch of the second mode. It should be noted that the graphs denoted by M_{11} , M_{21} , M_{12} and M_{22} and obtained for the case where $F = 0$ (i.e. for the case where the contact between the constituents is perfect) coincide with the corresponding ones given in the paper by Tolstoy and Usdin (1953). This situation gives a certain guarantee on the correctness of the algorithm-programs constructed for the numerical solution to the dispersion equation (3.23).

We also, consider similar results obtained for some pairs of the real materials. Values of the mechanical constants of these materials are given in Table 3.1 (i.e. the values of

Table 3.1: The values of elastic constants of the selected materials (Guz ,2004).

Materials	ρ (g/cm ³)	$\lambda \times 10^{-4}$ (MPa)	$\mu \times 10^{-4}$ (MPa)	$a \times 10^{-5}$ (MPa)	$b \times 10^{-5}$ (MPa)	$c \times 10^{-5}$ (MPa)
Steel 3	7.795	9.26	7.75	-2.35	-2.75	-4.90
Bronze	7.20	8.16	3.84	1.20	-3.10	4.80
Brass 59-1	7.20	9.49	4.47	-0.70	2.70	-3.40
Brass 62	7.20	9.49	4.47	-2.80	-2.10	-3.20
Plexiglas	1.16	0.404	0.19	2.68×10^{-3}	-3.12×10^{-2}	-6.77×10^{-2}

the mechanical constants which enter the expression (3.8) of the Murnaghan potential). We select four pairs from these materials. For the *I*, *II*, *III* and *IV* pairs, the material of the covering layer we take as *bronze*, *brass 59-1*, *brass 62* and *plexsiglas* respectively, but for all the pairs the material of the half-plane we take as *steel*. The graphs related to the foregoing pairs are given in Figure 3.3 (for the *I* pair), Figure 3.4 (for the pairs *II* and *III*) and Figure 3.5 (for the pair *IV*). It should be noted that, the results given in these figures and obtained for the case where $F = 0$ coincide with corresponding results obtained in the paper by Akbarov and Ozisik (2003).

It should be noted that, according to the expressions (3.11) and (3.12), as under calculation of the foregoing results it is assumed that $\sigma_{11}^{(1),0} = \sigma_{11}^{(2),0} = 0$, therefore the third order of elastic constants of the selected materials do not influence on these results.

Thus the dispersion curves obtained for the pairs *II* and *III* coincide because, according to the data given in Table 3.1, the constants ρ , λ and μ are the same for *brass 59-1* and *brass 62* (Figure 3.4). Moreover note that, for clarity of the illustration the first and second modes of the graphs obtained for the *IV* pair are given separately in Figure 3.5a and Figure 3.5b, respectively.

Now we analyze the foregoing numerical results which are obtained within the framework of the restriction (3.25). According to this restriction, it must be $c/c_2^{(2)} < 1$ and $c/c_1^{(1)} > 1$, i.e. the near-surface waves propagated in the system under consideration is subsonic in the half-plane, but it is supersonic in the covering layer. Thus, it follows from Figures 3.2, 3.3, 3.4 and 3.5 that the dimensionless wavenumber kh has cut off values for the second branch of the first mode, the first and second branches of the second mode. We denote these cut of values through $(kh)_{cf21}^P$, $(kh)_{cf12}^P$,

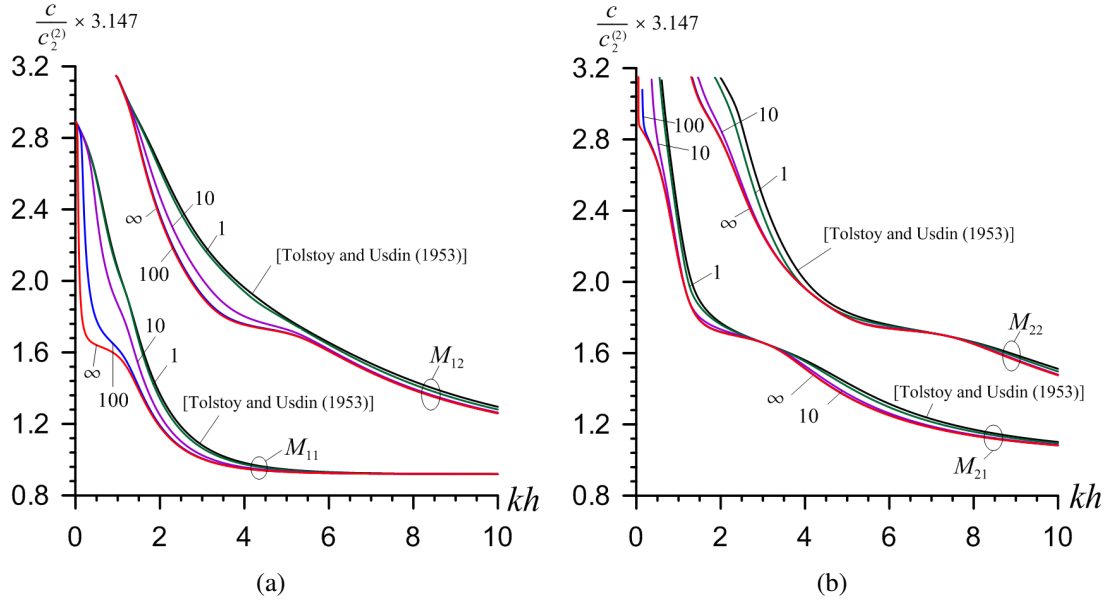


Figure 3.2: Dispersion curves for Poisson material (Tolstoy and Usdin, 1953): First and second branches of the first (a) and the second (b) modes.

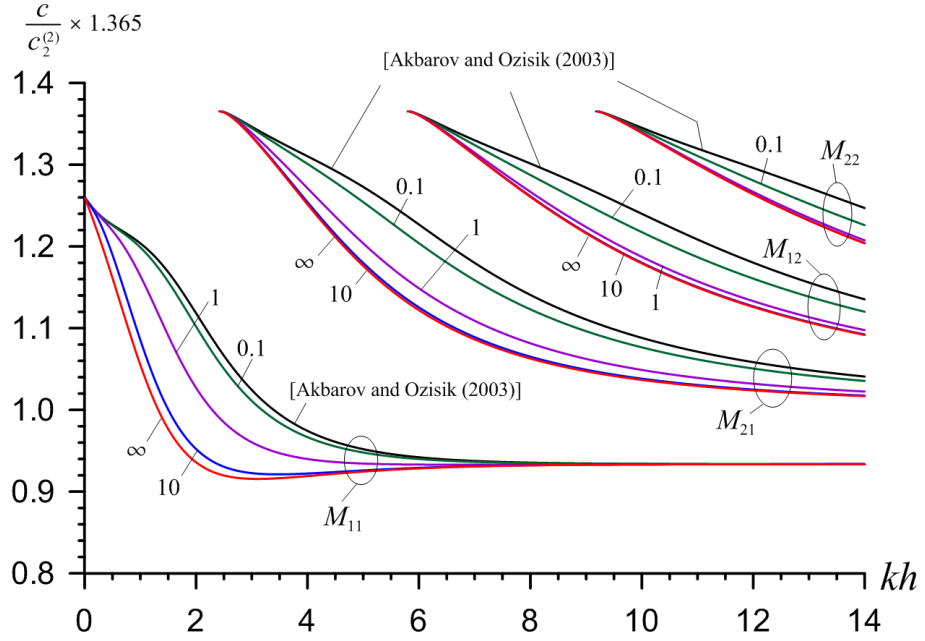


Figure 3.3: Dispersion curves for the I pair of materials.

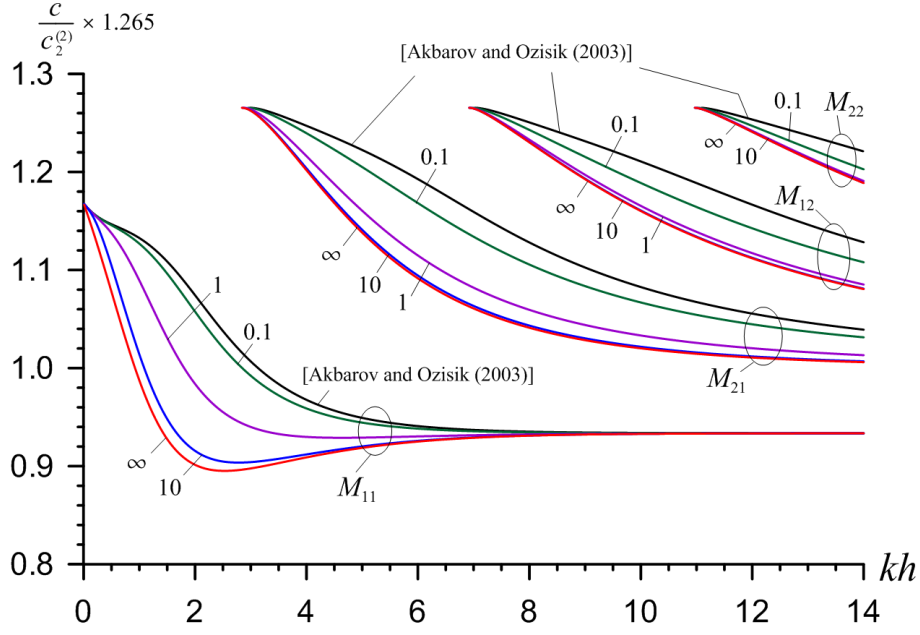


Figure 3.4: Dispersion curves for the *II* and *III* pair of materials.

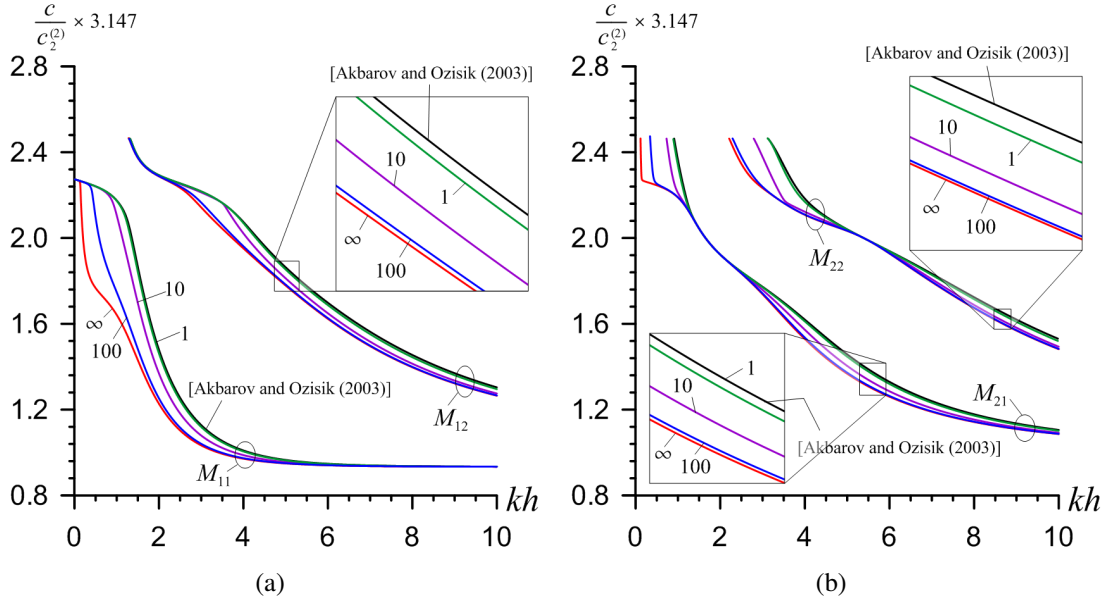


Figure 3.5: Dispersion curves for the *IV* pair of materials: The first and the second branches of the first (a) and the second (b) modes.

$(kh)_{cf22}^P$ or the pair of materials selected by Tolstoy and Usdin (1953) (Figure 3.2), through $(kh)_{cf21}^I, (kh)_{cf12}^I, (kh)_{cf22}^I$ for the I pair of materials (Figure 3.3), through $(kh)_{cf21}^{II}, (kh)_{cf12}^{II}, (kh)_{cf22}^{II}$ for the II pair of materials (Figure 3.4) and through $(kh)_{cf21}^{IV}, (kh)_{cf12}^{IV}, (kh)_{cf22}^{IV}$ for the IV pair of materials (Figure 3.5). Moreover, we introduce the notation $c_{11}^P, c_{21}^P (c_{12}^P, c_{22}^P)$ for the pair of materials selected by Tolstoy and Usdin (1953), $c_{11}^I, c_{21}^I (c_{12}^I, c_{22}^I)$ for the I pair of materials; $c_{11}^{II}, c_{21}^{II} (c_{12}^{II}, c_{22}^{II})$ for the II pair of materials and $c_{11}^{IV}, c_{21}^{IV} (c_{12}^{IV}, c_{22}^{IV})$ for the IV pair of materials for indication of the wave propagation velocity related to the first (second) branches of the first and the second modes.

According to the foregoing results, we can conclude that the imperfectness between the constituents causes to decrease of the wave propagation velocity of the all above-noted branches and modes. In this cases values of the velocity decrease monotonically with the shear-spring parameter F . This conclusion can be explained with the fact that the shear wave propagation velocity $c_2 = \sqrt{\mu/\rho}$ of the half-plane material (i.e. of the steel) is greater than that of the covering layer materials for the all considered pairs. Therefore the complete contact of the covering layer with the half-plane made of the steel makes the system under consideration more suitable ones for high wave propagation velocity.

We analyze the influence of the imperfectness of the contact conditions, i.e. the influence of the shear-spring type parameter F on the low and high wavenumber limit values of the wave propagation velocities of the first branch of the first mode. The foregoing results show that the low wavenumber limit values of the wave propagation velocity related to the first branches of the first mode obtained for the all pairs of materials denoted by $c_{11L}^P, c_{11L}^I, c_{11L}^{II}$ and c_{11L}^{IV} , and determined from the relations:

$$c_{11}^P \rightarrow c_{11L}^P, \quad c_{11}^I \rightarrow c_{11L}^I, \quad c_{11}^{II} \rightarrow c_{11L}^{II}, \quad c_{11}^{IV} \rightarrow c_{11L}^{IV} \text{ as } kh \rightarrow 0, \quad (3.26)$$

do not depend on the shear-spring type parameter F . At the same time, the foregoing results show that the wave propagation velocities related to the second branch of the first mode and the first and second branches of the second mode approach to the $c_2^{(2)}$ as the dimensionless wavenumber kh approach to its corresponding cut off values, i.e.

$$c_{12}^P \rightarrow c_2^{(2)} \text{ as } kh \rightarrow (kh)_{cf12}^P, \quad c_{12}^I \rightarrow c_2^{(2)} \text{ as } kh \rightarrow (kh)_{cf12}^I,$$

$$\begin{aligned}
c_{12}^{II} &\rightarrow c_2^{(2)} \text{ as } kh \rightarrow (kh)_{cf12}^{II}, & c_{12}^{IV} &\rightarrow c_2^{(2)} \text{ as } kh \rightarrow (kh)_{cf12}^{IV}, \\
c_{2n}^P &\rightarrow c_2^{(2)} \text{ as } kh \rightarrow (kh)_{cf2n}^P, & c_{2n}^I &\rightarrow c_2^{(2)} \text{ as } kh \rightarrow (kh)_{cf2n}^I, \\
c_{2n}^{II} &\rightarrow c_2^{(2)} \text{ as } kh \rightarrow (kh)_{cf2n}^{II}, & c_{2n}^{IV} &\rightarrow c_2^{(2)} \text{ as } kh \rightarrow (kh)_{cf2n}^{IV},
\end{aligned} \tag{3.27}$$

where $n = 1, 2$. In this cases the cut of values $(kh)_{cf12}^P$, $(kh)_{cf12}^I$, $(kh)_{cf2n}^I$ and $(kh)_{cf2n}^{II}$ do not depend on the parameter F , but cut off values $(kh)_{cf12}^{II}$, $(kh)_{cf12}^{IV}$, $(kh)_{cf2n}^P$ and $(kh)_{cf2n}^{IV}$ depend significantly on F and an increase in the values of the parameter F causes to decrease in the values of the $(kh)_{cf12}^{II}$, $(kh)_{cf12}^{IV}$, $(kh)_{cf2n}^P$ and $(kh)_{cf2n}^{IV}$. According to the well-known physical considerations, for the wave propagation velocity related to the first branch of the first mode of each pair of materials the following high wavenumber limit relation:

$$c \rightarrow \min \left(c_R^{(1)}, c_S \right), \text{ as } kh \rightarrow \infty \tag{3.28}$$

must satisfy, where $c_R^{(1)}$ is a velocity of the Rayleigh wave in the covering layer material, c_S is a velocity of the Stonoley wave for the corresponding pair of materials. It is known that the Stoneley waves exist for a few pairs of materials only and do not exist for the pairs of materials selected in the present investigation. This conclusion follows from nature of the problem under consideration. Consequently, the high wavenumber limit value of the wave propagation velocity related to the first branch of the first mode of each pair of materials is $c_R^{(1)}$. This conclusion is illustrated in Figure 3.6 for the pair of materials.

Moreover, the results illustrated in Figure 3.6 and other numerical results which are not given here show that the second branch of the first mode, the first and second branches of the second mode have the same high wavenumber limit value and this limit value is $c_2^{(1)}$. It follows from the foregoing discussions that, the high wavenumber limit values of the wave propagation velocities do not depend also on the parameter F . This and foregoing conclusions in the qualitative sense agree with corresponding ones obtained in works by Berger; Martin and McCaffery (2000), Kepceler (2010), Akbarov and Ipek (2010, 2012). Finally, we note the following consideration which follows from the results illustrated in Figure 3.3 and Figure 3.4. In the cases where $F \geq 10$ the dispersion curves obtained for the I and II pairs of materials have a point $kh = (kh)_*$

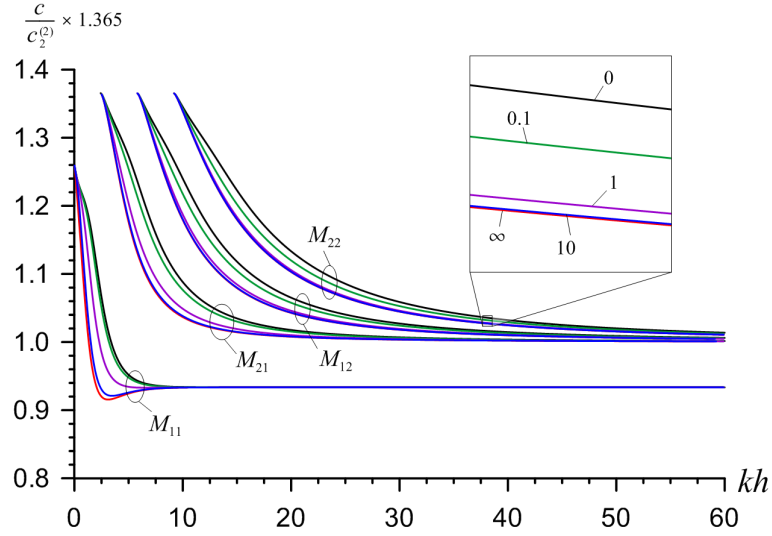


Figure 3.6: Asymptotic behavior of the dispersion curves for the *I* pair the materials as $kh \rightarrow \infty$.

($0 < (kh)_* < \infty$) at which:

$$\frac{dc}{d(kh)} = 0. \quad (3.29)$$

It is known that (see, Achenbach; Keshava and Hermann (1967), Akbarov and Ilhan (2008, 2009), Akbarov and Salmanova (2009) and others listed therein) velocities related to the case (3.29) is taken as a critical velocity for a moving load acting on the free face plane of the covering layer and under this velocity of the moving load a resonance type behavior of the system takes place. Moreover, at $kh = (kh)_*$ for which the relation (3.29) satisfies the group velocity becomes equal to the corresponding phase velocity and namely the velocity of the moving load which is equal to the group velocity is also called a critical velocity (see, Dieterman and Metrikine, 1997).

According to investigations carried out by Achenbach; Keshava and Hermann (1967), Akbarov and Ilhan (2008, 2009), Akbarov and Salmanova (2009) and other ones listed therein, under perfect contact between the constituents the foregoing type situation, i.e. the existence of the critical velocity of the mentioned moving load takes place in the cases where $c_2^{(1)}$ (shear wave velocity in the covering layer material) is greater than $c_2^{(2)}$ (shear wave velocity in the half-plane material) only. However, in the present case, i.e. in the case where the contact between the covering layer and half-plane is imperfect, the critical velocity may arise also in the cases where $c_2^{(1)} < c_2^{(2)}$. Consequently, the shear-spring type imperfectness between the constituents can acts on the dispersion

curves and, in general, on the dynamics of the system under consideration not only quantitatively, but also qualitatively.

Now we analyze the numerical results related to the influence of the initial stresses in the constituents on the wave propagation velocity. For estimation of the magnitude of the initial stresses we introduce the parameters:

$$\psi^{(1)} = \sigma_{11}^{(1),0}/\mu^{(1)}, \quad \psi^{(2)} = \sigma_{11}^{(2),0}/\mu^{(2)}. \quad (3.30)$$

Here we will present the results only for cases:

$$\begin{aligned} \text{Case 1.} \quad & \psi^{(1)} > 0, \quad \psi^{(2)} = 0; \\ \text{Case 2.} \quad & \psi^{(1)} = 0, \quad \psi^{(2)} < 0; \\ \text{Case 3.} \quad & \psi^{(1)} > 0, \quad \psi^{(2)} < 0; \\ \text{Case 4.} \quad & \psi^{(1)} > 0, \quad \psi^{(2)} > 0; \end{aligned} \quad (3.31)$$

Moreover, we introduce the notation:

$$\eta = \frac{c|_{\psi^{(1)} \neq 0; \text{ or } \psi^{(2)} \neq 0} - c|_{\psi^{(1)} = 0; \psi^{(2)} = 0}}{c|_{\psi^{(1)} = 0; \psi^{(2)} = 0}}, \quad (3.32)$$

for estimation of the influence of the initial stresses in the constituents, i.e. the influence of the parameters $\psi^{(1)}$ and $\psi^{(2)}$ on the wave propagation velocity.

Thus, through the graphs of the dependencies between η (3.32) and kh constructed for various values of the parameters F , $\psi^{(1)}$ and $\psi^{(2)}$ we analyze the effect of the imperfectness of the contact conditions between the covering layer and half-plane under the influence of the initial stresses in the constituents on the wave propagation velocity in the cases noted in (3.31). For the *I* and *III* pairs of materials in Case 1 these graphs are given in Figure 3.7 and Figure 3.8 respectively. Note that in these figures the graphs indicated by letters *a* and *c* (*b* and *d*) correspond to the first and second branches of the first (second) mode. Moreover, note that the results given in Figure 3.7 and Figure 3.8 and obtained in the case where $F = 0$ coincide with corresponding ones obtained in the paper by Akbarov and Ozisik (2003). The graphs show that for the *I* pair of the materials in Case 1 the initial stretching stress in the covering layer causes to increase the wave propagation velocity and in this case the values of $c/c_2^{(2)}$ increase

monotonically with $\psi^{(1)}$. Also, the graphs show that the wave propagation velocity related to the first branch of the first mode and to the second branch of the second mode increase monotonically with the parameter F . Consequently, the imperfectness of the contact conditions causes to increase the influence of the initial stress in the covering layer on the wave propagation velocity related to the first branch of the first mode and to the second branch of the second mode of the *I* pair of materials. However, the character of the effect of the imperfectness of the contact conditions, i.e. of the parameter F on the influence of the initial stress in the covering layer on the wave propagation velocity related to the second branch of the first mode and to the first branch of the second mode depends on the values of the dimensionless wavenumber kh . So, it follows from the Figure 3.7b and 3.7c that, before (after) a certain value of the kh , the imperfectness of the contact conditions causes to increase (decrease), the wave propagation velocity. Figure 3.8 shows that as a result of the initial stretching stress in the covering layer the wave propagation velocity related to the *III* pair of materials decreases. This conclusion was also noted in the paper by Akbarov and Ozisik (2003). In this case the imperfectness of the contact conditions, in general, causes to increase the wave propagation velocity related to the first branches of the first and the second modes. However, the imperfectness of the contact conditions before (after) a certain value of the kh causes to decrease (increase) the wave propagation velocity related to the second branches of the first and the second modes. At the same time, it should be noted that the influence of the parameter F on the graphs between η and kh which are shown in Figure 3.8, has a complicate character. For instance, in the cases where $0 < kh < 3.0$ the imperfectness of the contact conditions can cause to change the character of the influence of the initial stress in the covering layer on the wave propagation velocity related to the first branch of the first mode (Figure 3.8a). Moreover, the influence of the parameter F on the values η related to the first branch of the second mode (Figure 3.8b) is non-monotonic.

Now we analyze the effect of the imperfectness of the contact conditions on the influence of the initial compressional stress in the half-plane on the wave propagation velocity to the *II* (or *III*) and *IV* pairs of materials in Case 2. The graphs of the dependencies between η and kh related to the *II* (or *III*) and *IV* pairs of materials

and constructed for various values of the parameters F and $\psi^{(2)}$ are given in Figure 3.9 and Figure 3.10, respectively. Note that the graphs constructed in the case where $F = 0$ coincide with corresponding ones obtained in the paper by Akbarov and Ozisik (2003). It follows from the graphs given in Figure 3.9 and Figure 3.10 that as a result of the initial compression of the half-plane the wave propagation velocity related to the *II* (or *III*) and *IV* pairs of materials in Case 2 increase monotonically with the absolute values of the parameter $\psi^{(2)}$. In this case before (after) a certain value of the kh , the influence of the parameter F causes to increase (decrease) the wave propagation velocity related to the first branch of the first mode for the *II* pair of materials. At the same time, as a result of the influence of the parameter F the wave propagation velocities related to the second branch of the first mode, the first and second branches of the second mode of the *II* pair of materials decrease. The magnitude of this decreasing depends significantly on the values of the dimensionless wavenumber kh .

Analyses of the graphs given in Figures 3.10a, 3.10b and 3.10c show that the wave propagation velocity related to the first and second branches of the first mode and to the first branch of the second mode of the *IV* pair of materials decrease with the parameter F . However, the character of the influence of the parameter F on the wave propagation velocity related to the second branch of the second mode has a complicate character. This complication is also caused by decreasing of the cut off values of the kh with the parameter F . The similar situation also takes place for the first branch of the second mode. Consequently, the influence of the imperfectness of the contact conditions on the wave propagation velocities related to the first and second branch of the second mode has not only quantitative, but also qualitative character. Moreover, the graphs given in Figures 3.10b and 3.10d show that the results obtained for the first and second branch of the second mode for various values of the parameter F cannot be limited with the corresponding ones obtained in the cases where $F = 0$ (complete contact) and $F = \infty$ (full slipping). Note that this conclusion rises again the significance of the investigations carried out in the present study.

Now we consider the results obtained in Case 3 for the *II* pair of materials. These results are given in Figure 3.11 in the case where $\psi^{(2)} = -0.01$ for various values of the parameter $\psi^{(1)} (> 0)$. Note that the corresponding results obtained in the case

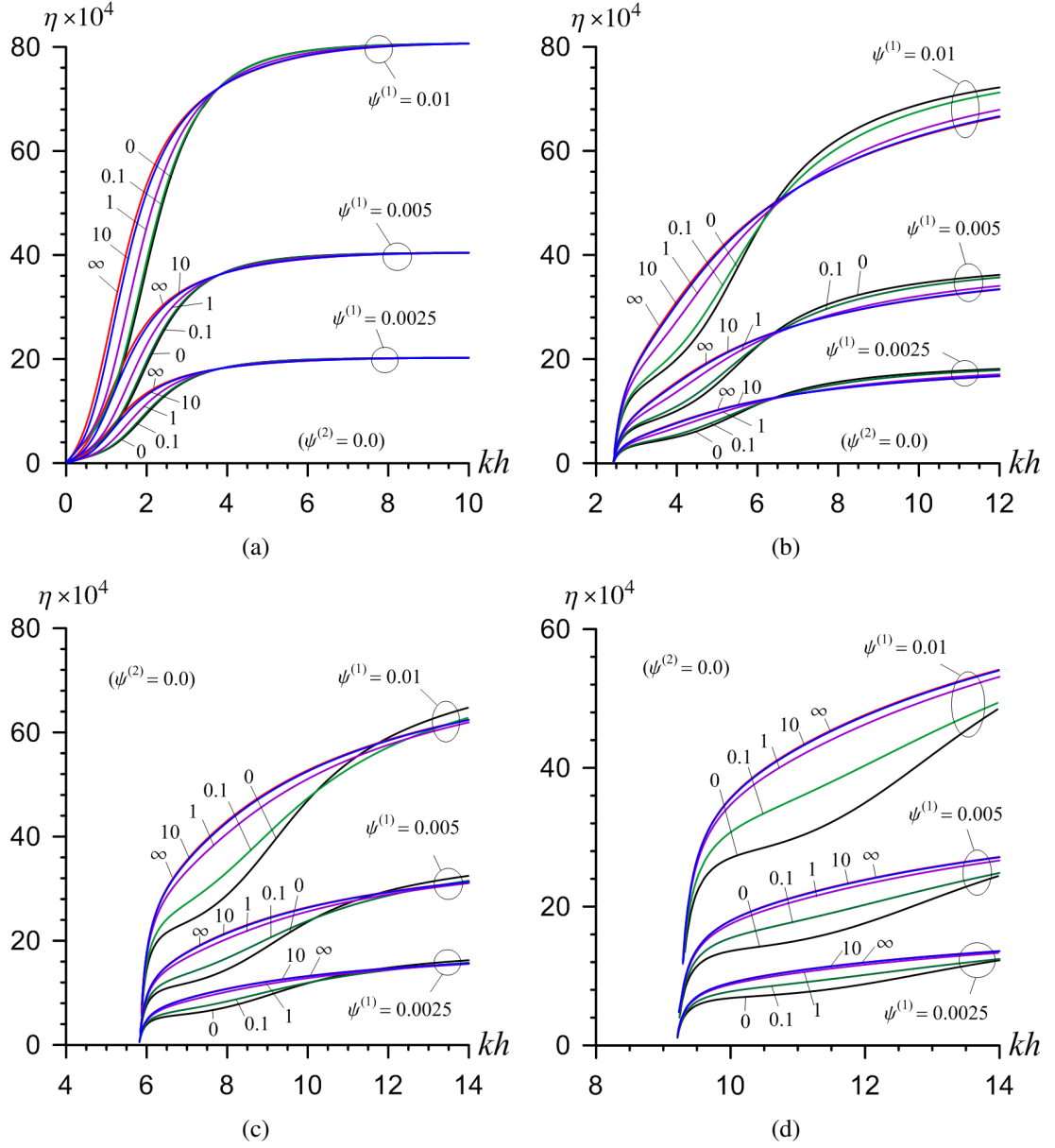


Figure 3.7: The influence of the imperfect bonding conditions and initial stresses to the dispersion of the generalized Rayleigh wave for the *I* pair of materials in Case 1: First (a) and second (b) branches of the first mode; First (c) and second (d) branches of the second mode.

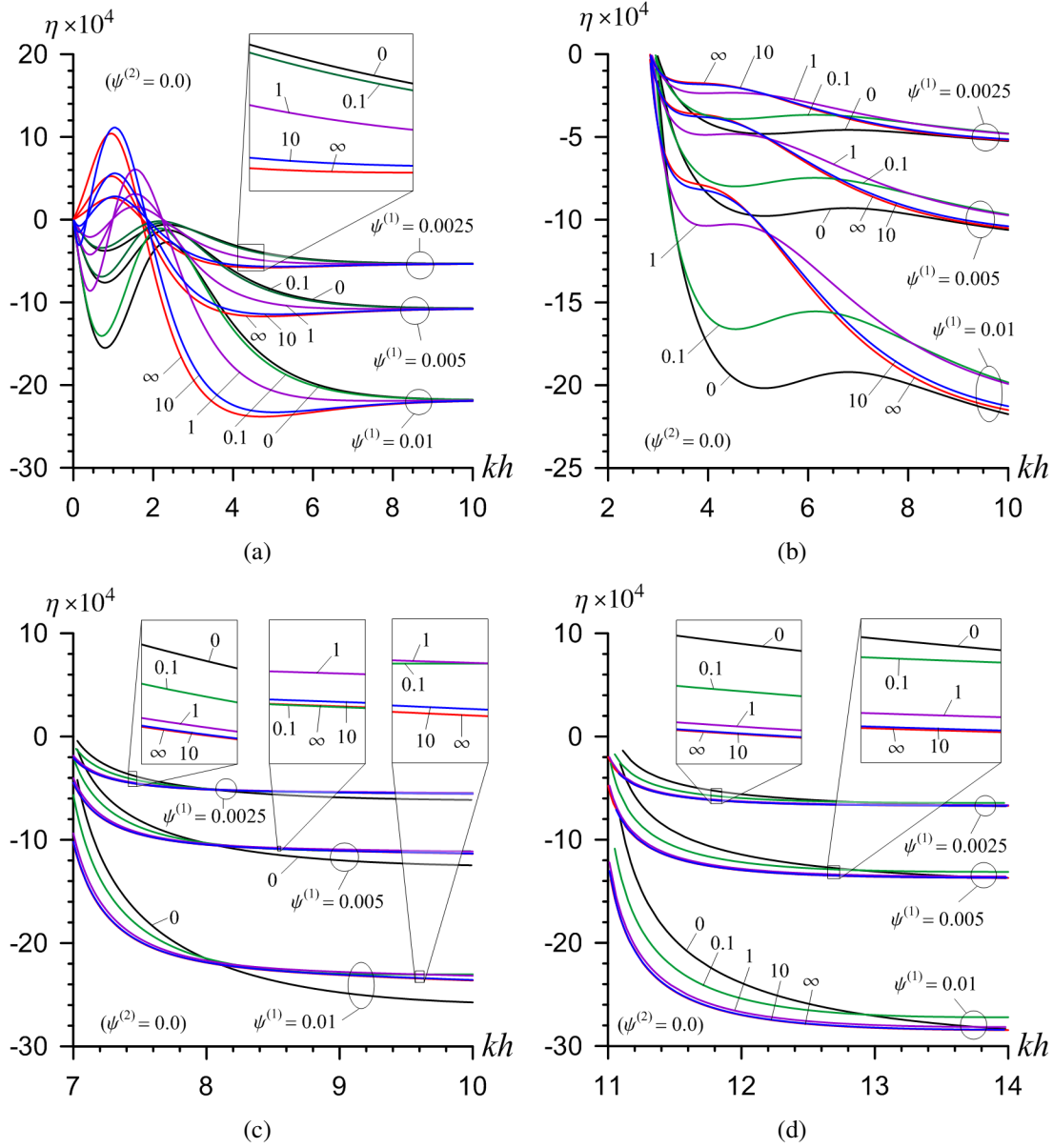


Figure 3.8: The influence of the imperfect bonding conditions and initial stresses to the dispersion of the generalized Rayleigh wave for the *III* pair of materials in Case 1: First (a) and second (b) branches of the first mode; First (c) and second (d) branches of the second mode.

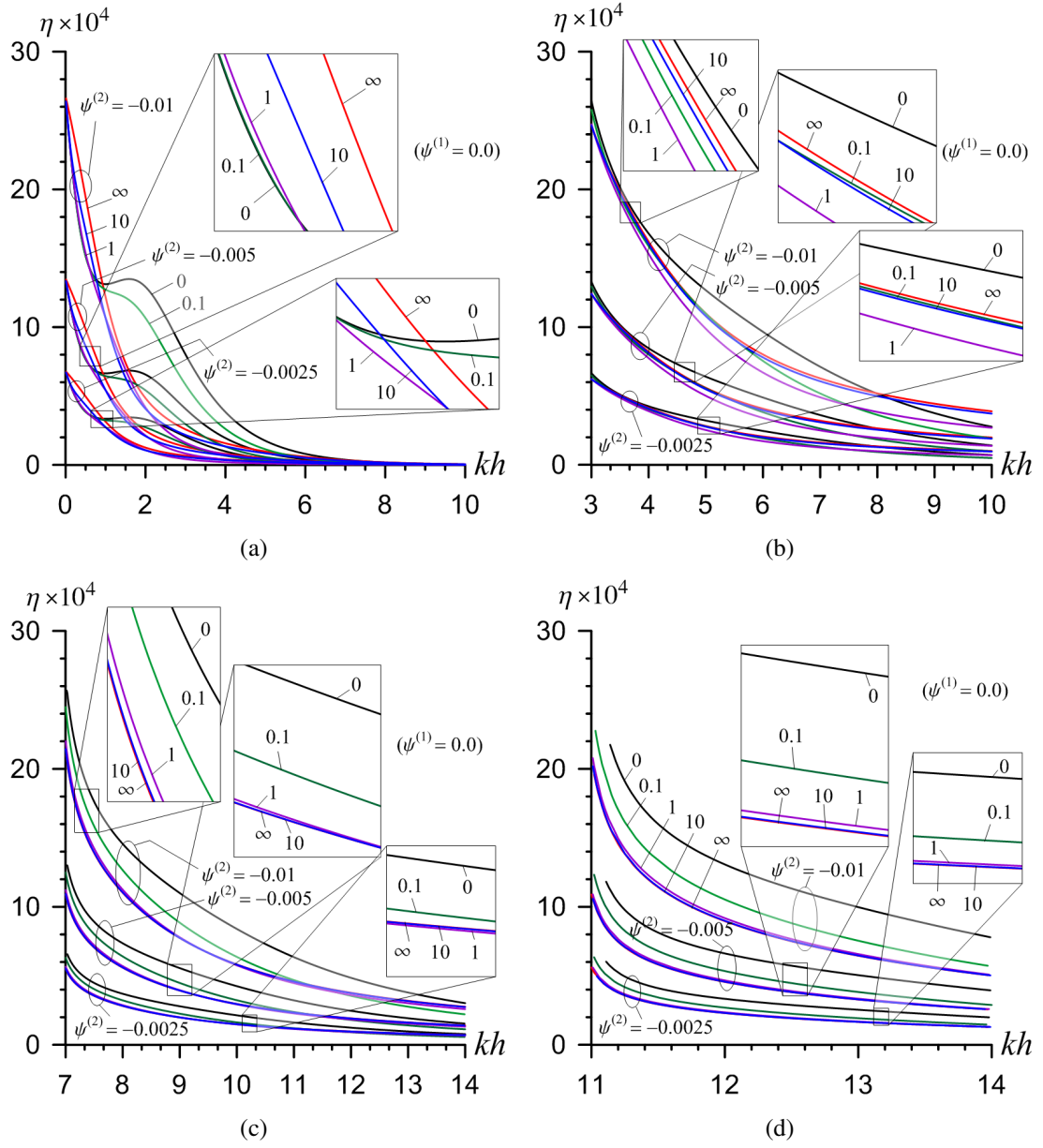


Figure 3.9: The influence of the imperfect bonding conditions and initial stresses to the dispersion of the generalized Rayleigh wave for the *II* and *III* pair materials in Case 2: First (a) and second (b) branches of the first mode; First (c) and second (d) branches of the second mode.

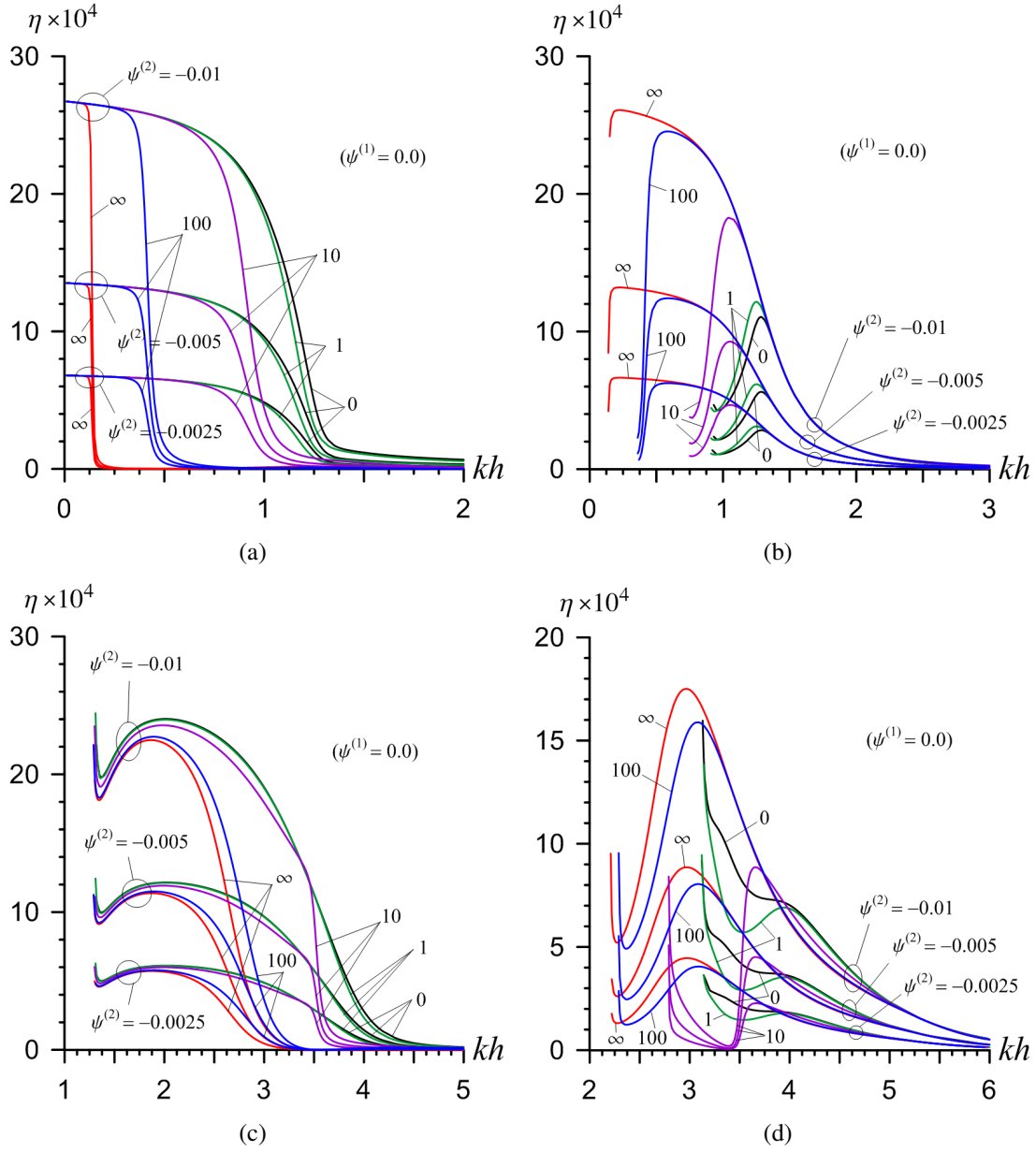


Figure 3.10: The influence of the imperfect bonding conditions and initial stresses to the dispersion of the generalized Rayleigh wave for the *IV* pair of materials in Case 2: First (a) and second (b) branches of the first mode; First (c) and second (d) branches of the second mode.

where $\psi^{(2)} = 0.0$ are given in Figure 3.7. Consequently, it can be conclude from the comparison of the results given in Figure 3.11 with the corresponding ones given in Figure 3.7, that how the initial compression of the half-plane acts on the influence of the parameter F on the wave propagation velocities under initial stretching of the covering layer. First, this comparison shows that the initial compression of the half-plane causes to considerable increase the wave propagation velocity with respect to the wave propagation velocity obtained in the case where the initial compression in the half-plane is absent. Moreover, this comparison shows that the influence of the parameter F on the wave propagation velocity in the latter case is more complicated than the influence of that on the wave propagation velocity obtained in the case where $\psi^{(2)} = 0.0$. At the same time, the analyses of the results given in Figure 3.11 shows that the graphs obtained for various values of the parameter F cannot be limited with corresponding ones obtained in the cases where $F = 0$ and $F = \infty$.

Finally, we consider the graphs given in Figure 3.12 which show the dependence between the η and kh for the *III* pair of materials in Case 4, i.e. in the case where the covering layer and half-plane are initially stretched simultaneously and $\psi^{(1)} = \psi^{(2)}$. Note that these graphs can be taken as generalization of the graphs given in Figure 3.8 for the case where the initial stretching exists not only in the covering layer, but also in the half-plane. Consequently, through the comparison of the graphs given in Figure 3.12 with the corresponding ones given in Figure 3.8 we can conclude on the action of the initial stretching of the half-plane under the influence of the initial stretching of the covering layer on the wave propagation velocity. It follows from this comparison that as a result of the initial stretching of the half plane the influence of the initial stretching of the covering layer on the wave propagation velocity related to the *III* pair of materials increase significantly and in this case the initial stretching of the covering layer causes to decrease of the wave propagation velocity. The analyses of the graphs given in Figure 3.12 show that the character of the influence of the parameter F on the behavior of these graphs is similar with the character of this influence on the graphs given in Figure 3.8.

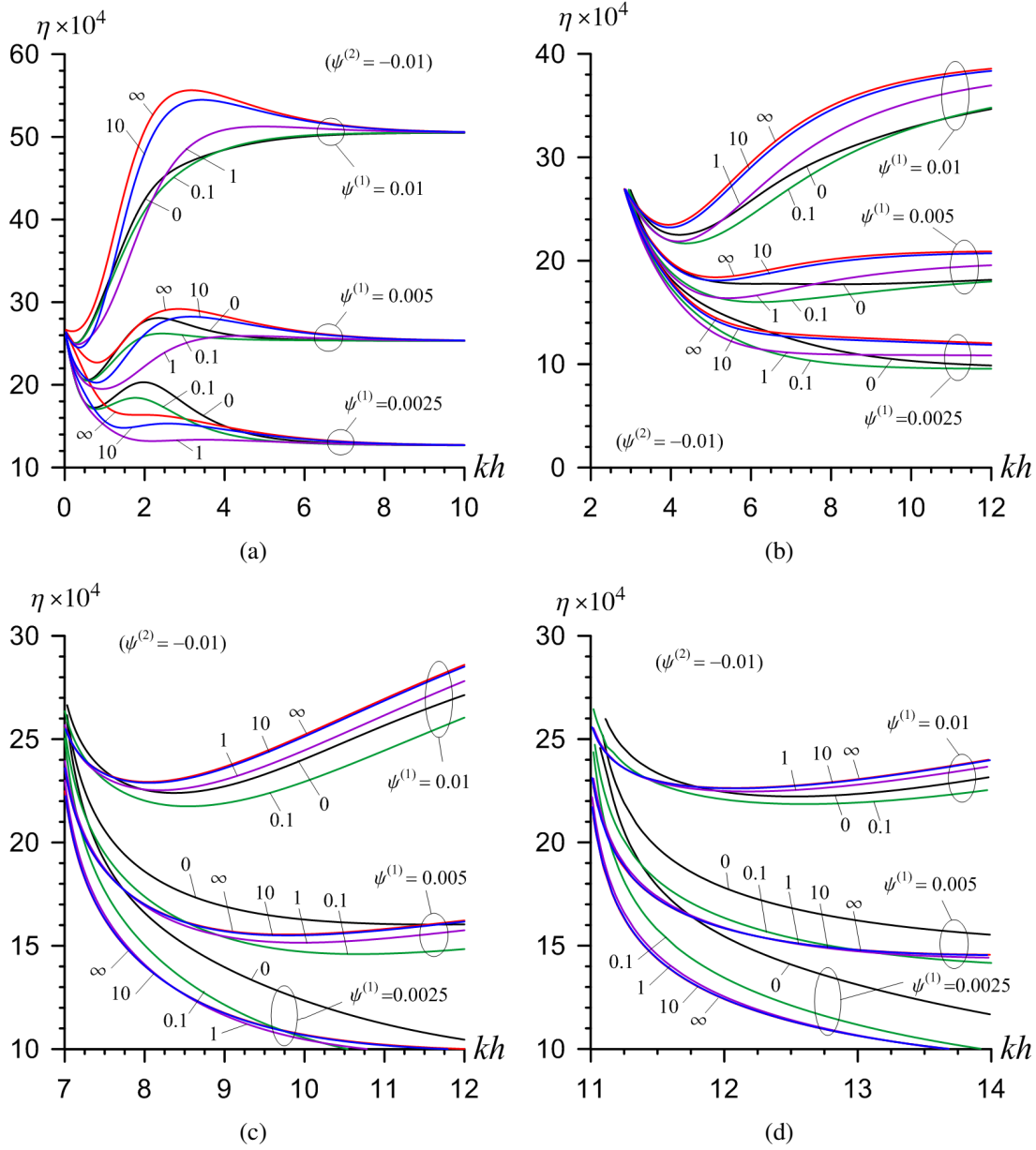


Figure 3.11: The influence of the imperfect bonding conditions and initial stresses to the dispersion of the generalized Rayleigh wave for the *II* pair of materials in Case 3: First (a) and second (b) branches of the first mode; First (c) and second (d) branches of the second mode.

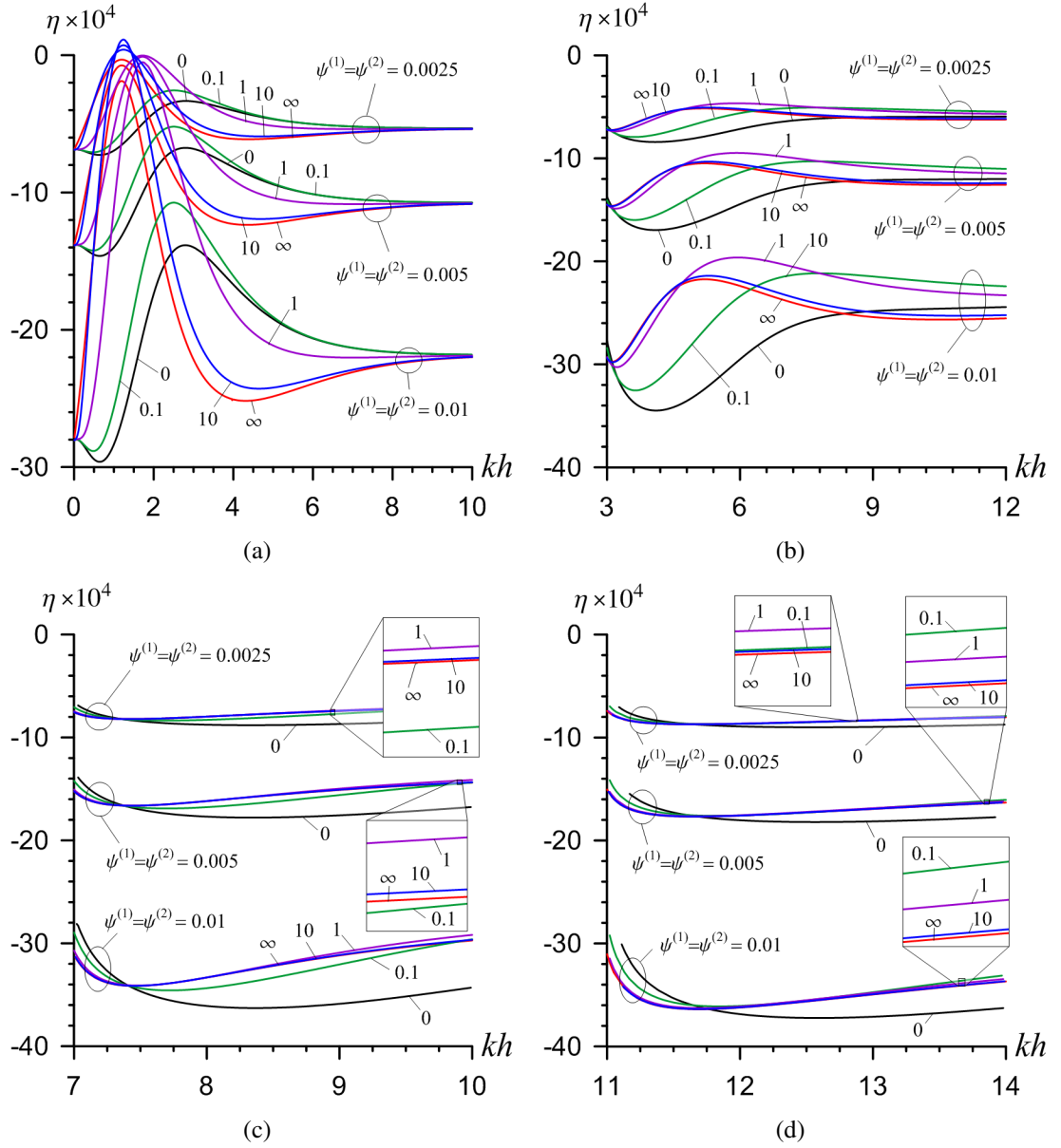


Figure 3.12: The influence of the imperfect bonding conditions and initial stresses to the dispersion of the generalized Rayleigh wave for the *III* pair of materials in Case 4: First (a) and second (b) branches of the first mode; First (c) and second (d) branches of the second mode.

This completes the analyses of the numerical results related to the four pairs of materials shown in Table 3.1. Note that these results are theoretical ones.

3.4 Some Applications and Experimental Verifications

The experimental studies on the generalized Rayleigh waves for the pair of materials was made in a paper by Lu; Zhang and Wang (2006). These studies was carried out within the complete contact condition between the Plexiglas (Lucite) covering layer and Steel half-plane and the dispersive characteristics of Rayleigh waves are investigated experimentally. Under these studies the thickness of the covering layer is taken $h = 5$ mm (Figure 3.1) and the experimental results were compared with the theoretical results obtained for the first branches of the first and second modes of the dispersion curves, i.e. the experimental results are compared with the theoretical results given in Figure 3.5a. However, in the paper by Lu; Zhang and Wang (2006) the mentioned dispersion curves are given as graphs of dependencies between the phase velocity c and frequency ω . For clarity, in Figure 3.13 the dispersion curves given in Figure 3.5a are reconstructed as a dependencies between the phase velocity c and frequency ω . Note that, namely, the curves obtained in the case where $F = 0$ and given in Figure 3.13 were used in the paper by Lu; Zhang and Wang (2006) for verification of the experimental results and this verification illustrate a very good agreement between the theoretical and corresponding experimental results. Consequently, the experimental method used in the paper by Lu; Zhang and Wang (2006) can also be employed for verification of the theoretical results obtained for the cases where $F > 0$, i.e. for verification of the imperfectness degree of the contact between covering layer and substrate. Note that the experimental methods based on the measurement of the Rayleigh waves for determination of the bonded defects in fiber-layered composites were developed in papers by Zurn and Mantell (2001) and Castaings; Hosten and Francois (2004) and others listed therein. Also, in the papers by Zurn and Mantell (2001) and Castaings; Hosten and Francois (2004) it was established that the mentioned bonded defects causes to decrease the generalized Rayleigh wave propagation velocity. Consequently, the theoretical results obtained in the present paper and related to the influence of the imperfectness of the contact conditions on

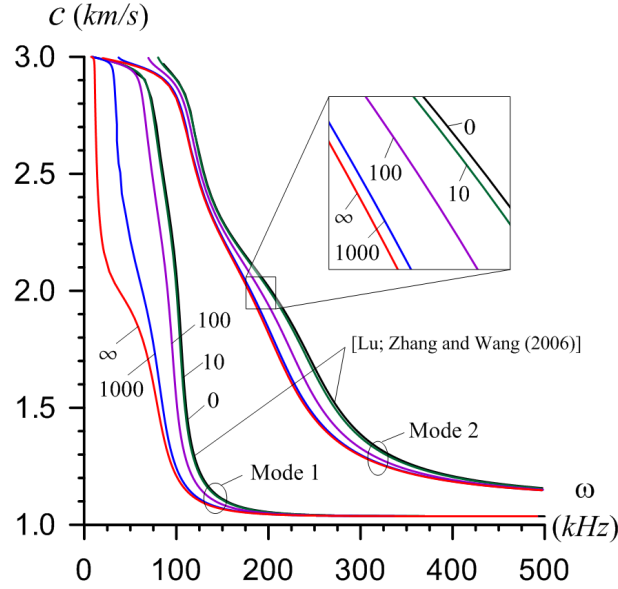


Figure 3.13: Dispersion curves for steel half-space covered by Lucite.

the generalized Rayleigh wave propagation velocity is validated with the experimental results obtained in the papers by Zurn and Mantell (2001) and Castaings; Hosten and Francois (2004) in the qualitative sense.

It is known that the experimental measurement of the generalized Rayleigh wave propagation is successfully used in the non-destructive determination of the structural parameters and residual stresses in the elements of constructions. It should be noted that under these determinations alongside with experimental data the theoretical results similar with the results presented in the present paper are also used. For example, in a paper by Lakestani; Coste and Denis (1995) generalized Rayleigh waves of various frequencies were generated using a broadband pulse and their velocities were measured as a function of the frequency and compared to the theoretical dispersion curve of the specimen. Experiments were carried out on AISI 316L specimens coated with vacuum plasma sprayed NiCoCrAlY of various thickness (190-330 μm). Figure 3.14 shows the dispersion curves, i.e. the dependence between the generalized Rayleigh wave propagation velocity c and the ratio h/λ , where h is a thickness of the coating and λ is a wave length, obtained for the mentioned pair of materials under various values of the shear-spring type parameter F . Note that the dispersion curve constructed under $F = 0$ and shown in Figure 3.14 is used in the paper by Lakestani; Coste and Denis (1995) as the theoretical results, according to which, using the experimental data the

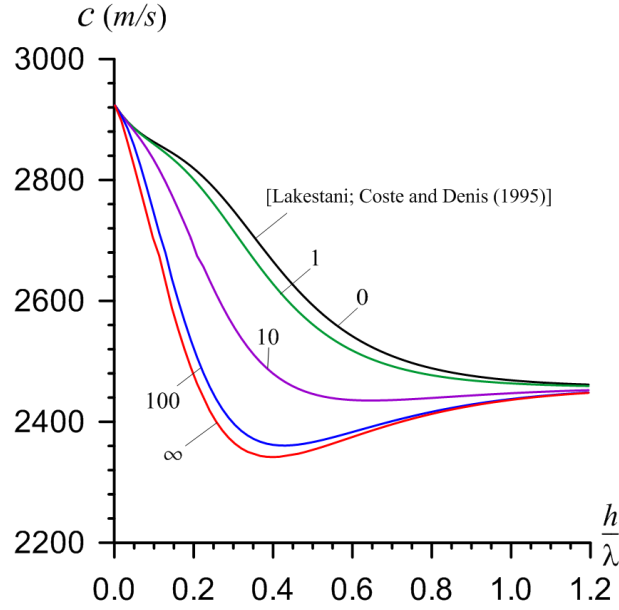


Figure 3.14: Dispersion curves for AISI 316L stainless steel coated with vacuum plasma sprayed NiCoCrAlY.

thickness of the coating is determined. Consequently, the dispersion curves obtained in the cases where $F > 0$ and shown in Figure 3.14 can also successfully be used for determination of the imperfectness between the coating and substrate material. Moreover, the results given in Figure 3.15 which illustrate the influence of the initial stresses in the constituents on the wave propagation velocity of the first branch of the first mode, i.e. on the parameter η (3.32) in Case 1 (Figure 3.15a), Case 2 (Figure 3.15b), Case 3 (Figure 3.15c) and Case 4 (Figure 3.15d) which are determined by the expression (3.31), can also be used as theoretical ones for determination of the quantities of the considered type initial stresses in the coating and substrate material used under the experimental investigations carried out in the paper by Lakestani; Coste and Denis (1995).

The other application field of the generalized Rayleigh wave measurement methods is the geophysical and geotechnical engineering. This method in these engineering fields is employed for determination of the soil stiffness profile. This profile is constructed with an inversion process starting from the experimentally determined dispersion behavior of the Rayleigh waves. After determination of the mentioned stiffness profile, the corresponding theoretical dispersion curves are also calculated for validation of the experimentally determined dispersion curves. Consequently, the dispersion curves

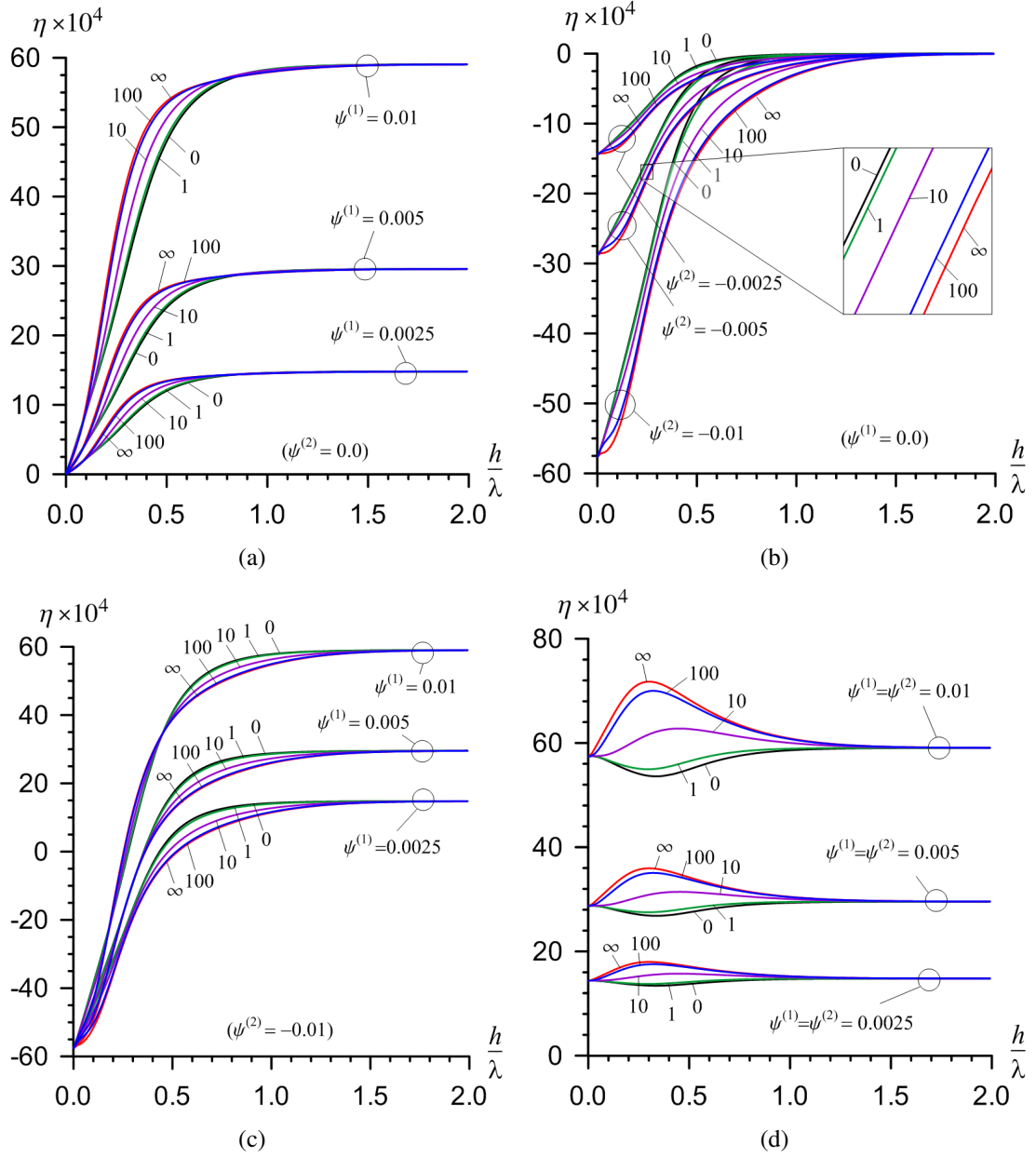


Figure 3.15: The influence of the imperfect bonding conditions and initial stresses to the dispersion of the generalized Rayleigh wave for AISI 316L steel coated with (VPS) NiCoCrAlY for the first branch of the first mode: (a) Case 1; (b) Case 2; (c) Case 3 and (d) Case 4.

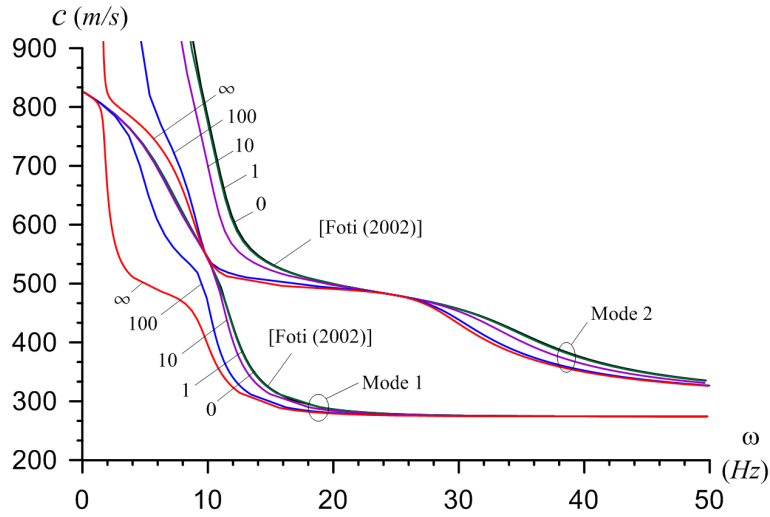


Figure 3.16: Dispersion curves related to surface waves in the soil which is modeled as a covering layer + half-plane (Foti, 2002).

constructed within the scope of the assumptions used in the present paper can also be used in the geophysical and geotechnical engineering under determination of the soil stiffness profile. As an example, we consider the case which was considered in a paper by Foti (2002), according to which the soil is modeled as covering layer + half-plane. The thickness of the covering layer is $h = 10$ m, the densities of the covering layer and half-plane materials are equal to each other and is 1800 kg/m^3 , shear and bulk waves velocities in the covering layer (half-plane) material are 300 m/s (900 m/s) and 500 m/s . Figure 3.16 shows the graphs of dependencies between the phase velocity and frequency and these graphs relate to the first branches of the first and the second modes of the dispersion curves constructed for the above mentioned case. Note that, namely the graphs constructed in the case where $F = 0$ and shown in Figure 3.16 were used in the paper by Foti (2002) for validation of the experimentally constructed dispersion curves. Consequently the other results show in Figure 3.16 and obtained in the case where $F > 0$ can also be used in the corresponding cases related to the geophysical and geotechnical engineering. Moreover, the results given in Figure 3.17, which shows the influence of the initial stresses in the soil constituents under consideration in Case 1 (Figure 3.17a), Case 2 (Figure 3.17b), Case 3 (Figure 3.17c) and Case 4 (Figure 3.17d), allows to determine the magnitude of the initial stresses in the soil layers using the experimentally constructed dispersion curves by employing

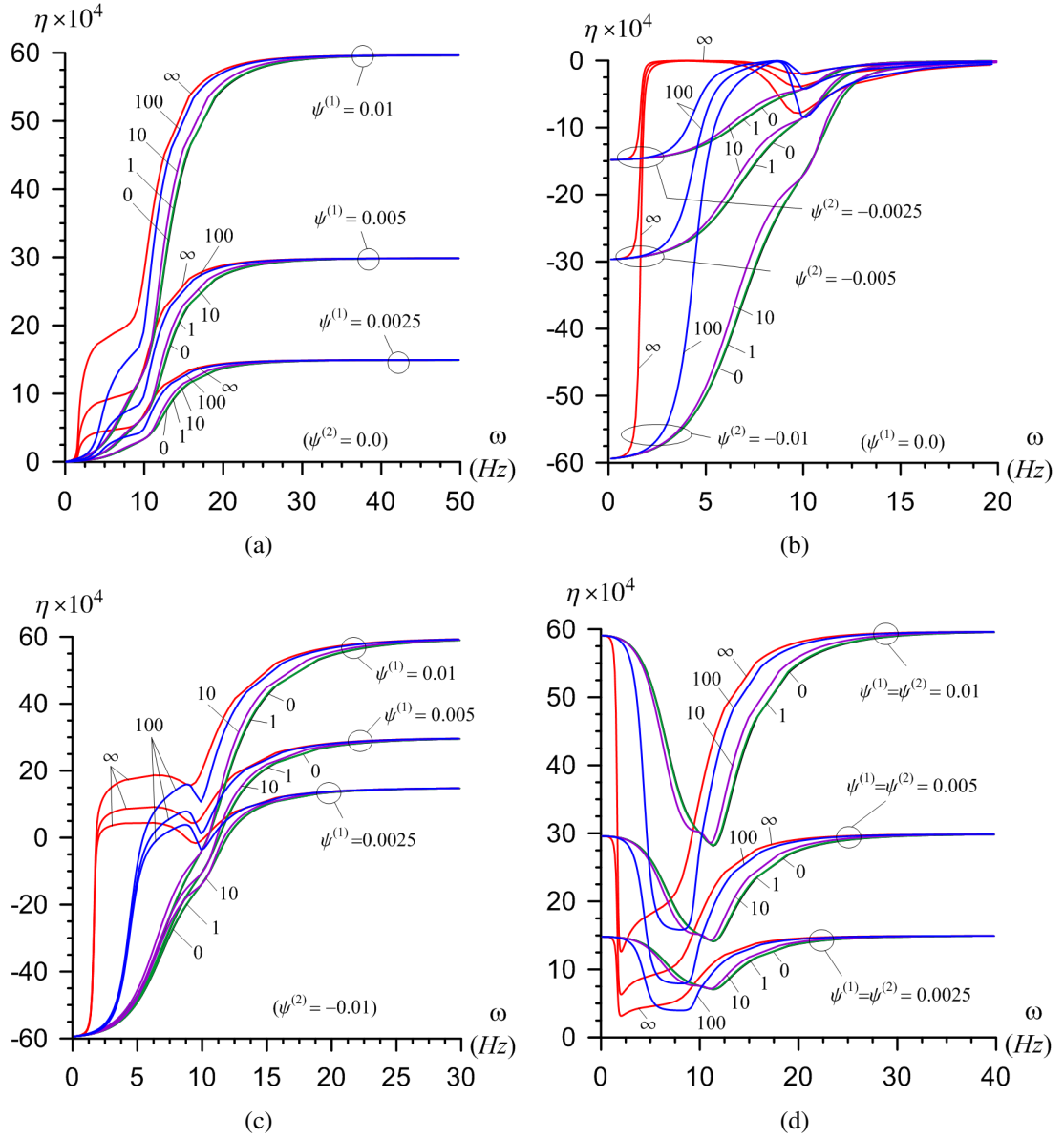


Figure 3.17: The influence of the imperfect bonding conditions and initial stresses to the dispersion of the generalized Rayleigh wave for AISI 316L steel coated with (VPS) NiCoCrAlY for the first branch of the first mode: (a) Case 1; (b) Case 2; (c) Case 3 and (d) Case 4.

the method described by Foti (2002). Note that the graphs constructed in Figure 3.17 relate to the first branch of the first mode.

3.5 Conclusions

Thus, in the present paper within the framework of the piecewise homogeneous body model with the use of the second version of the small initial deformation theory of the three-dimensional linearized theory of elastic waves in initially stressed bodies the influence of the shear-spring type imperfect contact conditions on the dispersion relation of the generalized Rayleigh waves in the system consisting of the initially stressed covering layer and initially stressed half plane has been investigated. The elasticity relations of the materials of the constituents are described by the Murnaghan potential. The magnitude of the mentioned imperfectness of the contact conditions on the wave propagation velocity has been estimated through the shear-spring type parameter F (3.6), where $0 \leq F < \infty$ and the case $F = 0$ ($F = \infty$) corresponds to the complete (full slipping) contact between the constituents. Consequently, the influence of the imperfectness of the contact conditions on the generalized Rayleigh wave propagation velocity has been studied through the influence of the parameter F on this velocity.

The numerical results are obtained and discussed for the pair of the Poisson materials by Tolstoy and Usdin (1953), and four pairs of materials composed from the materials the values of the mechanic constants of which are given in Table 3.1. From these discussions the following main conclusions are derived:

- The imperfectness of the contact conditions cause to decrease of the wave propagation velocity of the generalized Rayleigh waves.
- The dispersion curve constructed for each value of the parameter F is limited with corresponding ones obtained at $F = 0$ (upper limit) and $F = \infty$ (lower limit).
- The low wavenumber and high wavenumber limit values of the wave propagation velocity do not depend on the imperfectness of the contact conditions. However, the cut off values of the dimensionless wavenumber kh of the first and second branches

of the second modes for the pair of materials used by Tolstoy and Usdin (1953) and for the *IV* pair of materials depend significantly on the parameter F .

- In the case where the complete contact conditions are satisfied between the constituents the wave propagation velocity decrease monotonically with the dimensionless wavenumber kh , however in the case where there exists the shear-spring type imperfect conditions between the constituents the dependence between the wave propagation velocity and the dimensionless wavenumber kh may become non-monotonic for some pair of materials. Consequently, the imperfectness of the contact conditions acts on the dispersion curves and, in general, on the dynamics of the system under consideration not only quantitatively, but also qualitatively.

Note that the foregoing conclusions are made for the case where the initial stresses in the constituents are absent. In the paper the numerical results related to the action of the initial stresses in the constituents under the influence of the imperfectness parameter F on the wave propagation velocity are also presented and discussed for four pairs of materials (Table 3.1). Throughout these discussions the magnitude of the initial stresses is estimated by the parameters $\psi^{(1)}$ and $\psi^{(2)}$ (3.30), and four cases indicated in (3.31) with respect to the signs of the $\psi^{(1)}$ and $\psi^{(2)}$ are considered, but the change in the values of the wave propagation velocity is estimated through the parameter η (3.32). We can make the following main conclusions related to the action of the parameter F on the influence of the initial stresses on the wave propagation velocity:

- The imperfectness of the contact conditions causes to increase the influence of the initial stress in the covering layer on the wave propagation velocity related to the first branch of the first mode and to the second branch of the second mode of the *I* pair of materials. However, the character of the effect of the imperfectness of the contact conditions, i.e. of the parameter F on the influence of the initial stress in the covering layer on the wave propagation velocity related to the second branch of the first mode and to the first branch of the second mode depends on the values of the dimensionless wavenumber kh .

- As a result of the initial compression of the half-plane the wave propagation velocity related to the *II* (or *III*) and *IV* pairs of materials in Case 2 increase monotonically with the absolute values of the parameter $\psi^{(2)}$. In this case before (after) a certain value of the kh , the influence of the parameter F causes to increase (decrease) the wave propagation velocity related to the first branch of the first mode of the *II* pair of materials. At the same time, as a result of the influence of the parameter F the wave propagation velocities related to the second branch of the first mode, the first and second branches of the second mode of the *II* pair of materials decrease. The magnitude of this decreasing depends significantly on the values of the dimensionless wavenumber kh .
- In general, the graphs of the dependence between the parameters η and kh , i.e. the influence of the initial stresses on the wave propagation velocity obtained for each value of F cannot be limited with the corresponding ones obtained at $F = 0$ (complete contact) and $F = \infty$ (full slipping). This conclusion rises again the significance of the investigations carried out in the present paper.
- Numerical results obtained for the *IV* pair of materials under complete contact conditions are validated with the corresponding experimental ones which were detailed in the paper by Lu; Zhang and Wang (2006).
- The character of the influence of the imperfectness of the contact between the covering layer and half plane on the generalized Rayleigh wave propagation velocity in the qualitative sense is validated with the experimental ones given by Zurn and Mantell (2001) and Castaings; Hosten and Francois (2004).
- Dispersion curves for the pair of materials considered in the paper by Lakestani; Coste and Denis (1995) are also obtained and the possible application of the numerical results under determination of the structural parameters and residual stresses in the coated materials is proposed.
- The possible application of the numerical results which are similar to the obtained ones and relate to the determination of the soil structure and stiffness in the geophysical and geotechnical engineering is also discussed and corresponding numerical results are presented for the case considered in the paper by Foti (2002).

Many other details of the results obtained for the initially stressed cases are discussed in the text.

4. DISPERSION OF GENERALIZED RAYLEIGH WAVES IN A STRATIFIED HALF-SPACE WITH IMPERFECT INTERFACE UNDER TWO-AXIAL INITIAL STRESSES

4.1 Formulation of The Problem

Consider an elastic half-space covered by an elastic layer with thickness h as shown in Figure 4.1. We determine the positions of the points by the Lagrange coordinates in the Cartesian system of coordinates $Ox_1x_2x_3$. A plane-strain state in the Ox_1x_2 plane is considered, thus the displacement components along Ox_1 and Ox_2 directions, u_1 and u_2 are non-zero while displacement component u_3 along Ox_3 direction is zero. Assume that the Rayleigh waves propagate in the positive direction of Ox_1 axis. Note that the following notation will be used through the formulations: the values related to the layer and half-space are denoted by upper indices (1) and (2) respectively and the values related to the initial stress states are denoted by additional upper index 0. Let the system be under initial normal compressive stress $\sigma_{22}^{(m),0}$ along Ox_2 direction and compressive or tensile initial stress $\sigma_{11}^{(m),0}$ along Ox_1 direction, respectively. The initial stresses $\sigma_{22}^{(1),0} = \sigma_{22}^{(2),0} = \text{const}$, can be caused, for instance, by the weight of the fluid on the stratified half-space if the system is taken as a model for the soil of the bottom of the ocean or of the sea. Moreover, these initial stresses can be caused by the uniformly distributed normal "dead" forces with intensity $\sigma_{22}^{(1),0} = \sigma_{22}^{(2),0} = \text{const}$ and acting in the direction of the Ox_2 axis. The mentioned "dead" forces can also be taken as a model of the weight of the bodies which are located on the stratified half-space under consideration.

The homogeneous initial stresses $\sigma_{22}^{(1),0} \neq \sigma_{22}^{(2),0}$ are caused by the external forces acting at $|x_1| \rightarrow \infty$ in the direction of the Ox_1 axis. It can be assumed that the layer and half-space, at first, are stressed, i.e. are stretched or compressed in the Ox_1 axis direction, and then are contacted with each other. At the same time, it can be assumed that the initial stresses $\sigma_{22}^{(1),0} \neq \sigma_{22}^{(2),0}$ arise after contacting of the constituents by the

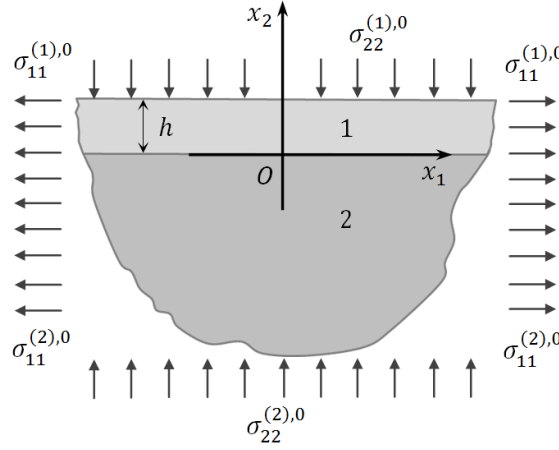


Figure 4.1: Geometry of the considered mechanical system.

uniformly distributed normal forces acting at infinity in the direction of the Ox_1 axis. Thus, taking the aforementioned assumptions into consideration, the initial stresses in the constituents are determined within the scope of the classical linear theory of elasticity as follows:

$$\sigma_{11}^{(m),0} = \text{const}_m \neq 0, \quad \sigma_{22}^{(1),0} = \sigma_{22}^{(2),0} \neq 0, \quad \sigma_{12}^{(m),0} = 0, \quad m = 1, 2. \quad (4.1)$$

According to Guz (2004), in the case where the initial stresses are determined as in (4.1), the equations of the TLTEWISB are obtained from the corresponding geometrical non-linear equations of motion by their linearization with respect to the perturbations of the stresses, strains and displacements:

$$\begin{aligned} \frac{\partial \sigma_{11}^{(m)}}{\partial x_1} + \frac{\partial \sigma_{12}^{(m)}}{\partial x_2} + \sigma_{11}^{(m),0} \frac{\partial^2 u_1^{(m)}}{\partial x_1^2} + \sigma_{22}^{(m),0} \frac{\partial^2 u_1^{(m)}}{\partial x_2^2} &= \rho^{(m)} \frac{\partial^2 u_1^{(m)}}{\partial t^2}, \\ \frac{\partial \sigma_{12}^{(m)}}{\partial x_1} + \frac{\partial \sigma_{22}^{(m)}}{\partial x_2} + \sigma_{11}^{(m),0} \frac{\partial^2 u_2^{(m)}}{\partial x_1^2} + \sigma_{22}^{(m),0} \frac{\partial^2 u_2^{(m)}}{\partial x_2^2} &= \rho^{(m)} \frac{\partial^2 u_2^{(m)}}{\partial t^2}. \end{aligned} \quad (4.2)$$

We assume that the following boundary conditions on the free face plane of the covering layer satisfy:

$$\sigma_{12}^{(1)} \Big|_{x_2=h} = 0, \quad \sigma_{22}^{(1)} \Big|_{x_2=h} = 0. \quad (4.3)$$

Now we consider the formulation of the imperfect contact conditions on the interface plane between the covering layer and the half-space. It should be noted that, in general, the imperfectness of the contact conditions is identified by discontinuities of the displacements and forces across the mentioned interface. According to the discussion

made in the previous subsection and according to Martin (1992) the mathematical formulation of the imperfectness of the contact conditions and these conditions are written as follows:

$$\sigma_{i2}^{(1)}|_{x_2=0} = \sigma_{i2}^{(2)}|_{x_2=0}, \quad i = 1, 2, \quad (4.4)$$

$$\begin{aligned} u_1^{(1)}|_{x_2=0} - u_1^{(2)}|_{x_2=0} &= F_1 \frac{h}{\mu^{(2)}} \sigma_{12}^{(2)}|_{x_2=0}, \quad F_1 > 0 \\ u_2^{(1)}|_{x_2=0} - u_2^{(2)}|_{x_2=0} &= F_2 \frac{h}{\mu^{(2)}} \sigma_{22}^{(2)}|_{x_2=0}, \quad F_2 > 0 \end{aligned} \quad (4.5)$$

where F_1 and F_2 are the non-dimensional shear- and normal-spring parameters. Note that the case where $F_1 = 0$ and $F_2 = 0$ means that the displacement component across the interface is continuous and therefore the half-space and the covering layer are perfectly bonded together or to say that they are in welded contact condition. At the other extreme, $F_1 = \infty$ and $F_2 = \infty$ implies that the half-space and the covering layer are completely unbounded together and the full slipping condition is satisfied. Thus, any other finite positive values of F_1 and F_2 expresses different imperfect interface conditions in the problem.

Moreover, we assume that the following decay conditions are satisfied:

$$\sigma_{ij}^{(2)}|_{x_2 \rightarrow -\infty} \rightarrow 0, \quad u_i^{(2)}|_{x_2 \rightarrow -\infty} \rightarrow 0, \quad i = 1, 2. \quad (4.6)$$

According to monograph by Guz (2004) and other references listed in these monographs, to obtain the results that are consistent with experimental studies of wave propagation patterns of small amplitudes (small perturbations) in mechanical systems containing a constituent made of compressible metal elastic material with initial stresses, it is necessary to use the Murnaghan type elastic potential to describe the elasticity relations of this material. This potential is given as follows (see, Guz and Makhort (2000)):

$$\Phi^{(m)} = \frac{1}{2} \lambda^{(m)} \left(A_1^{(m)} \right)^2 + \mu^{(m)} A_2^{(m)} + \frac{a^{(m)}}{3} \left(A_1^{(m)} \right)^3 + b^{(m)} A_1^{(m)} A_2^{(m)} + \frac{c^{(m)}}{3} A_3^{(m)}, \quad (4.7)$$

where $\lambda^{(m)}$ and $\mu^{(m)}$ are Lamé's and $a^{(m)}$, $b^{(m)}$ and $c^{(m)}$ are the third order elasticity constants. Here $A_1^{(m)}$, $A_2^{(m)}$ and $A_3^{(m)}$ are the first, second and the third algebraic invariants of Green's strain tensor respectively. For the case under consideration, the expressions of these invariants are:

$$A_1^{(m)} = \varepsilon_{11}^{(m)'} + \varepsilon_{22}^{(m)'},$$

$$\begin{aligned}
A_2^{(m)} &= \left(\varepsilon_{11}^{(m)'} \right)^2 + 2 \left(\varepsilon_{12}^{(m)'} \right)^2 + \left(\varepsilon_{22}^{(m)'} \right)^2, \\
A_3^{(m)} &= \left(\varepsilon_{11}^{(m)'} \right)^3 + 3 \left(\varepsilon_{12}^{(m)'} \right)^2 \left(\varepsilon_{11}^{(m)'} + \varepsilon_{22}^{(m)'} \right) + \left(\varepsilon_{22}^{(m)'} \right)^3,
\end{aligned} \tag{4.8}$$

where

$$\begin{aligned}
\varepsilon_{ij}^{(m)'} &= \frac{1}{2} \left(\frac{\partial u_i^{(m)'}}{\partial x_j} + \frac{\partial u_j^{(m)'}}{\partial x_i} + \frac{\partial u_n^{(m)'}}{\partial x_j} \frac{\partial u_n^{(m)'}}{\partial x_j} \right), \\
\sigma_{ij}^{(m)'} &= \frac{1}{2} \left(\frac{\partial}{\partial \varepsilon_{ij}^{(m)'}} + \frac{\partial}{\partial \varepsilon_{ji}^{(m)'}} \right) \Phi^{(m)}.
\end{aligned} \tag{4.9}$$

Note that in (4.7)–(4.9) the upper prime on the symbols $u_i^{(m)'} = (u_i^{(m),0} + u_i^{(m)})$, $\varepsilon_{ij}^{(m)'} = (\varepsilon_{ij}^{(m),0} + \varepsilon_{ij}^{(m)})$ and $\sigma_{ij}^{(m)'} = (\sigma_{ij}^{(m),0} + \sigma_{ij}^{(m)})$ denote the total values of the displacements, strains and stresses, respectively. Consequently, in the case under consideration by linearization of the non-linear relations (4.7)–(4.9) with respect to the perturbations, i.e. with respect to $u_i^{(m)}$, $\varepsilon_{ij}^{(m)}$ and $\sigma_{ij}^{(m)}$, the following linearized constitutive relations for the layer and the half-space materials are obtained.

$$\begin{aligned}
\sigma_{11}^{(m)} &= A_{11}^{(m)} \varepsilon_{11}^{(m)} + A_{12}^{(m)} \varepsilon_{22}^{(m)}, \\
\sigma_{22}^{(m)} &= A_{12}^{(m)} \varepsilon_{11}^{(m)} + A_{22}^{(m)} \varepsilon_{22}^{(m)}, \\
\sigma_{12}^{(m)} &= 2\mu_{12}^{(m)} \varepsilon_{12}^{(m)},
\end{aligned} \tag{4.10}$$

where

$$\begin{aligned}
A_{11}^{(m)} &= \lambda^{(m)} + 2\mu^{(m)} + \frac{\sigma_{11}^{(m),0}}{\mu^{(m)}} \left(2b^{(m)} + c^{(m)} \right) \\
&\quad + \frac{2 \left(\sigma_{11}^{(m),0} + \sigma_{22}^{(m),0} \right)}{3K_0^{(m)}} \left[\left(a^{(m)} + b^{(m)} \right) - \left(2b^{(m)} + c^{(m)} \right) \frac{\lambda^{(m)}}{2\mu^{(m)}} \right], \\
A_{22}^{(m)} &= \lambda^{(m)} + 2\mu^{(m)} + \frac{\sigma_{22}^{(m),0}}{\mu^{(m)}} \left(2b^{(m)} + c^{(m)} \right) \\
&\quad + \frac{2 \left(\sigma_{11}^{(m),0} + \sigma_{22}^{(m),0} \right)}{3K_0^{(m)}} \left[\left(a^{(m)} + b^{(m)} \right) - \left(2b^{(m)} + c^{(m)} \right) \frac{\lambda^{(m)}}{2\mu^{(m)}} \right], \\
A_{12}^{(m)} &= \lambda^{(m)} + \frac{b^{(m)}}{\mu^{(m)}} \left(\sigma_{11}^{(m),0} + \sigma_{22}^{(m),0} \right) + \frac{2 \left(\sigma_{11}^{(m),0} + \sigma_{22}^{(m),0} \right)}{3K_0^{(m)}} \left[a^{(m)} - b^{(m)} \frac{\lambda^{(m)}}{\mu^{(m)}} \right],
\end{aligned}$$

$$\begin{aligned}\mu_{12}^{(m)} &= \mu^{(m)} + \frac{b^{(m)}}{3K_0^{(m)}} \left(\sigma_{11}^{(m),0} + \sigma_{22}^{(m),0} \right) + \frac{c^{(m)} \left(\sigma_{11}^{(m),0} + \sigma_{22}^{(m),0} \right)}{4\mu^{(m)}} \left[\frac{\lambda^{(m)} + 2\mu^{(m)}}{3K_0^{(m)}} \right], \\ K_0^{(m)} &= \lambda^{(m)} + \frac{2\mu^{(m)}}{3}, \quad \varepsilon_{ij}^{(m)} = \frac{1}{2} \left(\frac{\partial u_i^{(m)}}{\partial x_j} + \frac{\partial u_j^{(m)}}{\partial x_i} \right).\end{aligned}\quad (4.11)$$

This completes the formulation of the problem and in the case where $\sigma_{11}^{(1),0} = \sigma_{11}^{(2),0} = \sigma_{22}^{(1),0} = \sigma_{22}^{(2),0} = 0$, this formulation transforms to the corresponding one made within the scope of the classical linear theory of elastodynamics. Moreover, in the case where $\sigma_{22}^{(1),0} = \sigma_{22}^{(2),0} = 0$ and $F_1 = F_2 = 0$ the foregoing formulation coincides with the corresponding one considered in the paper by Akbarov and Ozisik (2003).

4.2 Solution Procedure and Dispersion Equation

Each displacements component of the considered system are represent as follows:

$$\begin{aligned}u_1^{(m)} &= \varphi_1^{(m)}(x_2) \sin(kx_1 - \omega t), \\ u_2^{(m)} &= \varphi_2^{(m)}(x_2) \cos(kx_1 - \omega t).\end{aligned}\quad (4.12)$$

Substituting presentation (4.12) into the relations (4.11) and (4.10) we obtain the following equations for the $\varphi_1^{(m)}(x_2)$ and $\varphi_2^{(m)}(x_2)$ from the equation of motion (4.2):

$$\begin{aligned}\frac{d^2 \varphi_1^{(m)}}{d(kx_2)^2} + b_{21}^{(m)} \varphi_1^{(m)} + c_{21}^{(m)} \frac{d\varphi_2^{(m)}}{d(kx_2)} &= 0, \\ \frac{d^2 \varphi_2^{(m)}}{d(kx_2)^2} + b_{22}^{(m)} \varphi_2^{(m)} + c_{22}^{(m)} \frac{d\varphi_1^{(m)}}{d(kx_2)} &= 0,\end{aligned}\quad (4.13)$$

where

$$\begin{aligned}b_{21}^{(m)} &= -\frac{A_{11}^{(m)}}{\mu_{12}^{(m)} + \sigma_{22}^{(m),0}} - \frac{\sigma_{11}^{(m),0}}{\mu_{12}^{(m)} + \sigma_{22}^{(m),0}} + \frac{\rho^{(m)} \omega^2}{\left(\mu_{12}^{(m)} + \sigma_{22}^{(m),0} \right) k^2}, \\ b_{22}^{(m)} &= -\frac{\mu_{12}^{(m)}}{A_{22}^{(m)} + \sigma_{22}^{(m),0}} - \frac{\sigma_{11}^{(m),0}}{A_{22}^{(m)} + \sigma_{22}^{(m),0}} + \frac{\rho^{(m)} \omega^2}{\left(A_{22}^{(m)} + \sigma_{22}^{(m),0} \right) k^2}, \\ c_{21}^{(m)} &= \frac{-A_{12}^{(m)} - \mu_{12}^{(m)}}{\mu_{12}^{(m)} + \sigma_{22}^{(m),0}}, \quad c_{22}^{(m)} = \frac{\mu_{12}^{(m)} + A_{12}^{(m)}}{A_{22}^{(m)} + \sigma_{22}^{(m),0}}.\end{aligned}\quad (4.14)$$

After some mathematical procedures, we derive the following equation for $\varphi_2^{(m)}(x_2)$:

$$\frac{d^4 \varphi_2^{(m)}}{d(kx_2)^4} + B_2^{(m)} \frac{d^2 \varphi_2^{(m)}}{d(kx_2)^2} + C_2^{(m)} \varphi_2^{(m)} = 0,$$

$$B_2^{(m)} = b_{22}^{(m)} + b_{21}^{(m)} - c_{21}^{(m)} c_{22}^{(m)}, \quad C_2^{(m)} = b_{21}^{(m)} b_{22}^{(m)}. \quad (4.15)$$

We determine the solution to the equation (4.15) as follows:

$$\begin{aligned} \varphi_2^{(1)}(x_2) &= Z_1^{(1)} \exp(R_1^{(1)} k x_2) + Z_2^{(1)} \exp(-R_1^{(1)} k x_2) \\ &\quad + Z_3^{(1)} \exp(R_2^{(1)} k x_2) + Z_4^{(1)} \exp(-R_2^{(1)} k x_2), \\ \varphi_2^{(2)}(x_2) &= Z_1^{(2)} \exp(R_1^{(2)} k x_2) + Z_3^{(2)} \exp(R_2^{(2)} k x_2), \end{aligned} \quad (4.16)$$

where

$$R_1^{(m)} = \sqrt{-\frac{B_2^{(m)}}{2} + \sqrt{\frac{(B_2^{(m)})^2}{4} - C_2^{(m)}}}, \quad R_2^{(m)} = \sqrt{-\frac{B_2^{(m)}}{2} - \sqrt{\frac{(B_2^{(m)})^2}{4} - C_2^{(m)}}}. \quad (4.17)$$

In a similar way using (4.17) we can also determine the function $\varphi_1^{(m)}(x_2)$ from (4.13). Finally, we obtain the dispersion equation considering the conditions (4.3)–(4.6). This dispersion equation after some mathematical manipulations can be expressed formally as follows:

$$\det \left\| \alpha_{ij} \left(c, kh, F_1, F_2, \sigma_{11}^{(1),0}, \sigma_{11}^{(2),0}, \sigma_{22}^{(1),0}, \sigma_{22}^{(2),0}, a^{(1)}, b^{(1)}, c^{(1)}, a^{(2)}, b^{(2)}, c^{(2)} \right) \right\| = 0, \quad (4.18)$$

where $i, j = 1, 2, \dots, 6$ and

$$c = \frac{\omega}{k}, \quad c_1^{(m)} = \sqrt{\frac{\lambda^{(m)} + 2\mu^{(m)}}{\rho^{(m)}}}, \quad c_2^{(m)} = \sqrt{\frac{\mu^{(m)}}{\rho^{(m)}}}. \quad (4.19)$$

The explicit expressions of the α_{ij} ($i, j = 1, 2, \dots, 6$) in the dispersion equation (4.18) are given in Appendix A.2. This completes the solution method of the problem under consideration.

4.3 Numerical Results and Discussion

We will assume that,

$$\text{Re} R_1^{(1)} = \text{Re} R_2^{(1)} = 0, \quad R_1^{(2)} > 0, \quad R_2^{(2)} > 0. \quad (4.20)$$

This is concise way of saying that in order to satisfy the conditions (4.20) the following relations must hold:

$$B_2^{(1)} > 0, \quad C_2^{(1)} > 0, \quad B_2^{(2)} < 0, \quad C_2^{(2)} < 0, \quad (4.21)$$

The relations (4.21) hold when:

$$\max \left(\tilde{c}_1^{(1)}, \tilde{c}_2^{(1)}, \tilde{c}_3^{(1)} \right) < c < \min \left(\tilde{c}_1^{(2)}, \tilde{c}_2^{(2)}, \tilde{c}_3^{(2)} \right) \quad (4.22)$$

where

$$\begin{aligned} \tilde{c}_1^{(m)} &= \sqrt{\frac{A_{11}^{(m)}}{\rho^{(m)}} \left(1 + \frac{\sigma_{11}^{(m),0}}{A_{11}^{(m)}} \right)}, \quad \tilde{c}_2^{(m)} = \sqrt{\frac{\mu_{12}^{(m)}}{\rho^{(m)}} \left(1 + \frac{\sigma_{11}^{(m),0}}{\mu_{12}^{(m)}} \right)}, \\ \tilde{c}_3^{(m)} &= \sqrt{\frac{A_{11}^{(m)}}{\rho^{(m)}} \left(\frac{\frac{A_{22}^{(m)} + \sigma_{22}^{(m),0}}{\mu_{12}^{(m)} + A_{22}^{(m)} + 2\sigma_{22}^{(m),0}} + \frac{\sigma_{11}^{(m),0}}{A_{11}^{(m)}} + \frac{\mu_{12}^{(m)}}{A_{11}^{(m)}} \frac{\mu_{12}^{(m)} + \sigma_{22}^{(m),0}}{\mu_{12}^{(m)} + A_{22}^{(m)} + 2\sigma_{22}^{(m),0}} \right) - \frac{(\mu_{12}^{(m)} + A_{12}^{(m)})^2}{A_{11}^{(m)} (\mu_{12}^{(m)} + A_{22}^{(m)} + 2\sigma_{22}^{(m),0})}} \right)}. \end{aligned} \quad (4.23)$$

The relation (4.22) guarantee that $R_1^{(2)}, R_2^{(2)}$ always be real and positive, and $R_1^{(1)}, R_2^{(1)}$ always be pure imaginary. Note that the other cases under which the (4.20)–(4.23) are violated, in the present work do not considered. In this case, the solution (4.16) corresponds to such a wave propagation in the layered half-space that the layer undergoes an oscillatory motion in the Ox_2 direction propagating in the Ox_1 direction with velocity c . The disturbances in the layer decay exponentially with depth in the half-space and therefore the wave can be considered as a generalized Rayleigh wave confined to the pre-stressed covered layer, (Tolstoy and Usdin (1953)).

We consider two pairs of the real material. Values of the mechanical constants of these materials (i.e. the values of the mechanical constants which enter the expression (4.7) of the Murnaghan potential) are given in Table 4.1. Materials of the covering layer for the *I* and *II* pairs are taken as *bronze* and *Plexiglas* respectively, but for both pairs the material of the half-space is *steel*. Dispersion curves obtained from numerical solution of dispersion equation (4.18), for different imperfect conditions are given in Figure 4.2 for the *I* pair of materials. Note that, in order to compare the effect of contact imperfections in Ox_1 and Ox_2 directions, the graphs of the cases where imperfections exist only in transverse direction, i.e $F_1 \neq 0, F_2 = 0$ and the case where imperfections exist in both transverse and normal directions, i.e. $F_1 = F_2 \neq 0$, are given separately in Figures 4.2a and 4.2b respectively. It is worthy to notice that the results given in these figures which obtained for the case where $F_1 = F_2 = 0$ coincide with corresponding ones obtained in the paper by Akbarov and Ozisik (2003). The numbers labeled on the

Table 4.1: The values of elastic constants of the selected materials (Guz ,2004).

Materials	ρ (g/cm ³)	$\lambda \times 10^{-4}$ (MPa)	$\mu \times 10^{-4}$ (MPa)	$a \times 10^{-5}$ (MPa)	$b \times 10^{-5}$ (MPa)	$c \times 10^{-5}$ (MPa)
Steel 3	7.795	9.26	7.75	-2.35	-2.75	-4.90
Bronze	7.20	8.16	3.84	1.20	-3.10	4.80
Plexiglas	1.16	0.404	0.19	2.68×10^{-3}	-3.12×10^{-2}	-6.77×10^{-2}

curves correspond to the dimensionless shear- and normal-spring parameters F_1 and F_2 of the related curves.

The dispersion equation (4.18) has infinitely many modes unlike ordinary Rayleigh waves, which can propagate only in one mode. Moreover, it was established (Tolstoy and Usdin, 1953) that the dispersion curves related to each mode has two branches which were denoted by M_{1n} and M_{2n} respectively for the n -th mode. For the first M_{1n} branch the displacement of the layer circumscribes the ellipse similar to the ordinary Rayleigh waves, but for the second M_{2n} branch leads to an opposite type of motion. Moreover, according to the restriction (4.20), it must be $c/c_2^{(2)} < 1$ and $c/c_1^{(1)} > 1$, i.e. the near-surface waves propagated in the system under consideration is subsonic in the half-space, but it is supersonic in the covering layer. Thus, it follows from Figure 4.2 that the dimensionless wavenumber kh has cut off values for the second branch of the first mode, the first and second branches of the second mode.

Figure 4.3 shows the dispersion curves of the II pair of the materials for different values of the imperfect interface dimensionless parameters, i.e. for different values of $F_1 = F_2 \neq 0$. For clarity of the illustrations the graphs related to the first branches of the first and second modes and the graphs related to the second branches of the first and second modes are given separately in Figures 4.3a and 4.3b, respectively.

It follows from Figures 4.2 and 4.3 that the imperfectness between the constituents of the system decrease the wave propagation velocity of the all above-noted branches and modes. In addition, the dimensionless wavenumber kh has cut off values for the second branch of the first mode and for the first and second branches of the second mode. However, except the case where $F_2 = \infty$, the low and high wavenumber limit values of the wave propagation velocities as $kh \rightarrow 0$ and $kh \rightarrow \infty$, respectively, do not depend on the imperfectness of the interface, i.e., on the parameters F_1 and F_2 , though,

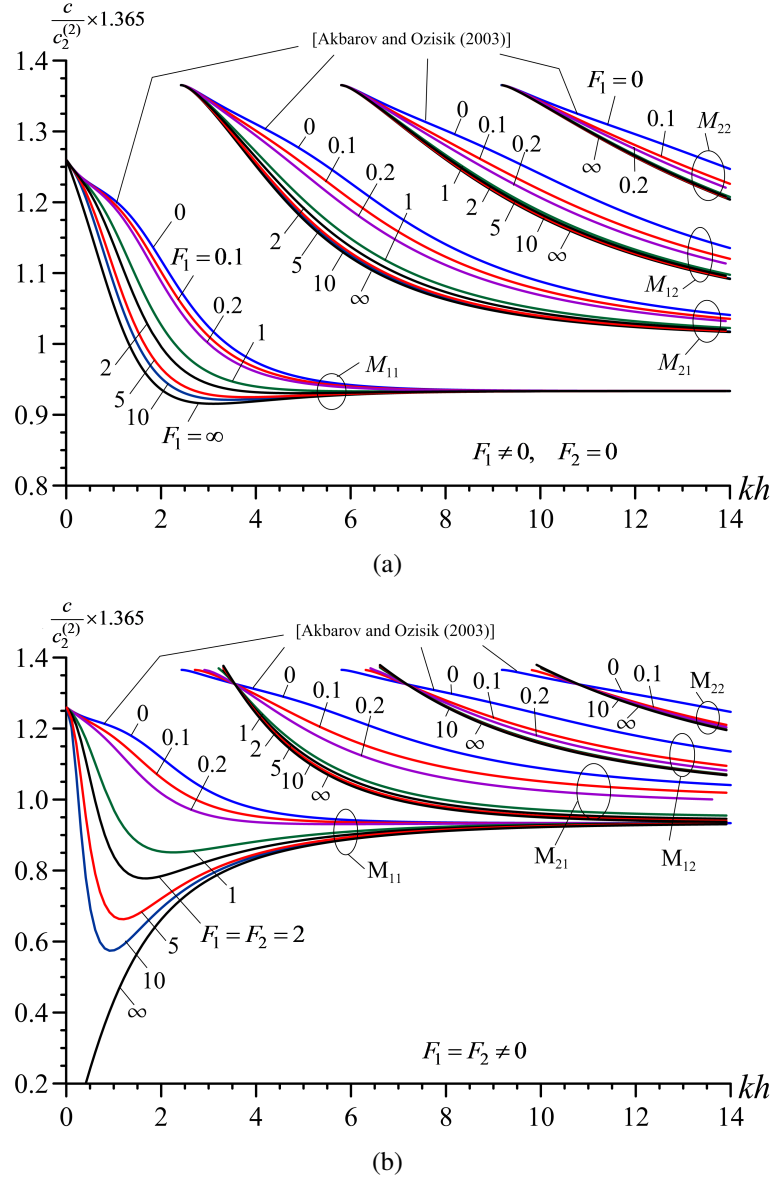


Figure 4.2: Dispersion curves for the I pair of materials: (a) Imperfection only in the transverse direction, $F_1 \neq 0, F_2 = 0$. The numbers in the figure fields show the values of the parameter F_1 ; (b) Imperfection both in the transverse and normal directions, $F_1 = F_2 \neq 0$. The numbers in the figure field show the values of the parameters $F_1 = F_2$.

existence of imperfections in the normal direction (i.e. in the case where $F_2 \neq 0$), slightly changes the cut off values of the second branch of the first mode and first and second branches of the second mode (Figure 4.2b and Figure 4.3). But, the case where $F_2 = \infty$ corresponds to the separation of the constituents from each other. Therefore, in the case where $F_2 = \infty$, in general, the first and second branches of the first mode correspond to the first mode of the flexural and the first mode of the extensional Lamb's waves in the covering layer.

Note that in Figure 4.2b the first mode of the flexural wave is illustrated for the *I* pair of materials only, because for the *I* pair of materials the velocity of the first mode of the extensional wave is out of the considered range of change of the wave propagation velocities. However, in the *II* pair of materials the dispersion curves related to the first mode of the flexural Lamb's wave (Figure 4.3a) and to the first mode of the extensional Lamb's wave (Figure 4.3b) are the limit ones (i.e. are the dispersion curves obtained under $F_2 = \infty$) of the dispersion curves under consideration. It should be noted that these situation agrees well with the known mechanical and physical consideration and proves the validity of the algorithm and PC programs used in the investigations. Moreover, Figures 4.2 and 4.3 show that the results obtained in the case where $F_1 = F_2 = 0$ coincide with the corresponding ones obtained in the paper by Akbarov and Ozisik (2003).

Now we analyze the numerical results related to the influence of the initial stresses in the constituents on the wave propagation velocity. For estimation of the magnitude of the initial stresses we introduce the parameters:

$$\psi^{(1)} = \sigma_{11}^{(1),0}/\mu^{(1)}, \quad \psi^{(2)} = \sigma_{11}^{(2),0}/\mu^{(2)}, \quad \psi^{(3)} = \sigma_{22}^{(1),0}/\mu^{(1)}. \quad (4.24)$$

Here we will present the results only for the following cases:

$$\begin{aligned} \text{Case 1.} \quad & \psi^{(1)} > 0, \quad \psi^{(2)} = 0; \\ \text{Case 2.} \quad & \psi^{(1)} = 0, \quad \psi^{(2)} < 0; \\ \text{Case 3.} \quad & \psi^{(1)} > 0, \quad \psi^{(2)} < 0; \\ \text{Case 4.} \quad & \psi^{(1)} > 0, \quad \psi^{(2)} > 0; \end{aligned} \quad (4.25)$$

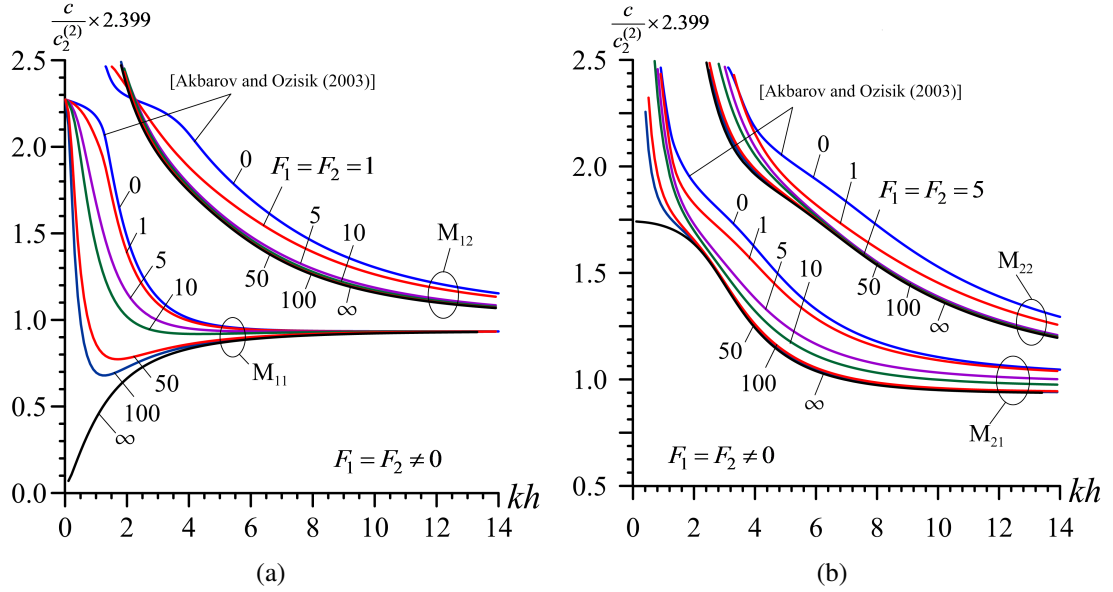


Figure 4.3: Dispersion curves for the II pair of materials: (a) first branches of the first and second modes; (b) second branches of the first and second modes. The numbers in the figures fields show the values of the parameters $F_1 = F_2$.

under $\psi^{(3)} < 0$. Moreover, we introduce the notation:

$$\eta = \frac{c|_{\psi^{(1)} \neq 0; \text{ or } \psi^{(2)} \neq 0; \text{ or } \psi^{(3)} \neq 0} - c|_{\psi^{(1)} = 0; \psi^{(2)} = 0; \psi^{(3)} = 0}}{c|_{\psi^{(1)} = 0; \psi^{(2)} = 0; \psi^{(3)} = 0}} \quad (4.26)$$

for estimation the influence of the initial stresses in the constituents, i.e. the influence of the parameters $\psi^{(1)}$, $\psi^{(2)}$ and $\psi^{(3)}$ on the wave propagation velocity.

Thus, through the graphs of the dependencies between η (4.23) and kh constructed for various values of the parameters F_1 , F_2 , $\psi^{(1)}$, $\psi^{(2)}$ and $\psi^{(3)}$ we analyze the effect of the imperfectness of the contact conditions between the covering layer and the half-space on the influence of the initial stresses in the constituents on the wave propagation velocity in the cases indicated in (4.22).

Figures 4.4 and 4.5 show the graphs of the dependence between η and kh for the first branch of the first mode for the *I* (in Case 1) and *II* (in Case 4) pairs of the materials respectively, for different values of the parameters F_1 and F_2 . Note that the graphs related to cases where the imperfection exists in the transverse direction only, i.e. $F_1 > 0$, $F_2 = 0$, are given in Figures 4.4a and 4.5a, however the graphs related to cases where $F_1 = F_2 > 0$ are given in Figures 4.4b and 4.5b. It follows from the graphs given in these figures that the effect of the parameter F_2 on the influence of the initial stresses on the wave propagation velocity is more significant than that of the parameter

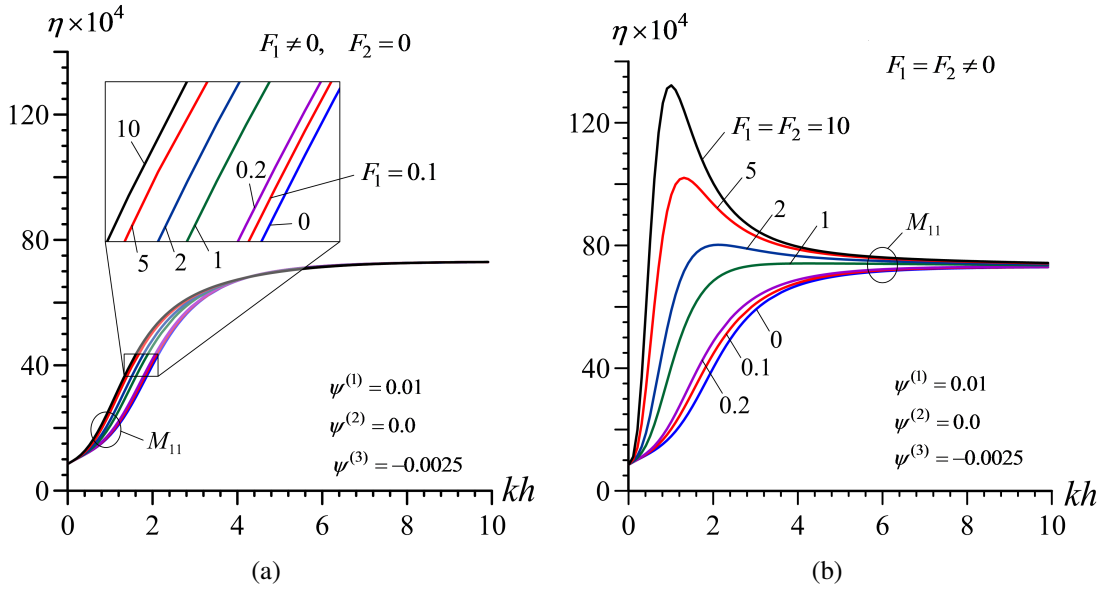


Figure 4.4: The influence of the contact imperfections on the dependence between η and kh for the first branch of the first mode for the *I* pair of materials in Case 1: (a) imperfection is only in the transverse direction, $F_1 \neq 0, F_2 = 0$; (b) imperfection is in both the transverse and normal directions, $F_1 = F_2 \neq 0$.

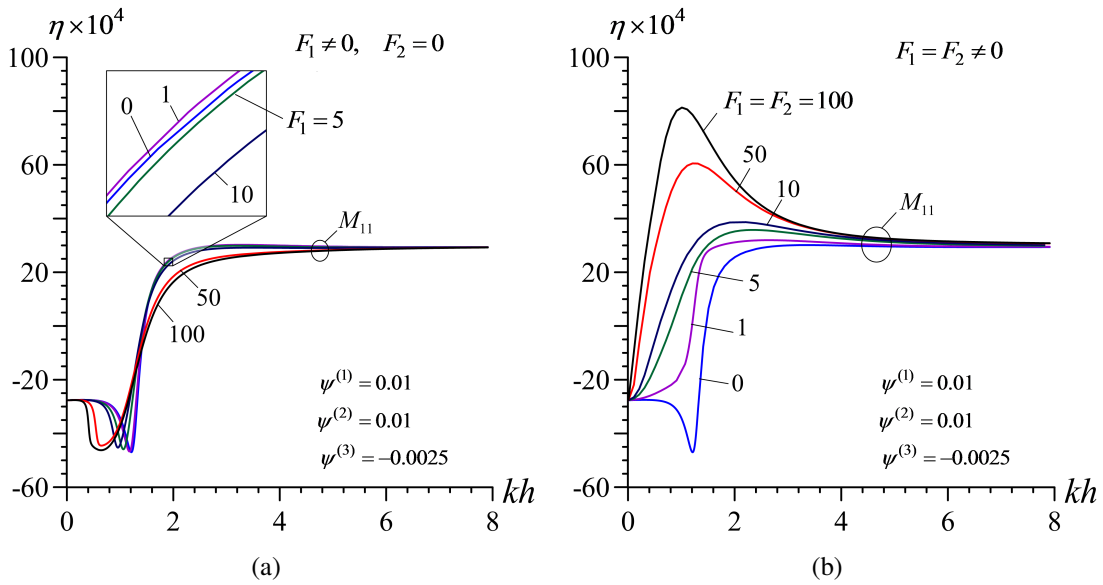


Figure 4.5: The influence of the contact imperfections on the dependence between η and kh for the first branch of the first mode for the *II* pair of materials in Case 4: (a) imperfection is only in the transverse direction, $F_1 \neq 0, F_2 = 0$; (b) imperfection is in both the transverse and normal directions, $F_1 = F_2 \neq 0$.

F_1 . However, it follows from these graphs that in the limit cases, i.e. in the cases where $kh \rightarrow 0$ and $kh \rightarrow \infty$ this effect disappears. Also, Figures 4.4b and 4.5b show that the effect of the parameter F_2 on the graphs between η and kh has not only quantitative character, but also qualitative character. Note that similar results on the effect of the parameter F_2 on the dependence between η and kh are also obtained for the second branches of the first mode and for the first and second branches of the second and subsequent modes. Taking this statement into account, below we will consider the case where $F_1 = F_2 > 0$ and analyze the effect of the parameter $\psi^{(3)}$ (< 0), i.e. the effect of the existence of the initial compressive stress $\sigma_{22}^{(1),0} (= \sigma_{22}^{(2),0})$ acting in the direction Ox_2 axis which is perpendicular to the wave propagation direction.

Thus, we consider the graphs given in Figures 4.6 – 4.9 which illustrate the dependence between η and kh constructed for the first branch of the first mode. Note that these results are obtained for the *I* pair of materials in Case 1 (Figure 4.6) and in Case 2 (Figure 4.7), and for the *II* pair of materials in Case 3 (Figure 4.8) and in Case 4 (Figure 4.9). It follows from the Figure 4.6 that in Case 1 the initial compressive stress $\sigma_{22}^{(1),0} (= \sigma_{22}^{(2),0})$ causes to decrease the wave propagation velocity for each selected values of the parameter $F_1 (= F_2)$. However, in Case 2 the character of the influence of the initial compressive stress $\sigma_{22}^{(1),0} (= \sigma_{22}^{(2),0})$ on the wave propagation velocity depends on the parameter $F_1 (= F_2)$. So that, for the relatively small values of $F_1 (= F_2)$ (for instance, under $F_1 (= F_2) \leq 0.2$ the wave propagation velocity increase, however, in the case where $F_1 (= F_2) \geq 2$, the wave propagation velocity decreases with absolute values of the parameter $\psi^{(3)}$.

The observation of the graphs given in Figures 4.6 and Figures 4.7 shows that in the relatively high degree of the imperfection of the contact conditions, i.e. in the cases where $F_1 (= F_2) \geq 2$ the absolute values of the $\eta = \eta(kh)$ has a local maximum. According to Figures 4.8 and 4.9, it can be concluded that such local maximum of the values $\eta = \eta(kh)$ obtained for the *II* pair of materials in Case 3 (Figure 4.8) and in Case 4 (Figure 4.9) arise also under perfect contact between the constituents of the system under consideration. Moreover, according to the Figures 4.8 and 4.9 we can conclude the mentioned local maximum increases with absolute values of the parameter $\psi^{(3)}$, i.e. under perfect contact condition the initial compressive stress $\sigma_{22}^{(1),0} (= \sigma_{22}^{(2),0})$ causes

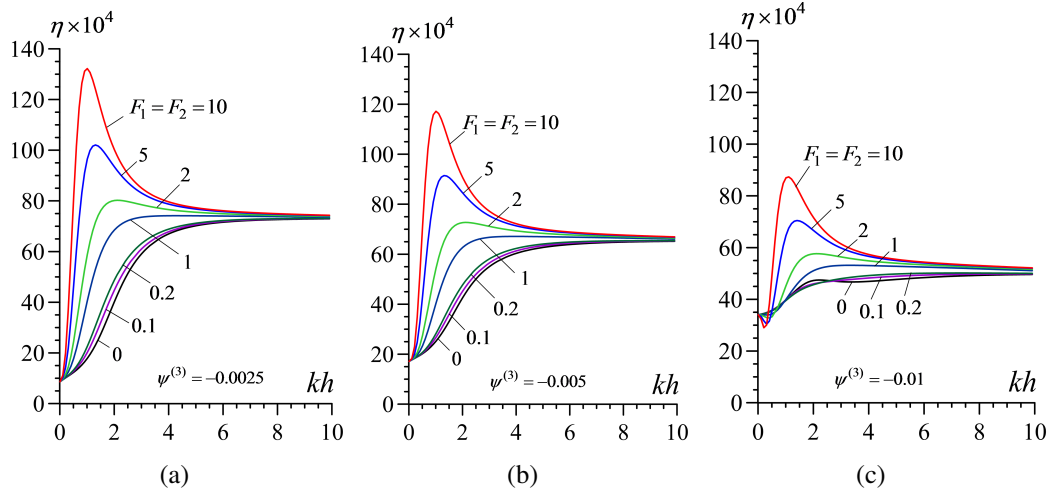


Figure 4.6: The graphs of the dependence between η and kh constructed for the first branch of the first mode of the I pair of materials in Case 1, ($\psi^{(1)} = 0.01$, $\psi^{(2)} = 0$) under $\psi^{(3)} = -0.0025$ (a), -0.005 (b) and -0.01 (c).

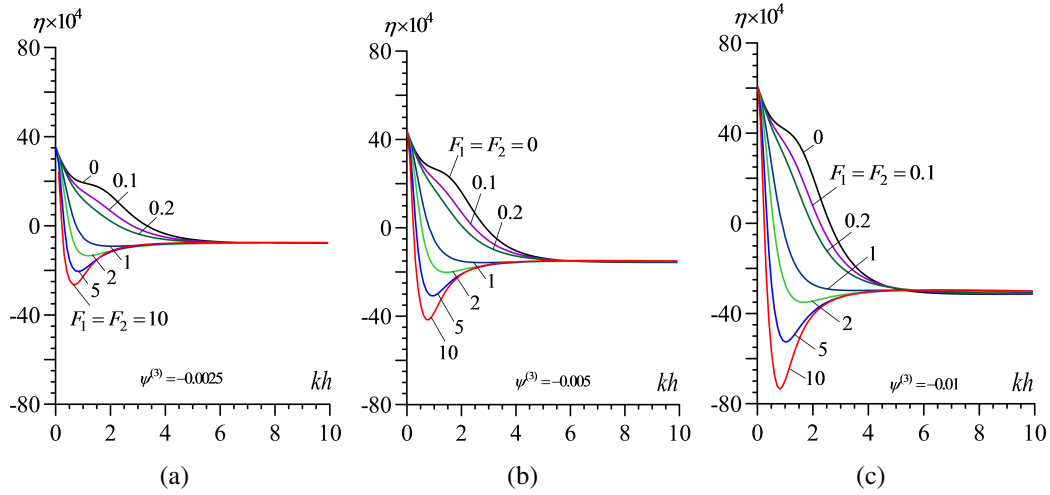


Figure 4.7: The graphs of the dependence between η and kh constructed for the first branch of the first mode of the I pair of materials in Case 2, ($\psi^{(1)} = 0$, $\psi^{(2)} = -0.01$) under $\psi^{(3)} = -0.0025$ (a), -0.005 (b) and -0.01 (c).

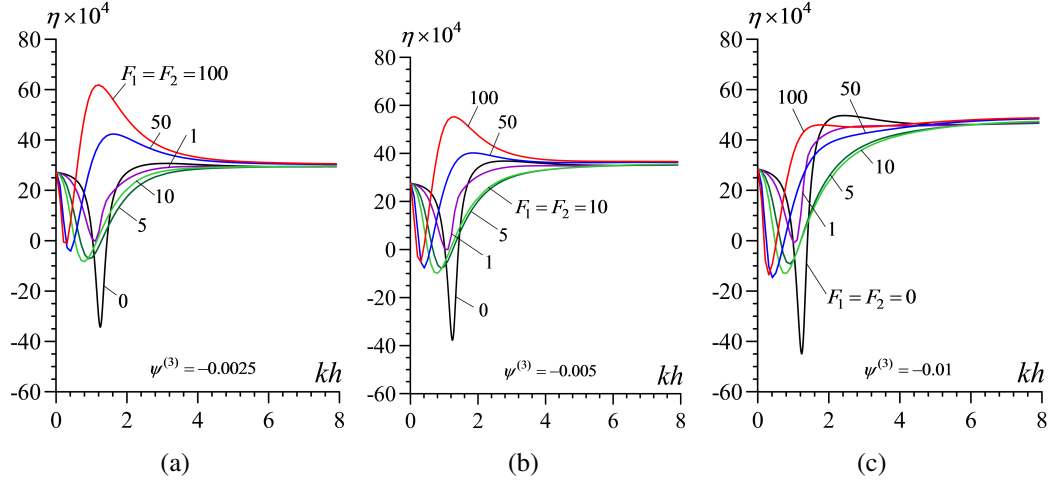


Figure 4.8: The graphs of the dependence between η and kh constructed for the first branch of the first mode of the II pair of materials in Case 3, ($\psi^{(1)} = 0.01, \psi^{(2)} = -0.01$) under $\psi^{(3)} = -0.0025(a), -0.005(b)$ and $-0.01(c)$.

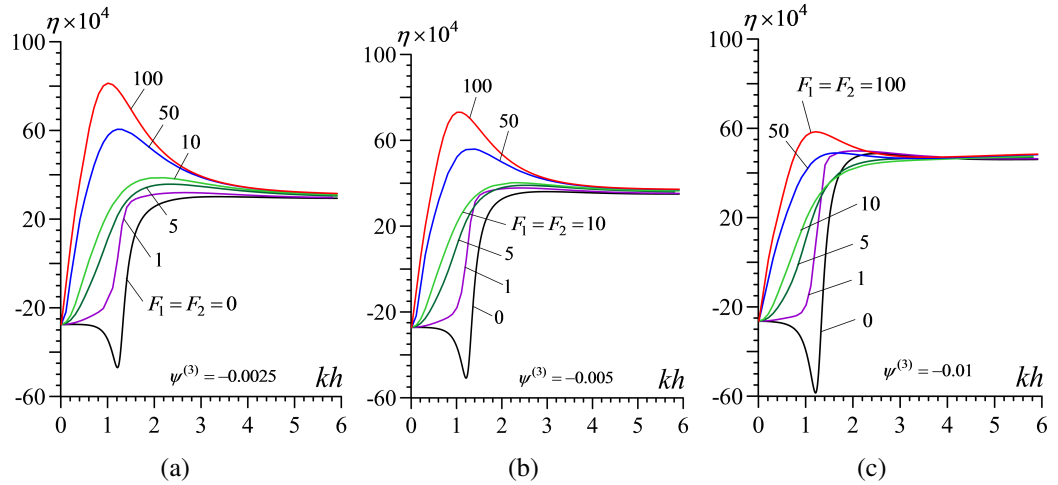


Figure 4.9: The graphs of the dependence between η and kh constructed for the first branch of the first mode of the II pair of materials in Case 4, ($\psi^{(1)} = 0, \psi^{(2)} = -0.01$) under $\psi^{(3)} = -0.0025(a), -0.005(b)$ and $-0.01(c)$.

to decrease the wave propagation velocity for the *II* pair of materials in Case 3 and Case 4. Similar conclusion can also be made for the case where the contact conditions are imperfect.

As an example in the influence of the initial stress $\sigma_{22}^{(1),0} (= \sigma_{22}^{(2),0})$ on the second branch of the first mode and on the first and second branches of the second mode we consider the graphs of the corresponding dependencies between $\eta = \eta(kh)$ related to the *I* pair of materials in Case 1 and in Case 2. The graphs related to the second branch of the first mode are given in Figure 4.10a and Figure 4.11a for Case 1 and Case 2 respectively, however, the graphs related to the first and second branches of the second mode obtained in Case 1 are presented in Figures 4.10b and 4.10c, but those obtained in Case 2 are presented in Figures 4.11b and 4.11c. Thus, it follows from the foregoing graphs that the near-surface wave propagation velocity in the system under consideration decreases with the absolute values of the initial compressive stress $\sigma_{22}^{(1),0} (= \sigma_{22}^{(2),0})$.

4.4 Conclusion

Thus, in the present section the generalized Rayleigh wave dispersion in the system consisting of a two-axially pre-stressed covering layer and two-axially pre-stressed half-space has been investigated by utilizing the three-dimensional linearized theory of elastic waves in initially stressed bodies. It has been assumed that the contact between the covering layer and the half-space is the shear-spring + normal-spring type imperfect, i.e. it has been assumed that on the interface plane the normal and tangential displacements have discontinuity simultaneously. The corresponding dispersion equation is solved numerically for the case where the half-space material is steel, but the covering layer material is bronze (the *I* pair) or Plexiglas (the *II* pair). With respect to the two-axial initial stresses the cases indicated in (4.22) are considered. Through the parameters F_1 and F_2 in (4.5) it is estimated the degree of the shear-spring and normal-spring type imperfections, respectively.

Numerical results, i.e. dispersion curves and the influence of the parameters F_1 and F_2 , as well as of the initial stresses on these curves are presented and discussed. According to these results the following main concrete conclusions can be made:

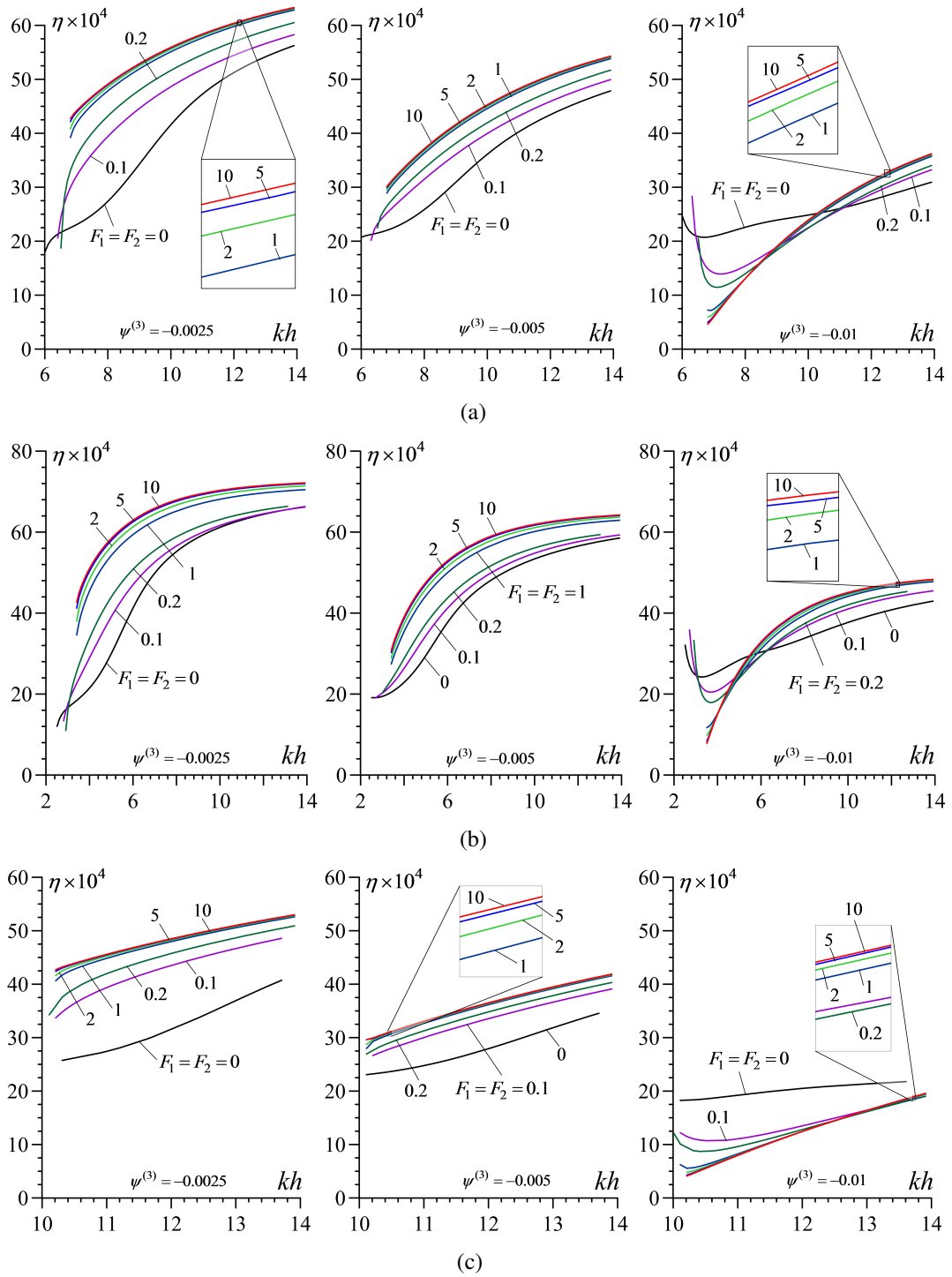


Figure 4.10: The graphs of the dependence between η and kh constructed for the second branch of the first mode (a), the first (b) and the second (c) branches of the second mode of the I pair of materials in Case 1, ($\psi^{(1)} = 0.01, \psi^{(2)} = 0$).

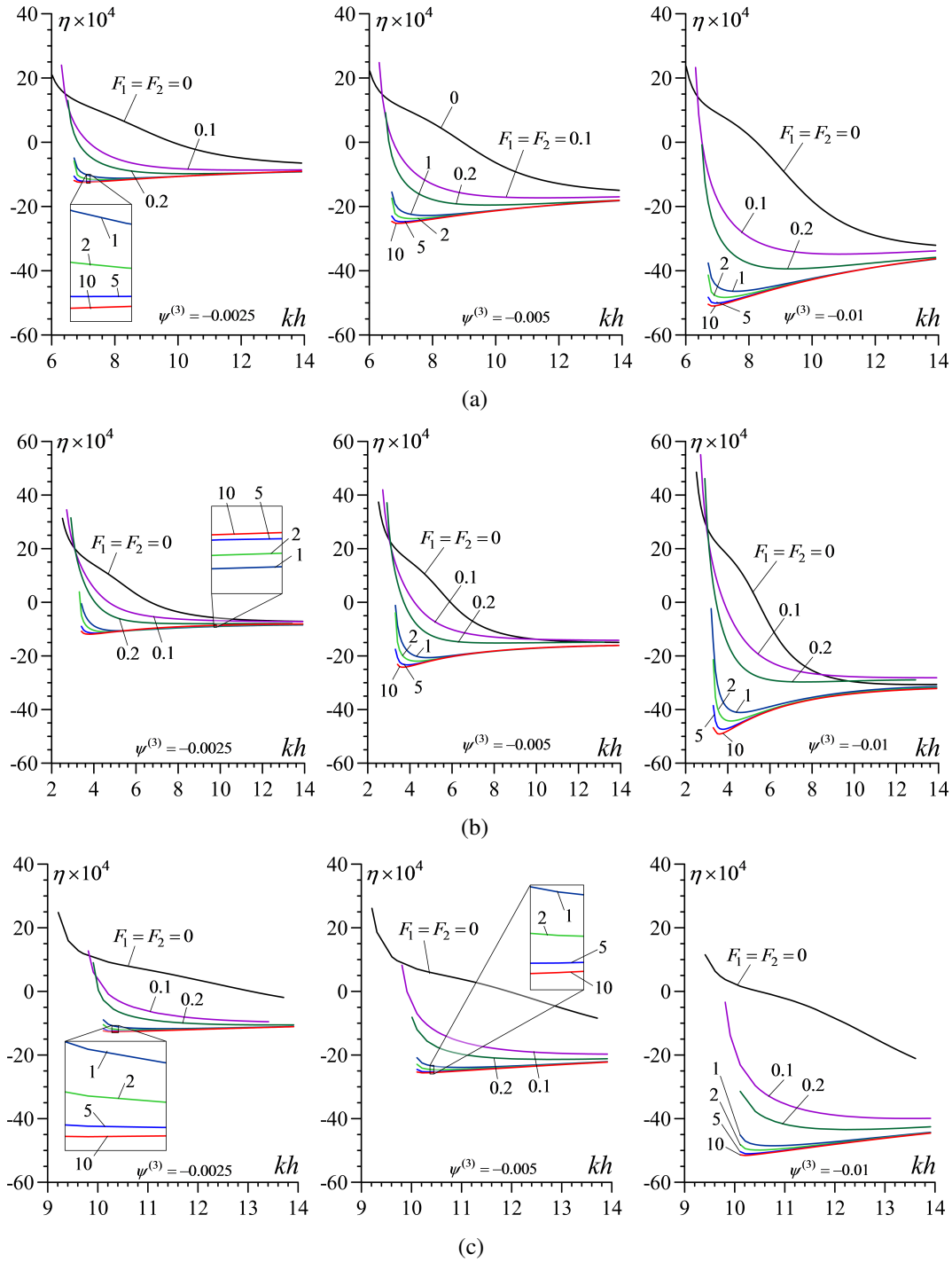


Figure 4.11: The graphs of the dependence between η and kh constructed for the second branch of the first mode (a), the first (b) and the second (c) branches of the second mode of the I pair of materials in Case 2, ($\psi^{(1)} = 0, \psi^{(2)} = -0.01$).

- The imperfectness of the contact conditions causes to decrease of the wave propagation velocity of the generalized Rayleigh waves.
- The low and high wavenumber limit values of the wave propagation velocity, i.e. the wave propagation velocity as $kh \rightarrow 0$ and as $kh \rightarrow \infty$ do not depend on the imperfection parameters F_1 and F_2 .
- Existence of the imperfection in normal direction considerably decreases the wave propagation velocity with respect to the velocity obtained in the case where the imperfections in the normal direction is absent.
- The existence of the initial compressive stress acting in the direction which is perpendicular to the wave propagation direction significantly changes, in quantitative and qualitative senses, the influence of the imperfection parameters on the wave propagation velocity.

5. GENERALIZED RAYLEIGH WAVE PROPAGATION IN A STRATIFIED HALF-SPACE WITH A LIQUID UPPER LAYER

5.1 Introduction

In the present chapter, the investigation by Negin et al. (2014) on propagation of the generalized Rayleigh waves in an initially stressed elastic half-space covered by an elastic layer is developed for the case where the initial stresses are caused by the uniformly distributed compression forces acting on the face surface of the layered half-space. The three-dimensional linearized theory of elastic waves in initially stressed bodies (TLTEWISB) is utilized and the plane-strain state is considered. Elasticity relations of the materials are described through the Murnaghan potential where the influence of the third order elastic constants is taken into consideration. The dispersion equation for this system is derived and a computer algorithm is developed for numerical solution to this equation. Numerical results for the dispersion of the generalized Rayleigh waves on the influence of the initial stresses and on the influence of the character of the external compressional forces are presented and discussed. Two cases are considered: Case 1: it is assumed that the external forces are "dead" forces. Therefore, in this case the external forces only cause the initial stresses and do not constrain the wave propagation in the layered half-space. Case 2: it is assumed that the external forces are "follower" forces. Consequently, in this case the external forces not only cause the initial stresses, but also constrain the wave propagation in the system. These distributed external forces, can be caused, for instance, by the weight of the liquid on the layered half-space if the system is taken as a model for the soil of the bottom of the oceans.

5.2 Formulation of The Problem

We consider an elastic half-space covered by an elastic layer with thickness h . Figure 5.1 shows the geometry of the problem. The layer and the half-plane occupy the

regions $\{-\infty < x_1 < +\infty, 0 \leq x_2 \leq h, -\infty < x_3 < +\infty\}$ and $\{-\infty < x_1 < +\infty, -\infty < x_2 \leq 0, -\infty < x_3 < +\infty\}$, respectively. Note that the values related to the layer and half-space are denoted by upper indices (1) and (2), respectively. Furthermore, the values relating to the initial state are denoted by the additional upper index 0. We determine the positions of the points by the Lagrange coordinates in the Cartesian system of coordinates $Ox_1x_2x_3$. A plane-strain state in the Ox_1x_2 plane is considered, thus the displacement components along Ox_1 and Ox_2 directions, u_1 and u_2 are non-zero while displacement component u_3 along Ox_3 direction is zero. We assume that the Rayleigh waves propagate in the positive direction of Ox_1 axis.

It is assumed that the considered system is compressed with the uniformly distributed normal forces with the intensity P_0 along its thickness. The uniformly distributed normal force P_0 , as mentioned before, can be caused for instance, by the weight of the fluid on the stratified half-space if the system is taken as a model for the soil of the bottom of the ocean or of the sea or it can also be taken as a model of the weight of the bodies which are located on the stratified half-space under consideration.

According to Guz (2004), the equations of the TLTEWISB are obtained from the corresponding geometrical non-linear equations of motion by their linearization with respect to the perturbations of the stresses, strains and displacements:

$$\begin{aligned}\frac{\partial \sigma_{11}^{(m)}}{\partial x_1} + \frac{\partial \sigma_{12}^{(m)}}{\partial x_2} + P_0 \frac{\partial^2 u_1^{(m)}}{\partial x_2^2} &= \rho^{(m)} \frac{\partial^2 u_1^{(m)}}{\partial t^2}, \\ \frac{\partial \sigma_{12}^{(m)}}{\partial x_1} + \frac{\partial \sigma_{22}^{(m)}}{\partial x_2} + P_0 \frac{\partial^2 u_2^{(m)}}{\partial x_2^2} &= \rho^{(m)} \frac{\partial^2 u_2^{(m)}}{\partial t^2}.\end{aligned}\quad (5.1)$$

Now we formulate the boundary conditions. We assume that the following complete contact conditions between the layer and half-space are satisfied:

$$\begin{aligned}\sigma_{12}^{(1)}|_{x_2=0} &= \sigma_{12}^{(2)}|_{x_2=0}, \quad \sigma_{22}^{(1)}|_{x_2=0} = \sigma_{22}^{(2)}|_{x_2=0}, \\ u_1^{(1)}|_{x_2=0} &= u_1^{(2)}|_{x_2=0}, \quad u_2^{(1)}|_{x_2=0} = u_2^{(2)}|_{x_2=0}.\end{aligned}\quad (5.2)$$

As has been noted in the previous section we consider two cases with respect to the boundary conditions: Case 1: we assume that the external compression forces with intensity P_0 are "dead" forces, i.e. any magnitude in either direction does not change

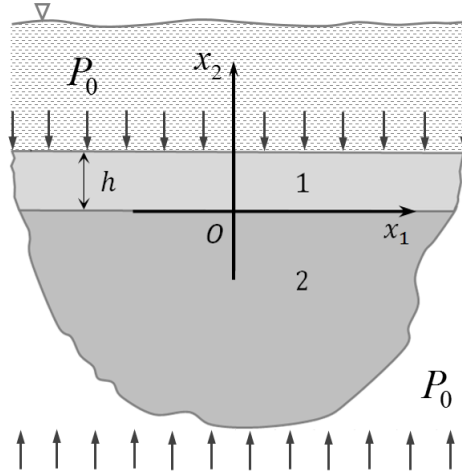


Figure 5.1: Geometry of the considered mechanical system.

in the perturbation state. Therefore, in this case the boundary conditions are as follows:

$$\sigma_{12}^{(1)} \Big|_{x_2=h} = 0, \quad \sigma_{22}^{(1)} \Big|_{x_2=h} = 0. \quad (5.3)$$

Case 2: in this case we assume that the aforementioned forces are "follower" forces. The load is said to be "follower" if it is applied normally to the surface of a body and does not change its direction and magnitude during deformation, i.e. if it acts normally on the surface in the deformed state too. According to this definition of the "follower" forces, we have the boundary conditions written below:

$$\begin{aligned} \sigma_{12}^{(1)} \Big|_{x_2=h} &= -P_0 \frac{\partial u_2^{(1)}}{\partial x_1} \Big|_{x_2=h}, \\ \sigma_{22}^{(1)} \Big|_{x_2=h} &= P_0 \frac{\partial u_1^{(1)}}{\partial x_1} \Big|_{x_2=h}. \end{aligned} \quad (5.4)$$

The expression for the calculation of the "follower" forces acting on the surface, which is also used for writing the conditions (5.4), is given in the monograph by Guz (1999). Moreover, we assume that the following decay conditions also are satisfied:

$$\sigma_{ij}^{(2)} \Big|_{x_2 \rightarrow -\infty} \rightarrow 0, \quad u_i^{(2)} \Big|_{x_2 \rightarrow -\infty} \rightarrow 0, \quad i = 1, 2. \quad (5.5)$$

As stated above, we assume that the constitutive relations of the materials of the constituents are given by the Murnaghan potential. In fact, experimental data detailed in the monograph by Guz (2004) and other references listed therein, show that the absolute values of the influence of the initial stretching and the initial compressing

stresses on the wave propagation velocity in the pre-stressed bodies fabricated from the materials such as those which are chosen in this study, differ from each other in the quantitative sense. Consequently, in a theoretical sense such experimental results can be described only by employing the strain energy potential containing not only the second and the square of the first algebraic invariants of Green's strain tensor, but also the cube of the first invariant, the multiplication of the first and second invariants and the third invariant with corresponding coefficients, i.e. with the third order elastic constants. The Murnaghan potential can be taken as an example of such potential. These third order elastic constants enter into the relations of the TDLTEWISB and through these constants the aforementioned effect of the difference between the absolute values of the influence of the initial stretching and the initial compressing stresses on the wave propagation velocity in the pre-stressed bodies is described and estimated. Therefore, in the present investigation we use the Murnaghan potential which is given as follow (Guz and Makhort (2000)):

$$\Phi^{(m)} = \frac{1}{2}\lambda^{(m)}\left(A_1^{(m)}\right)^2 + \mu^{(m)}A_2^{(m)} + \frac{a^{(m)}}{3}\left(A_1^{(m)}\right)^3 + b^{(m)}A_1^{(m)}A_2^{(m)} + \frac{c^{(m)}}{3}A_3^{(m)}, \quad (5.6)$$

where $\lambda^{(m)}$ and $\mu^{(m)}$ are Lamé's and $a^{(m)}$, $b^{(m)}$ and $c^{(m)}$ are the third order elasticity constants. Here $A_1^{(m)}$, $A_2^{(m)}$ and $A_3^{(m)}$ are the first, second and the third algebraic invariants of Green's strain tensor respectively. For the case under consideration, the expressions of these invariants are:

$$\begin{aligned} A_1^{(m)} &= \varepsilon_{11}^{(m)'} + \varepsilon_{22}^{(m)'}, \\ A_2^{(m)} &= \left(\varepsilon_{11}^{(m)'}\right)^2 + 2\left(\varepsilon_{12}^{(m)'}\right)^2 + \left(\varepsilon_{22}^{(m)'}\right)^2, \\ A_3^{(m)} &= \left(\varepsilon_{11}^{(m)'}\right)^3 + 3\left(\varepsilon_{12}^{(m)'}\right)^2\left(\varepsilon_{11}^{(m)'} + \varepsilon_{22}^{(m)'}\right) + \left(\varepsilon_{22}^{(m)'}\right)^3, \end{aligned} \quad (5.7)$$

where

$$\begin{aligned} \varepsilon_{ij}^{(m)'} &= \frac{1}{2} \left(\frac{\partial u_i^{(m)'}}{\partial x_j} + \frac{\partial u_j^{(m)'}}{\partial x_i} + \frac{\partial u_n^{(m)'}}{\partial x_j} \frac{\partial u_n^{(m)'}}{\partial x_j} \right), \\ \sigma_{ij}^{(m)'} &= \frac{1}{2} \left(\frac{\partial}{\partial \varepsilon_{ij}^{(m)'}} + \frac{\partial}{\partial \varepsilon_{ji}^{(m)'}} \right) \Phi^{(m)}. \end{aligned} \quad (5.8)$$

Note that the upper prime on the symbols $u_i^{(m)'} = (u_i^{(m),0} + u_i^{(m)})$, $\varepsilon_{ij}^{(m)'} = (\varepsilon_{ij}^{(m),0} + \varepsilon_{ij}^{(m)})$ and $\sigma_{ij}^{(m)'} = (\sigma_{ij}^{(m),0} + \sigma_{ij}^{(m)})$ denote the total values of the displacements, strains and

stresses, respectively. Consequently, in the case under consideration by linearization of the non-linear relations with respect to the perturbations, i.e. with respect to $u_i^{(m)}$, $\varepsilon_{ij}^{(m)}$ and $\sigma_{ij}^{(m)}$, the following linearized constitutive relations for the layer and the half-space materials are obtained.

$$\begin{aligned}\sigma_{11}^{(m)} &= A_{11}^{(m)} \varepsilon_{11}^{(m)} + A_{12}^{(m)} \varepsilon_{22}^{(m)}, \\ \sigma_{22}^{(m)} &= A_{12}^{(m)} \varepsilon_{11}^{(m)} + A_{22}^{(m)} \varepsilon_{22}^{(m)}, \\ \sigma_{12}^{(m)} &= 2\mu_{12}^{(m)} \varepsilon_{12}^{(m)},\end{aligned}\tag{5.9}$$

where

$$A_{11}^{(m)} = \lambda^{(m)} + 2\mu^{(m)} + \frac{2P_0}{3K_0^{(m)}} \left[\left(a^{(m)} + b^{(m)} \right) - \left(2b^{(m)} + c^{(m)} \right) \frac{\lambda^{(m)}}{2\mu^{(m)}} \right],$$

$$\begin{aligned}A_{22}^{(m)} &= \lambda^{(m)} + 2\mu^{(m)} + \frac{P_0}{\mu^{(m)}} \left(2b^{(m)} + c^{(m)} \right) \\ &\quad + \frac{2P_0}{3K_0^{(m)}} \left[\left(a^{(m)} + b^{(m)} \right) - \left(2b^{(m)} + c^{(m)} \right) \frac{\lambda^{(m)}}{2\mu^{(m)}} \right],\end{aligned}$$

$$A_{12}^{(m)} = \lambda^{(m)} + \frac{b^{(m)}}{\mu^{(m)}} P_0 + \frac{2P_0}{3K_0^{(m)}} \left[a^{(m)} - b^{(m)} \frac{\lambda^{(m)}}{\mu^{(m)}} \right],$$

$$\mu_{12}^{(m)} = \mu^{(m)} + \frac{b^{(m)}}{3K_0^{(m)}} P_0 + \frac{c^{(m)} P_0}{4\mu^{(m)}} \left[\frac{\lambda^{(m)} + 2\mu^{(m)}}{3K_0^{(m)}} \right],$$

$$K_0^{(m)} = \lambda^{(m)} + \frac{2\mu^{(m)}}{3},$$

$$\varepsilon_{ij}^{(m)} = \frac{1}{2} \left(\frac{\partial u_i^{(m)}}{\partial x_j} + \frac{\partial u_j^{(m)}}{\partial x_i} \right).\tag{5.10}$$

This completes the formulation of the problem and in the case where P_0 , this formulation transforms to the corresponding one made within the scope of the classical linear theory of elastodynamics.

5.3 Method of the Solution

Each displacements component of the considered system are represent as follows:

$$\begin{aligned} u_1^{(m)} &= \varphi_1^{(m)}(x_2) \sin(kx_1 - \omega t), \\ u_2^{(m)} &= \varphi_2^{(m)}(x_2) \cos(kx_1 - \omega t). \end{aligned} \quad (5.11)$$

Substituting presentation (5.11) into the relations (5.10) and (5.9) we obtain the following equations for the $\varphi_1^{(m)}(x_2)$ and $\varphi_2^{(m)}(x_2)$ from the equation of motion (5.1):

$$\begin{aligned} \frac{d^2 \varphi_1^{(m)}}{d(kx_2)^2} + b_{21}^{(m)} \varphi_1^{(m)} + c_{21}^{(m)} \frac{d \varphi_2^{(m)}}{d(kx_2)} &= 0, \\ \frac{d^2 \varphi_2^{(m)}}{d(kx_2)^2} + b_{22}^{(m)} \varphi_2^{(m)} + c_{22}^{(m)} \frac{d \varphi_1^{(m)}}{d(kx_2)} &= 0, \end{aligned} \quad (5.12)$$

where

$$\begin{aligned} b_{21}^{(m)} &= -\frac{A_{11}^{(m)}}{\mu_{12}^{(m)} + \sigma_{22}^{(m),0}} - \frac{\sigma_{11}^{(m),0}}{\mu_{12}^{(m)} + \sigma_{22}^{(m),0}} + \frac{\rho^{(m)} \omega^2}{\left(\mu_{12}^{(m)} + \sigma_{22}^{(m),0}\right) k^2}, \\ b_{22}^{(m)} &= -\frac{\mu_{12}^{(m)}}{A_{22}^{(m)} + \sigma_{22}^{(m),0}} - \frac{\sigma_{11}^{(m),0}}{A_{22}^{(m)} + \sigma_{22}^{(m),0}} + \frac{\rho^{(m)} \omega^2}{\left(A_{22}^{(m)} + \sigma_{22}^{(m),0}\right) k^2}, \\ c_{21}^{(m)} &= \frac{-A_{12}^{(m)} - \mu_{12}^{(m)}}{\mu_{12}^{(m)} + \sigma_{22}^{(m),0}}, \quad c_{22}^{(m)} = \frac{\mu_{12}^{(m)} + A_{12}^{(m)}}{A_{22}^{(m)} + \sigma_{22}^{(m),0}}. \end{aligned} \quad (5.13)$$

After some mathematical procedures, we derive the following equation for $\varphi_2^{(m)}(x_2)$:

$$\begin{aligned} \frac{d^4 \varphi_2^{(m)}}{d(kx_2)^4} + B_2^{(m)} \frac{d^2 \varphi_2^{(m)}}{d(kx_2)^2} + C_2^{(m)} \varphi_2^{(m)} &= 0, \\ B_2^{(m)} &= b_{22}^{(m)} + b_{21}^{(m)} - c_{21}^{(m)} c_{22}^{(m)}, \quad C_2^{(m)} = b_{21}^{(m)} b_{22}^{(m)}. \end{aligned} \quad (5.14)$$

We determine the solution to the equation (5.14) as follows:

$$\begin{aligned} \varphi_2^{(1)}(x_2) &= Z_1^{(1)} \exp\left(R_1^{(1)} kx_2\right) + Z_2^{(1)} \exp\left(-R_1^{(1)} kx_2\right) \\ &\quad + Z_3^{(1)} \exp\left(R_2^{(1)} kx_2\right) + Z_4^{(1)} \exp\left(-R_2^{(1)} kx_2\right), \\ \varphi_2^{(2)}(x_2) &= Z_1^{(2)} \exp\left(R_1^{(2)} kx_2\right) + Z_3^{(2)} \exp\left(R_2^{(2)} kx_2\right), \end{aligned} \quad (5.15)$$

where

$$R_1^{(m)} = \sqrt{-\frac{B_2^{(m)}}{2} + \sqrt{\frac{\left(B_2^{(m)}\right)^2}{4} - C_2^{(m)}}}, \quad R_2^{(m)} = \sqrt{-\frac{B_2^{(m)}}{2} - \sqrt{\frac{\left(B_2^{(m)}\right)^2}{4} - C_2^{(m)}}}. \quad (5.16)$$

In a similar way using (5.16) we can also determine the function $\varphi_1^{(m)}(x_2)$ from (5.12). Finally, we obtain the dispersion equation considering the conditions (5.3) – (5.5). This dispersion equation after some mathematical manipulations can be expressed formally as follows:

$$\det \left\| \alpha_{ij} \left(c, kh, P_0, a^{(1)}, b^{(1)}, c^{(1)}, a^{(2)}, b^{(2)}, c^{(2)} \right) \right\| = 0, \quad (5.17)$$

where $i, j = 1, 2, \dots, 6$ and

$$c = \frac{\omega}{k}, \quad c_1^{(m)} = \sqrt{\frac{\lambda^{(m)} + 2\mu^{(m)}}{\rho^{(m)}}}, \quad c_2^{(m)} = \sqrt{\frac{\mu^{(m)}}{\rho^{(m)}}}. \quad (5.18)$$

We will assume that,

$$\operatorname{Re} R_1^{(1)} = \operatorname{Re} R_2^{(1)} = 0, \quad R_1^{(2)} > 0, \quad R_2^{(2)} > 0. \quad (5.19)$$

This is concise way of saying that in order to satisfy the conditions (5.19) the following relations must hold:

$$B_2^{(1)} > 0, \quad C_2^{(1)} > 0, \quad B_2^{(2)} < 0, \quad C_2^{(2)} < 0, \quad (5.20)$$

The relations (5.20) hold when:

$$\max \left(\tilde{c}_1^{(1)}, \tilde{c}_2^{(1)}, \tilde{c}_3^{(1)} \right) < c < \min \left(\tilde{c}_1^{(2)}, \tilde{c}_2^{(2)}, \tilde{c}_3^{(2)} \right) \quad (5.21)$$

where

$$\begin{aligned} \tilde{c}_1^{(m)} &= \sqrt{\frac{A_{11}^{(m)}}{\rho^{(m)}} \left(1 + \frac{\sigma_{11}^{(m),0}}{A_{11}^{(m)}} \right)}, \quad \tilde{c}_2^{(m)} = \sqrt{\frac{\mu_{12}^{(m)}}{\rho^{(m)}} \left(1 + \frac{\sigma_{11}^{(m),0}}{\mu_{12}^{(m)}} \right)}, \\ \tilde{c}_3^{(m)} &= \sqrt{\frac{A_{11}^{(m)}}{\rho^{(m)}} \left(\frac{\frac{A_{22}^{(m)} + P_0}{\mu_{12}^{(m)} + A_{22}^{(m)} + 2P_0} + \frac{\mu_{12}^{(m)}}{A_{11}^{(m)}} \frac{\mu_{12}^{(m)} + P_0}{\mu_{12}^{(m)} + A_{22}^{(m)} + 2P_0} \right) - \frac{\left(\mu_{12}^{(m)} + A_{12}^{(m)} \right)^2}{A_{11}^{(m)} \left(\mu_{12}^{(m)} + A_{22}^{(m)} + 2P_0 \right)}}. \end{aligned} \quad (5.22)$$

The relation (5.21) guarantee that $R_1^{(2)}, R_2^{(2)}$ always be real and positive and $R_1^{(1)}, R_2^{(1)}$ always be pure imaginary. Note that the other cases under which the (5.20) – (5.22) are violated, in the present work do not considered. This completes the solution method of the problem under consideration.

The explicit expressions of the α_{ij} ($i, j = 1, 2, \dots, 6$) in the dispersion equation (5.17) are given in Appendix A.3. This completes the solution method of the problem under consideration.

5.4 Numerical Results and Discussion

In the cases where the assumptions (5.19) – (5.22) are satisfied the solution (15) corresponds to such a wave propagation in the layered half-space that the layer undergoes an oscillatory motion in the Ox_2 direction propagating in the Ox_1 direction with velocity c . The disturbances in the layer decay exponentially with depth in the half-space and therefore the wave can be considered as a generalized Rayleigh wave confined to the pre-stressed covered layer. The dispersion equation (5.17) has infinitely many modes unlike ordinary Rayleigh waves, which can propagate only in one mode. Moreover, the dispersion curves related to each mode has two branches which were denoted by M_{1n} and M_{2n} respectively for the n -th mode. For the first M_{1n} branches the displacement of the layer circumscribes the ellipse similar to the ordinary Rayleigh waves, but for the second M_{2n} branches leads to an opposite type of motion. Moreover, according to the restriction (5.19), it must be $c/c_2^{(2)} < 1$ and $c/c_1^{(1)} > 1$, i.e. the near-surface waves propagated in the system under consideration is subsonic in the half-space, but it is supersonic in the covering layer (Tolstoy and Usdin (1953)).

In this study we consider some pairs of the real materials, values of the mechanical constants of which are given in Table 5.1 (i.e. the values of the mechanical constants which enter the expression (5.6) of the Murnaghan potential). We select four pairs from these materials. For the *I*, *II*, *III* and *IV* pairs, the material of the covering layer we take as *bronze*, *brass 59-1*, *brass 62* and *Plexiglas*, respectively, but for all the pairs the material of the half-space we take as *steel*.

For estimation of the magnitude of the initial stresses we introduce the parameter:

$$\psi = P_0/\mu^{(2)}. \quad (5.23)$$

Moreover, we introduce the notation:

$$\eta = \frac{c|_{\psi \neq 0} - c|_{\psi=0}}{c|_{\psi=0}}, \quad (5.24)$$

for estimation of the influence of the initial stresses in the constituents, i.e. the influence of the parameters ψ on the wave propagation velocity. Thus, through the graphs of the dependencies between η (5.24) and kh constructed for various values of the parameters ψ we analyze the effect of the initial stresses in the constituents on the wave propagation velocity.

Table 5.1: The values of elastic constants of the selected materials (Guz ,2004).

Materials	ρ (g/cm ³)	$\lambda \times 10^{-4}$ (MPa)	$\mu \times 10^{-4}$ (MPa)	$a \times 10^{-5}$ (MPa)	$b \times 10^{-5}$ (MPa)	$c \times 10^{-5}$ (MPa)
Steel 3	7.795	9.26	7.75	-2.35	-2.75	-4.90
Bronze	7.20	8.16	3.84	1.20	-3.10	4.80
Brass 59–1	7.20	9.49	4.47	-0.70	2.70	-3.40
Brass 62	7.20	9.49	4.47	-2.80	-2.10	-3.20
Plexiglas	1.16	0.404	0.19	2.68×10^{-3}	-3.12×10^{-2}	-6.77×10^{-2}

Figure 5.2 shows the dispersion curves obtained for the first branch of the first mode of the generalized Rayleigh wave for the *I* pair of the materials for both dead and follower forces. Figure 5.2a shows the results for the case when the third order elasticity constants are not considered. It follows from this figure, that for all values of the kh , under the action of the dead forces the wave propagation velocity c decreases with increasing ψ , i.e. with increasing absolute values of the compressional forces that cause the initial stresses. However, under the action of the follower forces the character of the influence of the ψ on the values of c changes completely in the opposite direction, i.e. under the action of the follower forces wave propagation velocity increases with increasing ψ .

Figure 5.2b shows the results for the case when the third order elasticity constants are not zero. It follows from these graphs that considering the effect of third order elasticity constants into account, for both dead and follower cases, first of all the character of dispersion curves will be similar for dead and follower forces and the second, not only the effect of initial compressional forces increases dramatically in this cases, but the character of the dispersion curves changes completely. For example in the case of dead forces (follower forces) wave propagation velocity increases with increasing before some value of the wavenumber, say $kh \approx 2.3$ ($kh \approx 3.4$ in the case of follower forces) and decreases after that value with increasing ψ .

Figure 5.3 shows the dispersion curves obtained for the first branch of the first mode for the *II* and *III* pairs of the materials for both dead and follower forces for the case when the third order elasticity constants are not zero. As can be seen from these figures for both these material pairs and for both cases of the initial stresses the wave propagation velocity increases as the absolute values of the compressional forces increase.

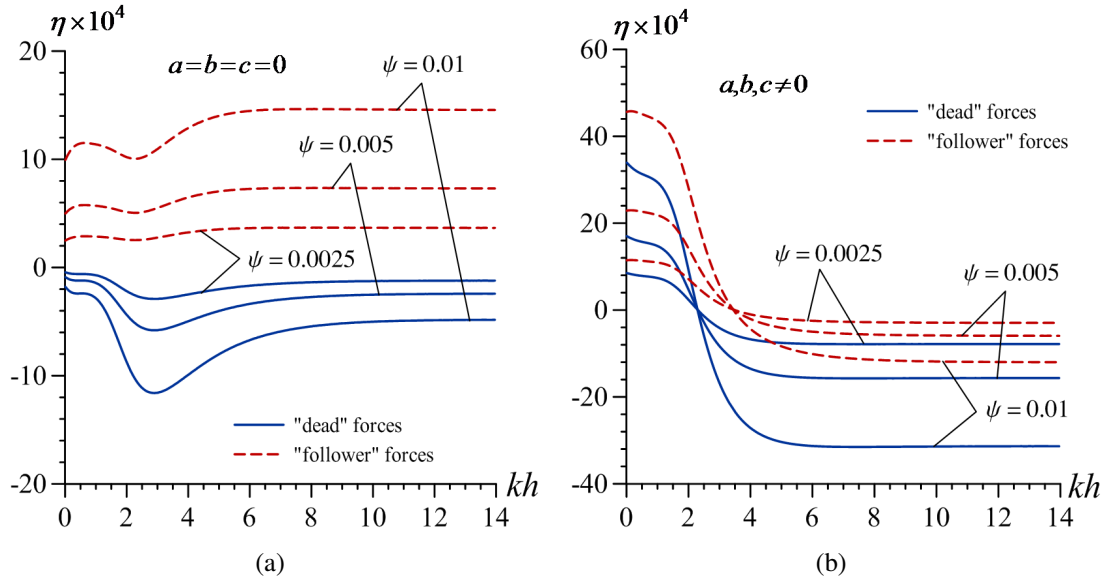


Figure 5.2: Influence of the compressional "dead" and "following" forces to the dispersion of the generalized Rayleigh wave for the *I* pair of the materials for the first branch of the first mode when (a) $a = b = c = 0$ and (b) $a, b, c \neq 0$.

Figure 5.4 illustrate the dispersion curves of the first branch of the first mode for the *IV* pair of the materials and influence of the dead and follower forces on the wave dispersion curves for the cases when the third order elasticity constants are taken to be zero (a) and when they are considered to not to be zero (b). It follows from these graphs that as in the case of the *I* pair of the materials considering the effect of the third order elasticity constants into account the influence of initial compressional forces increases dramatically. Furthermore, character of the wave propagation curves depends on the wavenumbers, for example in the case of follower forces (Figure 5.4a) wave propagation velocity decreases with increasing ψ before some value of the wavenumber (say $kh \approx 3$) and increases after that value with increasing ψ . Finally, for this material case the low wavenumber limit values of the wave propagation velocity as $kh \rightarrow 0$ do not depend on the character of the initial compressional forces, i.e. dead or follower forces.

Dispersion curves related to the second branch of the first mode for all four material pairs have been shown in Figure 5.5 for the case where the third order elasticity constants are considered in the analysis. Thus, it follows from Figure 5.5 that the dimensionless wavenumber kh has cut off values for the second branch of the first

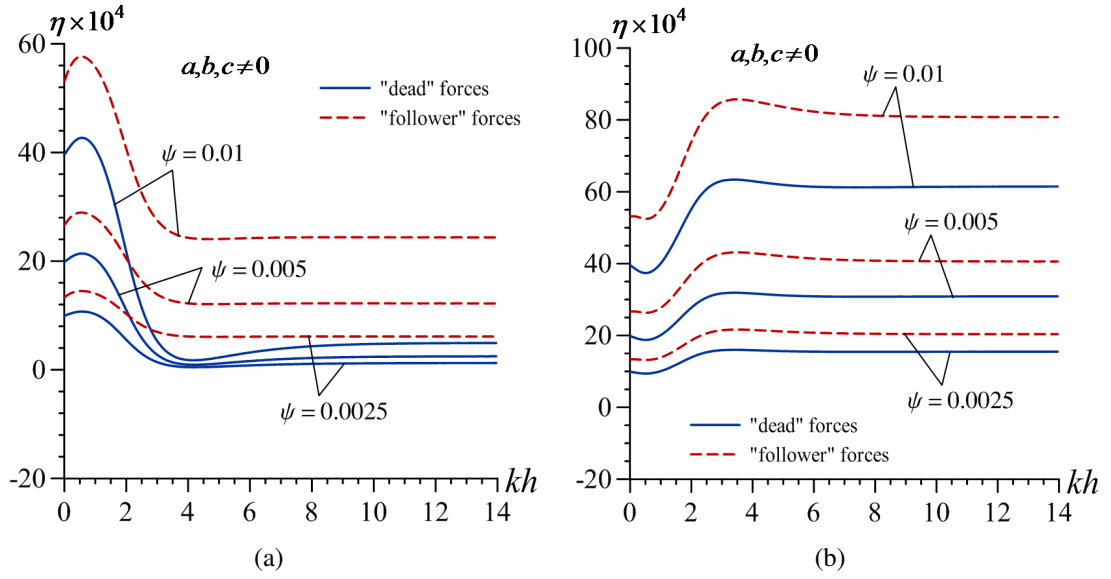


Figure 5.3: Influence of the compressional "dead" and "following" forces to the dispersion of the generalized Rayleigh wave for the (a) *II* pair and (b) *III* pair of the materials for the first branch of the first mode when $a, b, c \neq 0$.

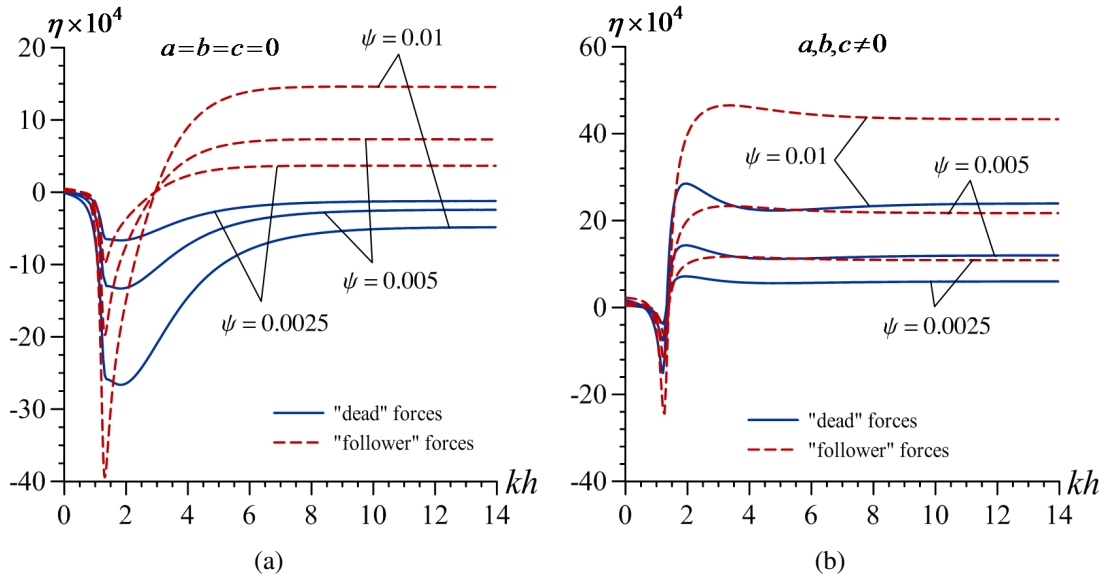


Figure 5.4: Influence of the compressional "dead" and "following" forces to the dispersion of the generalized Rayleigh wave for the *IV* pair of the materials for the first branch of the first mode when (a) $a = b = c = 0$ and (b) $a, b, c \neq 0$.

mode. Furthermore, low and high wavenumber limit values of the wave propagation velocity as $kh \rightarrow 0$ and $kh \rightarrow \infty$, respectively, do not depend on the character of the initial compressional forces, i.e. on the dead or follower forces. It follows from Figure 5.5b and Figure 5.5c that in the case of the *II* and the *III* pairs of the materials the wave propagation velocity increase monotonically as the values of initial compressional forces, i.e. ψ increase. However, in the case of the *I* and the *IV* pairs of the materials, Figure 5.5a and Figure 5.5d respectively, the character of the wave propagation curves depend on the wavenumbers. For example, in Figure 5.5a the wave propagation velocity decreases with increasing the absolute values of ψ after some value of the wavenumber (say $kh \approx 4.8$) and increases after that value with increasing ψ . Or in Figure 5.5d the wave propagation velocity decreases with increasing the absolute values of ψ after some value of the wavenumber (say $kh \approx 4.3$) and increases after that value with increasing ψ .

Finally, we consider the graphs given in Figure 5.6 and Figure 5.7 which illustrate the dependence between η and kh constructed for the first and second branches of the second mode for the *IV* pair of the materials. Similar results as previous ones can be obtained here. First of all, it follows from these figures that for the first and second branch of the second mode the dimensionless wavenumber kh also has cut off values. Figure 5.6 shows the results for the case when the third order elasticity constants are taken to be zero. It follows from this figure, that for all values of the kh , under the action of the dead forces the wave propagation velocity c decreases with increasing the absolute value of the compressional forces that cause the initial stresses. Figure 5.7 shows the results for the case when the third order elasticity constants are not zero. It follows from these graphs that considering the third order elasticity constants into account, has similar effects on both dead and follower cases, and the character of the influence of the ψ on the values of wave propagation velocity c changes completely. For example in Figure 5.7a wave propagation velocity decreases with increasing ψ before some value of the wavenumber (say $kh \approx 6.7$) and increases after that value with increasing ψ for the first branch of the second mode or in Figure 5.7b wave propagation velocity behavior changes after some value of the wavenumber (say $kh \approx 9.3$) for the second branch of the second mode.

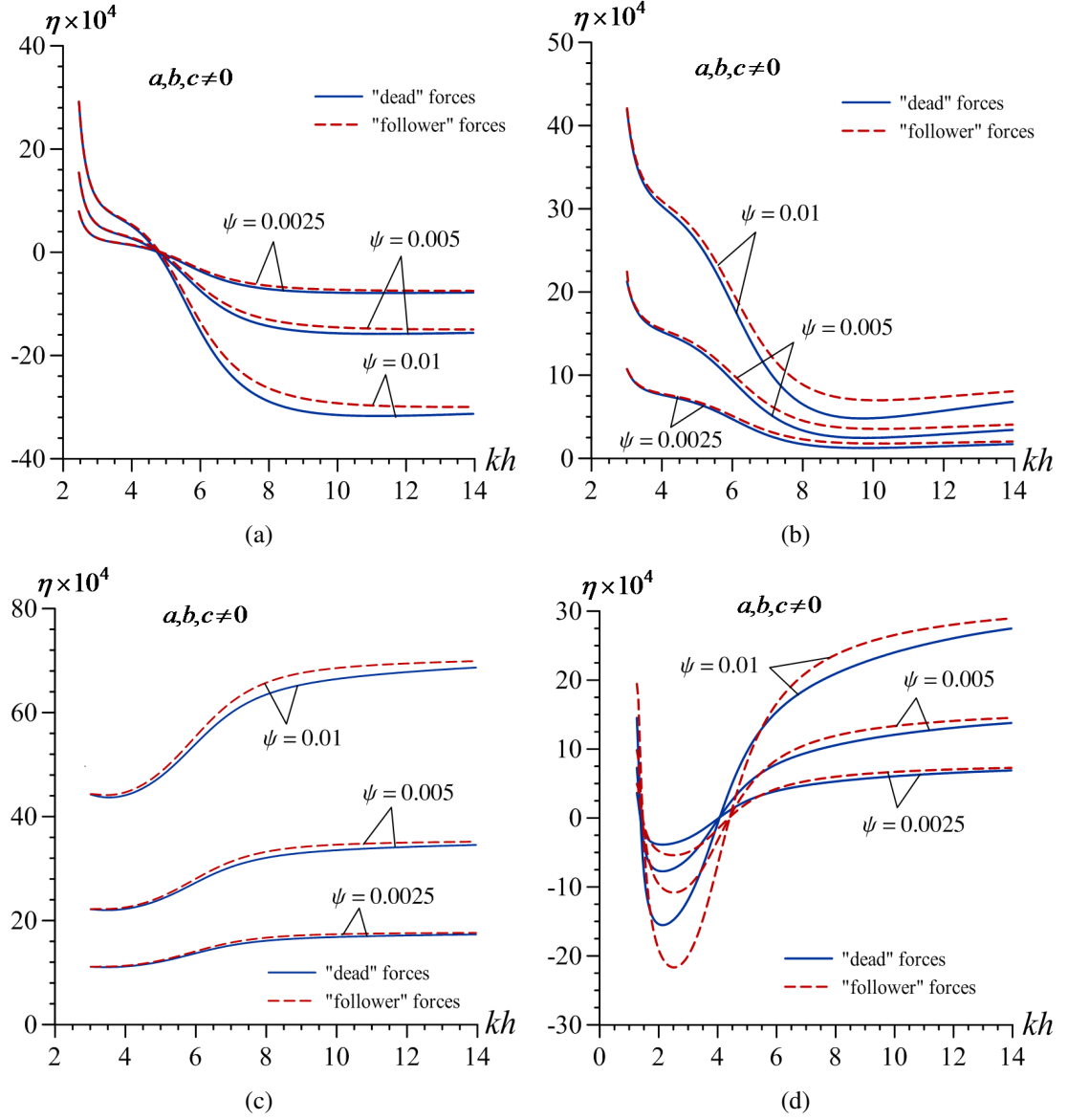


Figure 5.5: The influence compressional "dead" and "following" forces to the dispersion of the generalized Rayleigh wave for the (a) I, (b) II, (c) III and (d) IV pairs of materials for the second branch of the first mode when $a, b, c \neq 0$.

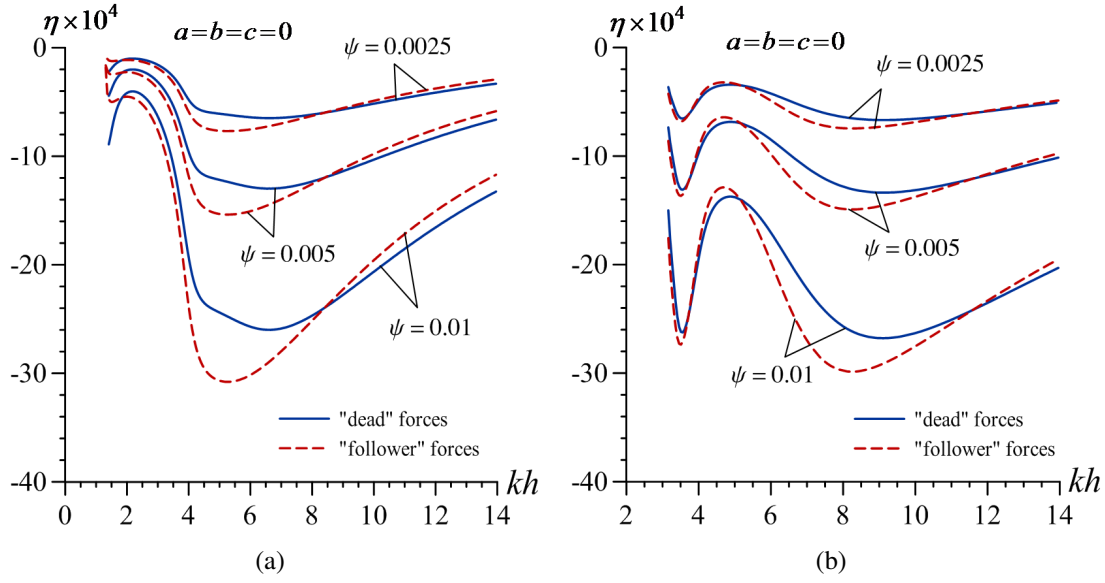


Figure 5.6: Influence of the compressional "dead" and "following" forces to the dispersion of the generalized Rayleigh wave for the *IV* pair of the materials for the (a) first and (b) second branches of the second mode when $a = b = c = 0$.

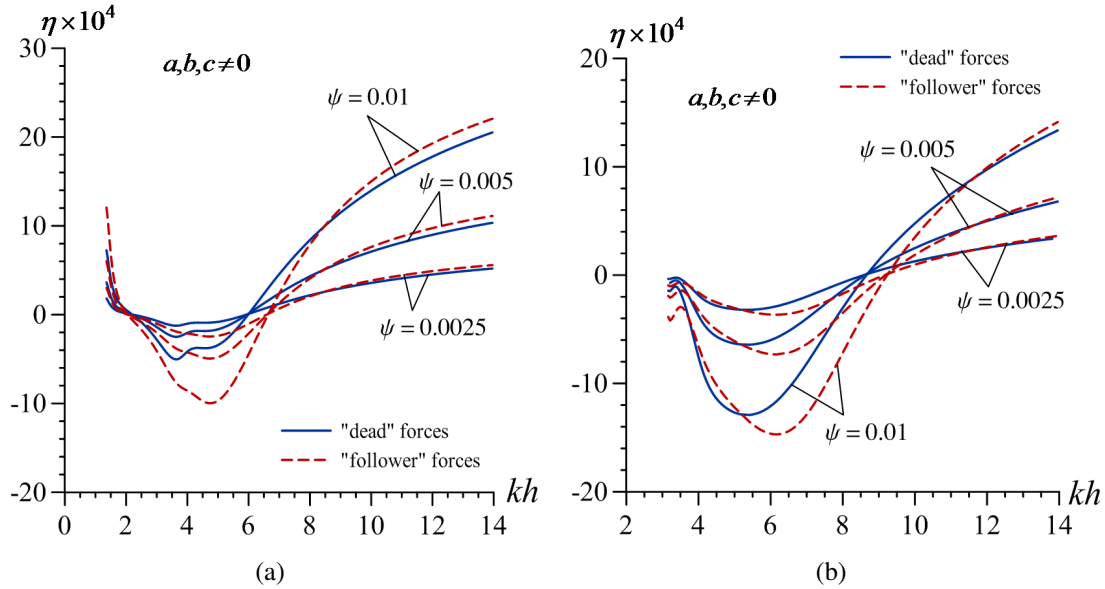


Figure 5.7: Influence of the compressional "dead" and "following" forces to the dispersion of the generalized Rayleigh wave for the *IV* pair of the materials for the (a) first and (b) second branches of the second mode when $a, b, c \neq 0$.

5.5 Conclusion

In the present paper within the scope of the piecewise homogeneous body model with the use of the three-dimensional linearized theory of elastic waves in initially stressed bodies, dispersion of the generalized Rayleigh waves in an initially stressed elastic half-space covered by an elastic layer is investigated. It is assumed that the initial stresses are caused by the uniformly distributed normal compressional forces acting on the face surface of the covering layer. Two cases are considered: in Case 1 it is supposed that the compressional forces are "dead" forces, while in Case 2 it is assumed that they are "follower" ones. The dispersion equations for each case are obtained and an algorithm was developed to do numerical investigations. The basic numerical results for the low and high wave number limit values of the wave propagation velocity are presented and discussed. Moreover, the numerical results related to different branches of the first and second modes are presented and the effect of third order elasticity constants are considered yielding the following main conclusions:

- In the case where the initial stresses in the considered system are caused by the compressional "dead" forces which act on the face surface of the covering layer, for all values of kh the propagation velocity of the generalized Rayleigh wave decreases with the absolute values of the compressional forces (i.e., with decreasing ψ).
- In the case where the above mentioned forces are the "follower" ones, the character of the influence of the initial stresses on the wave propagation velocity is more complicated and in general depends on the values of kh . For example, in the case of first branch of first mode for the I pair of the materials wave propagation velocity increases with increasing ψ before a value of the wavenumber and decreases after that value with increasing ψ .
- Taking the third order elastic constants into account the character of the influence of the initial stresses on the velocity of wave propagation vary for different material pairs and before (after) some values of kh decrease (increases) the velocity of wave propagation.

6. CONCLUSIONS AND RECOMMENDATIONS

The influence of shear-spring + normal-spring type imperfect interface conditions on the dispersion of the generalized Rayleigh waves in the system consisting of a covering layer and a half-space with two-axial homogeneous initial stresses is investigated. The three-dimensional linearized theory of elastic waves in initially stressed bodies (TLTEWISB) is employed and the plane-strain state is considered. The elasticity relations of the materials of the constituents are described through the Murnaghan potential and the influence of the third order elastic constants which enter the expression of this potential is taken into consideration. The corresponding dispersion equation is derived and the algorithm is developed for numerical solution to this equation. Numerical results on the action of the parameters which enter the formulation of the imperfect contact conditions on the wave dispersion curves are presented and discussed. The results of these investigations can be successfully used for estimation of the degree of the bonded defects between the covering layer and half-space. According to these results the following main conclusions can be made:

- The imperfectness of the contact conditions causes to decrease of the wave propagation velocity of the generalized Rayleigh waves.
- The low and high wavenumber limit values of the wave propagation velocity, i.e. the wave propagation velocity as $kh \rightarrow 0$ and as $kh \rightarrow \infty$ do not depend on the imperfection parameters F_1 and F_2 .
- The dispersion curve constructed for each value of the parameter F is limited with corresponding ones obtained at $F = 0$ (upper limit) and $F = \infty$ (lower limit).
- Existence of the imperfection in normal direction considerably decreases the wave propagation velocity with respect to the velocity obtained in the case where the imperfections in the normal direction is absent.

- The existence of the initial compressive stress acting in the direction which is perpendicular to the wave propagation direction significantly changes, in quantitative and qualitative senses, the influence of the imperfection parameters on the wave propagation velocity.
- The low wavenumber and high wavenumber limit values of the wave propagation velocity do not depend on the imperfectness of the contact conditions. However, the cut off values of the dimensionless wavenumber kh of the first and second branches of the second modes for the pair of materials used by Tolstoy and Usdin (1953) and for the *IV* pair of materials depend significantly on the parameter F .
- In the case where the complete contact conditions are satisfied between the constituents the wave propagation velocity decrease monotonically with the dimensionless wavenumber kh , however in the case where there exists the shear-spring type imperfect conditions between the constituents the dependence between the wave propagation velocity and the dimensionless wavenumber kh may become non-monotonic for some pair of materials. Consequently, the imperfectness of the contact conditions acts on the dispersion curves and, in general, on the dynamics of the system under consideration not only quantitatively, but also qualitatively.

Numerical results related to the action of the initial stresses in the constituents under the influence of the imperfectness parameter F on the wave propagation velocity are presented and discussed for four pairs of materials (Table 3.1). Throughout these discussions the magnitude of the initial stresses is estimated by the parameters $\psi^{(1)}$ and $\psi^{(2)}$ (3.30), and four cases indicated in (3.31) with respect to the signs of the $\psi^{(1)}$ and $\psi^{(2)}$ are considered, but the change in the values of the wave propagation velocity is estimated through the parameter η (3.32). We can make the following main conclusions related to the action of the parameter F on the influence of the initial stresses on the wave propagation velocity:

- The imperfectness of the contact conditions causes to increase the influence of the initial stress in the covering layer on the wave propagation velocity related to the

first branch of the first mode and to the second branch of the second mode of the *I* pair of materials. However, the character of the effect of the imperfectness of the contact conditions, i.e. of the parameter F on the influence of the initial stress in the covering layer on the wave propagation velocity related to the second branch of the first mode and to the first branch of the second mode depends on the values of the dimensionless wavenumber kh .

- As a result of the initial compression of the half-plane the wave propagation velocity related to the *II* (or *III*) and *IV* pairs of materials in Case 2 increase monotonically with the absolute values of the parameter $\psi^{(2)}$. In this case before (after) a certain value of the kh , the influence of the parameter F causes to increase (decrease) the wave propagation velocity related to the first branch of the first mode of the *II* pair of materials. At the same time, as a result of the influence of the parameter F the wave propagation velocities related to the second branch of the first mode, the first and second branches of the second mode of the *II* pair of materials decrease. The magnitude of this decreasing depends significantly on the values of the dimensionless wavenumber kh .
- In general, the graphs of the dependence between the parameters η and kh , i.e. the influence of the initial stresses on the wave propagation velocity obtained for each value of F cannot be limited with the corresponding ones obtained at $F = 0$ (complete contact) and $F = \infty$ (full slipping). This conclusion rises again the significance of the investigations carried out in the present paper.
- In the case where the initial stresses in the considered system are caused by the compressional "dead" forces which act on the face surface of the covering layer, for all values of kh the propagation velocity of the generalized Rayleigh wave decreases with the absolute values of the compressional forces (i.e., with decreasing ψ).
- In the case where the above mentioned forces are the "follower" ones, the character of the influence of the initial stresses on the wave propagation velocity is more complicated and in general depends on the values of kh . For example, in the case of first branch of first mode for the *I* pair of the materials wave propagation velocity

increases with increasing ψ before a value of the wavenumber and decreases after that value with increasing ψ .

- Numerical results obtained for the *IV* pair of materials under complete contact conditions are validated with the corresponding experimental ones which were detailed in the paper by Lu; Zhang and Wang (2006).
- The character of the influence of the imperfectness of the contact between the covering layer and half plane on the generalized Rayleigh wave propagation velocity in the qualitative sense is validated with the experimental ones given by Zurn and Mantell (2001) and Castaings; Hosten and Francois (2004).
- Dispersion curves for the pair of materials considered in the paper by Lakestani; Coste and Denis (1995) are also obtained and the possible application of the numerical results under determination of the structural parameters and residual stresses in the coated materials is proposed.
- The possible application of the numerical results which are similar to the obtained ones and relate to the determination of the soil structure and stiffness in the geophysical and geotechnical engineering is also discussed and corresponding numerical results are presented for the case considered in the paper by Foti (2002).

Many other details of the results obtained for the initially stressed cases are discussed in the text.

Rapid development of electronic devices, specially, has revolutionized elastic surface waves applications in many engineering fields through the last decade. Indeed, variety of mechanical, material and structural properties, presence of damages or cracks, etc. make the study of these wave processes an active field of research. In our study, we consider the effects of some of those parameters, namely the effect of constant initial stresses and imperfect contact conditions in the problem, however, in the future works it is desirable to consider the effect of different patterns of inhomogeneous initial stresses rather than only the constant ones. It is also possible to consider the effects of lateral inhomogeneity in material properties of the medium. It is desirable to consider

the role of viscosity in the interface and its influence on the dispersion of surface waves.
This study can be extended to include such interesting type of problems.

REFERENCES

- Achenbach, J. D., Keshava, S. P., & Herrmann, G.** (1967). Moving load on a plate resting on an elastic half space. *Journal of Applied Mechanics*, 34(4), 910-914.
- Acosta-Colon, A., Pyrak-Nolte, L. J., & Nolte, D. D.** (2009). Laboratory-scale study of field of view and the seismic interpretation of fracture specific stiffness. *Geophysical Prospecting*, 57(2), 209-224.
- Akbarov, S. D., & Ozisik, M.** (2003). The influence of the third order elastic constants to the generalized Rayleigh wave dispersion in a pre-stressed stratified half-plane. *International journal of engineering science*, 41(17), 2047-2061.
- Akbarov, S. D.** (2007). Recent investigations on dynamic problems for an elastic body with initial (residual) stresses (review). *International Applied Mechanics*, 43(12), 1305-1324.
- Akbarov, S., & İlhan, N.** (2008). Dynamics of a system comprising a pre-stressed orthotropic layer and pre-stressed orthotropic half-plane under the action of a moving load. *International Journal of Solids and Structures*, 45(14), 4222-4235.
- Akbarov, S., & İlhan, N.** (2009). Dynamics of a system comprising an orthotropic layer and orthotropic half-plane under the action of an oscillating moving load. *International Journal of Solids and Structures*, 46(21), 3873-3881.
- Akbarov, S. D., & Salmanova, K. A.** (2009). On the dynamics of a finite pre-strained bi-layered slab resting on a rigid foundation under the action of an oscillating moving load. *Journal of Sound and Vibration*, 327(3), 454-472.
- Akbarov, S. D., & Ipek, C.** (2010). The influence of the imperfectness of the interface conditions on the dispersion of the axisymmetric longitudinal waves in the pre-strained compound cylinder. *Computer Modeling in Engineering and Sciences*, 70(2), 93-121.
- Akbarov, S. D., Agasiyev, E. R., & Zamanov, A. D.** (2011). Wave propagation in a pre-strained compressible elastic sandwich plate. *European Journal of Mechanics-A/Solids*, 30(3), 409-422.
- Akbarov, S. D.** (2012). The influence of third order elastic constants on axisymmetric wave propagation velocity in the two-layered pre-stressed hollow cylinder. *Computers, Materials, & Continua*, 32(1), 29-60.

- Akbarov, S. D., & Ipek, C.** (2012). Dispersion of Axisymmetric Longitudinal Waves in a Pre-Strained Imperfectly Bonded Bi-Layered Hollow Cylinder. *Computers Materials and Continua*, 30(2), 99-144.
- Berger, J. R., Martin, P. A., & McCaffery, S. J.** (2000). Time-harmonic torsional waves in a composite cylinder with an imperfect interface. *The Journal of the Acoustical Society of America*, 107(3), 1161-1167.
- Biot, M. A.** (1965). *Mechanics of incremental deformations: theory of elasticity and viscoelasticity of initially stressed solids and fluids, including thermodynamic foundations and applications to finite strain*. New York, Wiley.
- Castaings, M., Hosten, B., & François, D.** (2004). The sensitivity of surface guided modes to the bond quality between a concrete block and a composite plate. *Ultrasonics*, 42(1), 1067-1071.
- Dieterman, H. A., & Metrikine, A.** (1997). Critical velocities of a harmonic load moving uniformly along an elastic layer. *Journal of applied mechanics*, 64(3), 596-600.
- Dowaikh, M. A., & Ogden, R. W.** (1991). Interfacial waves and deformations in pre-stressed elastic media. *Proceedings of the Royal Society of London. Series A: Mathematical and Physical Sciences*, 433(1888), 313-328.
- Eringen, A. C., & Suhubi, E. S.** (1975). *Elastodynamics, Volume I, Finite Motions*, Academic Press.
- Eringen, A. C., & Suhubi, E. S.** (1975). *Elastodynamics, Volume II, Linear Theory*, Academic Press.
- Fan, H., Yang, J., & Xu, L.** (2006). Antiplane piezoelectric surface waves over a ceramic half-space with an imperfectly bonded layer. *IEEE transactions on ultrasonics, ferroelectrics, and frequency control*, 53(9), 1695-1698.
- Foti, S.** (2002). Numerical and experimental comparison between 2-station and multistation methods for spectral analysis of surface waves. *Rivista Italiana di Geotecnica*, 36, 11-22.
- Gupta, S., Majhi, D. K., & Vishwakarma, S. K.** (2012). Torsional surface wave propagation in an initially stressed non-homogeneous layer over a non-homogeneous half-space. *Applied Mathematics and Computation*, 219(6), 3209-3218.
- Guz, A. N.** (2002). Elastic waves in bodies with initial (residual) stresses. *International Applied Mechanics*, 38(1), 23-59.
- Guz, A. N.** (2004). *Elastic waves in Bodies with Initial (Residual) Stresses*, "A.S.K", Kiev, (in Russian).

- Guz, A. N.** (2005). On foundations of the ultrasonic non-destructive method of determination of stresses in near-the-surface layers of solid bodies. *CMES: Computer Modeling in Engineering and Sciences*, 8(3), 217-230.
- Guz, A. N., Makhort, F.G.** (2000). Physical principles of ultrasonic non-destructive method of determination of stresses in rigid solids. *International Applied Mechanics*, 36, 3-34.
- Huang, Y., & Li, X. F.** (2010). Shear waves guided by the imperfect interface of two magnetoelectric materials. *Ultrasonics*, 50(8), 750-757.
- Jones, J. P., & Whittier, J. S.** (1967). Waves at a flexibly bonded interface. *Journal of Applied Mechanics*, 34(4), 905-909.
- Kepceler, T.** (2010). Torsional wave dispersion relations in a pre-stressed bi-material compounded cylinder with an imperfect interface. *Applied Mathematical Modelling*, 34(12), 4058-4073.
- Kumar, R., & Singh, M.** (2009). Effect of rotation and imperfection on reflection and transmission of plane waves in anisotropic generalized thermoelastic media. *Journal of Sound and Vibration*, 324(3), 773-797.
- Lakestani, F., Coste, J. F., & Denis, R.** (1995). Application of ultrasonic Rayleigh waves to thickness measurement of metallic coatings. *NDT & E International*, 28(3), 171-178.
- Leungvichcharoen, S., & Wijeyewickrema, A. C.** (2003). Dispersion effects of extensional waves in pre-stressed imperfectly bonded incompressible elastic layered composites. *Wave Motion*, 38(4), 311-325.
- Liu, J., Wang, Y., & Wang, B.** (2010). Propagation of shear horizontal surface waves in a layered piezoelectric half-space with an imperfect interface. *Ultrasonics, Ferroelectrics and Frequency Control, IEEE Transactions on*, 57(8), 1875-1879.
- Lu, L. Y., Zhang, B. X., & Wang, C. H.** (2006). Experiment and Inversion Studies on Rayleigh Wave Considering Higher Modes. *Chinese Journal of Geophysics*, 49(4), 974-985.
- Martin, P. A.** (1992). Boundary integral equations for the scattering of elastic waves by elastic inclusions with thin interface layers. *Journal of nondestructive evaluation*, 11(3-4), 167-174.
- Melkumyan, A., & Mai, Y. W.** (2008). Influence of imperfect bonding on interface waves guided by piezoelectric/piezomagnetic composites. *Philosophical Magazine*, 88(23), 2965-2977.
- Mindlin, R. D.** (1960). Waves and vibrations in isotropic, elastic plates. *Structural mechanics*, 1960, 199-232.

- Myer, L. R., Hopkins, D., & Cook, N. G. W.** (1985, March). Effects of contact area of an interface on acoustic wave transmission characteristics. In *Presented at the 26th US Symp. on Rock Mech., Rapid City, SD, 26-28 Jun. 1985* (Vol. 1, pp. 26-28).
- Nagy, P. B.** (1992). Ultrasonic classification of imperfect interfaces. *Journal of Nondestructive evaluation*, 11(3-4), 127-139.
- Negin, M., Akbarov, S. D., & Erguven, M. E.** (2014). Generalized Rayleigh Wave Dispersion Analysis in a Pre-stressed Elastic Stratified Half-space with Imperfectly Bonded Interfaces. *CMC: Computers, Materials & Continua*, 42(1), 25-61.
- Nihei, K. T., Gu, B., Myer, L. R., Pyrak, L. J., & Cook, N. G.** (1995, January). Elastic interface wave propagation along a fracture. In *8th ISRM Congress*. International Society for Rock Mechanics.
- Ogden, R., & Singh, B.** (2011). Propagation of waves in an incompressible transversely isotropic elastic solid with initial stress: Biot revisited. *Journal of Mechanics of Materials and Structures*, 6(1), 453-477.
- Pang, Y., & Liu, J. X.** (2011). Reflection and transmission of plane waves at an imperfectly bonded interface between piezoelectric and piezomagnetic media. *European Journal of Mechanics-A/Solids*, 30(5), 731-740.
- Pecorari, C.** (2001). Scattering of a Rayleigh wave by a surface-breaking crack with faces in partial contact. *Wave Motion*, 33(3), 259-270.
- Pymk-Nolte, L. J., Cook, N. G. W., & Myer, L. R.** (1987, January). Seismic Visibility Of Fractures. In *The 28th US Symposium on Rock Mechanics (USRMS)*. American Rock Mechanics Association.
- Pyrak-Nolte, L. J., & Cook, N. G. W.** (1987) Elastic interface waves along a fracture, *Geophysical Research Letters*, 14(11), 1107–1110.
- Pyrak-Nolte, L. J., Myer, L. R., & Cook, N. G.** (1990). Anisotropy in seismic velocities and amplitudes from multiple parallel fractures. *Journal of Geophysical Research: Solid Earth (1978–2012)*, 95(B7), 11345-11358.
- Pyrak-Nolte, L. J., Myer, L. R., & Cook, N. G.** (1990). Transmission of seismic waves across single natural fractures. *Journal of Geophysical Research: Solid Earth (1978–2012)*, 95(B6), 8617-8638.
- Pyrak-Nolte, L. J., Myer, L. R., & Cook, N. G.** (1990). Anisotropy in seismic velocities and amplitudes from multiple parallel fractures. *Journal of Geophysical Research: Solid Earth (1978–2012)*, 95(B7), 11345-11358.
- Pyrak-Nolte, L. J., Xu, J. J., & Haley, G. M.** (1992, January). Elastic interface waves along a fracture: Theory and experiment. In *The 33th US Symposium on Rock Mechanics (USRMS)*. American Rock Mechanics Association.

- Pyrak-Nolte, L. J., & Nolte, D. D.** (1995). Wavelet analysis of velocity dispersion of elastic interface waves propagating along a fracture. *Geophysical Research Letters*, 22(11), 1329-1332.
- Rogerson, G. A., & Fu, Y. B.** (1995). An asymptotic analysis of the dispersion relation of a pre-stressed incompressible elastic plate. *Acta Mechanica*, 111(1-2), 59-74.
- Rokhlin, S. I., & Wang, Y. J.** (1991). Analysis of boundary conditions for elastic wave interaction with an interface between two solids. *The Journal of the Acoustical Society of America*, 89(2), 503-515.
- Roy, S., & Pyrak-Nolte, L. J.** (1995). Interface waves propagating along tensile fractures in dolomite. *Geophysical Research Letters*, 22(20), 2773-2776.
- Schoenberg, M.** (1980). Elastic wave behavior across linear slip interfaces. *The Journal of the Acoustical Society of America*, 68(5), 1516-1521.
- Shams, M., & Ogden, R. W.** (2014). On Rayleigh-type surface waves in an initially stressed incompressible elastic solid. *IMA Journal of Applied Mathematics*, 79(2), 360-376.
- Sotiropoulos D. A.** (1998). Interfacial waves in pre-stressed compressible elastic media. *Computational mechanics*, 21(4-5), 293-299.
- Tolstoy, I., & Usdin, E.** (1953). Dispersive properties of stratified elastic and liquid media: A ray theory. *Geophysics*, 18(4), 844-870.
- Truesdell, C.** (1961). General and exact theory of waves in finite elastic strain. *Archive for rational mechanics and analysis*, 8(1), 263-296.
- Vlasie, V., & Rousseau, M.** (2005). Non destructive tests of structural bonds by guided ultrasonic waves: Effect of a surface pretreatment or a localized defect. *American Journal of Applied Sciences*, 2(3), 739-745.
- Vishwakarma, S. K., Gupta, S., & Verma, A. K.** (2014) Torsional wave propagation in Earth's crustal layer under the influence of imperfect interface. *Journal of Vibration and Control*, 20(3), 355-369.
- Wijeyewickrema, A., Ushida, Y. & Kayestha, P.** (2008) Wave propagation in a pre-stressed compressible elastic layer with constrained boundaries. *Journal of Mechanics of Materials and Structures*, 3(10), 1963-1976.
- Xian, C., Nolte, D. D., & Pyrak-Nolte, L. J.** (2001). Compressional waves guided between parallel fractures. *International Journal of Rock Mechanics and Mining Sciences*, 38(6), 765-776.
- Zang, A., Stephansson, O., & Stephansson, O.** (2010). *Stress field of the Earth's crust* (pp. 115-193). Berlin: Springer.

- Zerwer, A., Polak, M. A., & Santamarina, J. C.** (2005). Detection of surface breaking cracks in concrete members using Rayleigh waves. *Journal of Environmental & Engineering Geophysics*, 10(3), 295-306.
- Zhang, R., Pang, Y., & Feng, W.** (2014). Propagation of Rayleigh Waves in a Magneto-Electro-Elastic Half-Space with Initial Stress. *Mechanics of Advanced Materials and Structures*, 21(7), 538-543.
- Zhou, Y. Y., Lü, C. F., & Chen, W. Q.** (2012). Bulk wave propagation in layered piezomagnetic/piezoelectric plates with initial stresses or interface imperfections. *Composite Structures*, 94(9), 2736-2745.
- Zurn, B., & Mantell, S. C.** (2001). Nondestructive evaluation of laminated composites using rayleigh waves. *Journal of composite materials*, 35(12), 1026-1044.

APPENDICES

APPENDIX A.1: The explicit expressions of the α_{ij} in the dispersion equation (3.23).

APPENDIX A.2: The explicit expressions of the α_{ij} in the dispersion equation (4.18).

APPENDIX A.3: The explicit expressions of the α_{ij} in the dispersion equation (5.17).

APPENDIX A.1

The explicit expressions of the α_{ij} in the dispersion equation (3.23)

$$\begin{aligned}
\alpha_{11} &= -\frac{R_1^{(1)}}{c_{22}^{(1)}} - \frac{b_{22}^{(1)}}{R_1^{(1)} c_{22}^{(1)}}, & \alpha_{12} &= \frac{R_1^{(1)}}{c_{22}^{(1)}} + \frac{b_{22}^{(1)}}{R_1^{(1)} c_{22}^{(1)}}, \\
\alpha_{13} &= -\frac{R_2^{(1)}}{c_{22}^{(1)}} - \frac{b_{22}^{(1)}}{R_2^{(1)} c_{22}^{(1)}}, & \alpha_{14} &= \frac{R_2^{(1)}}{c_{22}^{(1)}} + \frac{b_{22}^{(1)}}{R_2^{(1)} c_{22}^{(1)}}, \\
\alpha_{15} &= \frac{R_1^{(2)}}{c_{22}^{(2)}} + \frac{b_{22}^{(2)}}{R_1^{(2)} c_{22}^{(2)}} + \frac{{}^{(2)}Fkh}{({}^{(2)}\mu)} \left(\frac{(R_1^{(2)})^2 + b_{22}^{(2)}}{c_{22}^{(2)}} + 1 \right), \\
\alpha_{16} &= \frac{R_2^{(2)}}{c_{22}^{(2)}} + \frac{b_{22}^{(2)}}{R_2^{(2)} c_{22}^{(2)}} + \frac{{}^{(2)}\mu_{12} Fkh}{\mu^{(2)}} \left(\frac{(R_2^{(2)})^2 + b_{22}^{(2)}}{c_{22}^{(2)}} + 1 \right), \\
\alpha_{21} &= 1, & \alpha_{22} &= 1, & \alpha_{23} &= 1, & \alpha_{24} &= 1, & \alpha_{25} &= -1, & \alpha_{26} &= -1, \\
\alpha_{31} &= -\mu_{12}^{(1)} \left(\frac{(R_1^{(1)})^2 + b_{22}^{(1)}}{c_{22}^{(1)}} + 1 \right), \\
\alpha_{32} &= -\mu_{12}^{(1)} \left(\frac{(R_1^{(1)})^2 + b_{22}^{(1)}}{c_{22}^{(1)}} + 1 \right), \\
\alpha_{33} &= -\mu_{12}^{(1)} \left(\frac{(R_2^{(1)})^2 + b_{22}^{(1)}}{c_{22}^{(1)}} + 1 \right), \\
\alpha_{34} &= -\mu_{12}^{(1)} \left(\frac{(R_2^{(1)})^2 + b_{22}^{(1)}}{c_{22}^{(1)}} + 1 \right), \\
\alpha_{35} &= \mu_{12}^{(2)} \left(\frac{(R_1^{(2)})^2 + b_{22}^{(2)}}{c_{22}^{(2)}} + 1 \right), \\
\alpha_{36} &= \mu_{12}^{(2)} \left(\frac{(R_2^{(2)})^2 + b_{22}^{(2)}}{c_{22}^{(2)}} + 1 \right), \\
\alpha_{41} &= A_{22}^{(1)} R_1^{(1)} - A_{12}^{(1)} \left(\frac{R_1^{(1)}}{c_{22}^{(1)}} + \frac{b_{22}^{(1)}}{R_1^{(1)} c_{22}^{(1)}} \right), \\
\alpha_{42} &= -A_{22}^{(1)} R_1^{(1)} + A_{12}^{(1)} \left(\frac{R_1^{(1)}}{c_{22}^{(1)}} + \frac{b_{22}^{(1)}}{R_1^{(1)} c_{22}^{(1)}} \right), \\
\alpha_{43} &= A_{22}^{(1)} R_2^{(1)} - A_{12}^{(1)} \left(\frac{R_2^{(1)}}{c_{22}^{(1)}} + \frac{b_{22}^{(1)}}{R_2^{(1)} c_{22}^{(1)}} \right), \\
\alpha_{44} &= -A_{22}^{(1)} R_2^{(1)} + A_{12}^{(1)} \left(\frac{R_2^{(1)}}{c_{22}^{(1)}} + \frac{b_{22}^{(1)}}{R_2^{(1)} c_{22}^{(1)}} \right), \\
\alpha_{45} &= -A_{22}^{(2)} R_1^{(2)} + A_{12}^{(2)} \left(\frac{R_1^{(2)}}{c_{22}^{(2)}} + \frac{b_{22}^{(2)}}{R_1^{(2)} c_{22}^{(2)}} \right), \\
\alpha_{46} &= -A_{22}^{(2)} R_2^{(2)} + A_{12}^{(2)} \left(\frac{R_2^{(2)}}{c_{22}^{(2)}} + \frac{b_{22}^{(2)}}{R_2^{(2)} c_{22}^{(2)}} \right),
\end{aligned}$$

$$\begin{aligned}
\alpha_{51} &= -e^{R_1^{(1)kh}} \left(1 + \frac{(R_1^{(1)})^2}{c_{22}^{(1)}} + \frac{b_{22}^{(1)}}{c_{22}^{(1)}} \right), \\
\alpha_{52} &= -e^{-R_1^{(1)kh}} \left(1 + \frac{(R_1^{(1)})^2}{c_{22}^{(1)}} + \frac{b_{22}^{(1)}}{c_{22}^{(1)}} \right), \\
\alpha_{53} &= -e^{R_2^{(1)kh}} \left(1 + \frac{(R_2^{(1)})^2}{c_{22}^{(1)}} + \frac{b_{22}^{(1)}}{c_{22}^{(1)}} \right), \\
\alpha_{54} &= -e^{-R_2^{(1)kh}} \left(1 + \frac{(R_2^{(1)})^2}{c_{22}^{(1)}} + \frac{b_{22}^{(1)}}{c_{22}^{(1)}} \right), \\
\alpha_{55} &= 0, \quad \alpha_{56} = 0, \\
\alpha_{61} &= e^{R_1^{(1)kh}} \left(A_{22}^{(1)} R_1^{(1)} - A_{12}^{(1)} \left(\frac{R_1^{(1)}}{c_{22}^{(1)}} + \frac{b_{22}^{(1)}}{R_1^{(1)} c_{22}^{(1)}} \right) \right), \\
\alpha_{62} &= e^{-R_1^{(1)kh}} \left(A_{12}^{(1)} \left(\frac{R_1^{(1)}}{c_{22}^{(1)}} + \frac{b_{22}^{(1)}}{R_1^{(1)} c_{22}^{(1)}} \right) - A_{22}^{(1)} R_1^{(1)} \right), \\
\alpha_{63} &= e^{R_2^{(1)kh}} \left(A_{22}^{(1)} R_2^{(1)} - A_{12}^{(1)} \left(\frac{R_2^{(1)}}{c_{22}^{(1)}} + \frac{b_{22}^{(1)}}{R_2^{(1)} c_{22}^{(1)}} \right) \right), \\
\alpha_{64} &= e^{-R_2^{(1)kh}} \left(A_{12}^{(1)} \left(\frac{R_2^{(1)}}{c_{22}^{(1)}} + \frac{b_{22}^{(1)}}{R_2^{(1)} c_{22}^{(1)}} \right) - A_{22}^{(1)} R_2^{(1)} \right), \\
\alpha_{65} &= 0, \quad \alpha_{66} = 0.
\end{aligned}$$

APPENDIX A.2

The explicit expressions of the α_{ij} in the dispersion equation (4.18)

$$\begin{aligned}
\alpha_{11} &= -\frac{R_1^{(1)}}{c_{22}^{(1)}} - \frac{b_{22}^{(1)}}{R_1^{(1)} c_{22}^{(1)}}, & \alpha_{12} &= \frac{R_1^{(1)}}{c_{22}^{(1)}} + \frac{b_{22}^{(1)}}{R_1^{(1)} c_{22}^{(1)}}, \\
\alpha_{13} &= -\frac{R_2^{(1)}}{c_{22}^{(1)}} - \frac{b_{22}^{(1)}}{R_2^{(1)} c_{22}^{(1)}}, & \alpha_{14} &= \frac{R_2^{(1)}}{c_{22}^{(1)}} + \frac{b_{22}^{(1)}}{R_2^{(1)} c_{22}^{(1)}}, \\
\alpha_{15} &= \frac{R_1^{(2)}}{c_{22}^{(2)}} + \frac{b_{22}^{(2)}}{R_1^{(2)} c_{22}^{(2)}} + \frac{\mu_{12}^{(2)} F_1 k h}{\mu^{(2)}} \left(\frac{(R_1^{(2)})^2 + b_{22}^{(2)}}{c_{22}^{(2)}} + 1 \right), \\
\alpha_{16} &= \frac{R_2^{(2)}}{c_{22}^{(2)}} + \frac{b_{22}^{(2)}}{R_2^{(2)} c_{22}^{(2)}} + \frac{\mu_{12}^{(2)} F_1 k h}{\mu^{(2)}} \left(\frac{(R_2^{(2)})^2 + b_{22}^{(2)}}{c_{22}^{(2)}} + 1 \right), \\
\alpha_{21} &= 1, & \alpha_{22} &= 1, & \alpha_{23} &= 1, & \alpha_{24} &= 1, \\
\alpha_{25} &= -\frac{F_2 k h}{\mu^{(2)}} \left(A_{22}^{(2)} R_1^{(2)} - \frac{A_{12}^{(2)} \left((R_1^{(2)})^2 + b_{22}^{(2)} \right)}{R_1^{(2)} c_{22}^{(2)}} \right) - 1, \\
\alpha_{26} &= -\frac{F_2 k h}{\mu^{(2)}} \left(A_{22}^{(2)} R_2^{(2)} - \frac{A_{12}^{(2)} \left((R_2^{(2)})^2 + b_{22}^{(2)} \right)}{R_2^{(2)} c_{22}^{(2)}} \right) - 1, \\
\alpha_{31} &= -\mu_{12}^{(1)} \left(\frac{(R_1^{(1)})^2 + b_{22}^{(1)}}{c_{22}^{(1)}} + 1 \right), \\
\alpha_{32} &= -\mu_{12}^{(1)} \left(\frac{(R_1^{(1)})^2 + b_{22}^{(1)}}{c_{22}^{(1)}} + 1 \right), \\
\alpha_{33} &= -\mu_{12}^{(1)} \left(\frac{(R_2^{(1)})^2 + b_{22}^{(1)}}{c_{22}^{(1)}} + 1 \right), \\
\alpha_{34} &= -\mu_{12}^{(1)} \left(\frac{(R_2^{(1)})^2 + b_{22}^{(1)}}{c_{22}^{(1)}} + 1 \right), \\
\alpha_{35} &= \mu_{12}^{(2)} \left(\frac{(R_1^{(2)})^2 + b_{22}^{(2)}}{c_{22}^{(2)}} + 1 \right), \\
\alpha_{36} &= \mu_{12}^{(2)} \left(\frac{(R_2^{(2)})^2 + b_{22}^{(2)}}{c_{22}^{(2)}} + 1 \right), \\
\alpha_{41} &= A_{22}^{(1)} R_1^{(1)} - A_{12}^{(1)} \left(\frac{R_1^{(1)}}{c_{22}^{(1)}} + \frac{b_{22}^{(1)}}{R_1^{(1)} c_{22}^{(1)}} \right), \\
\alpha_{42} &= -A_{22}^{(1)} R_1^{(1)} + A_{12}^{(1)} \left(\frac{R_1^{(1)}}{c_{22}^{(1)}} + \frac{b_{22}^{(1)}}{R_1^{(1)} c_{22}^{(1)}} \right), \\
\alpha_{43} &= A_{22}^{(1)} R_2^{(1)} - A_{12}^{(1)} \left(\frac{R_2^{(1)}}{c_{22}^{(1)}} + \frac{b_{22}^{(1)}}{R_2^{(1)} c_{22}^{(1)}} \right), \\
\alpha_{44} &= -A_{22}^{(1)} R_2^{(1)} + A_{12}^{(1)} \left(\frac{R_2^{(1)}}{c_{22}^{(1)}} + \frac{b_{22}^{(1)}}{R_2^{(1)} c_{22}^{(1)}} \right),
\end{aligned}$$

$$\begin{aligned}
\alpha_{45} &= -A_{22}^{(2)} R_1^{(2)} + A_{12}^{(2)} \left(\frac{R_1^{(2)}}{c_{22}^{(2)}} + \frac{b_{22}^{(2)}}{R_1^{(2)} c_{22}^{(2)}} \right), \\
\alpha_{46} &= -A_{22}^{(2)} R_2^{(2)} + A_{12}^{(2)} \left(\frac{R_2^{(2)}}{c_{22}^{(2)}} + \frac{b_{22}^{(2)}}{R_2^{(2)} c_{22}^{(2)}} \right), \\
\alpha_{51} &= -e^{R_1^{(1)} kh} \left(1 + \frac{(R_1^{(1)})^2}{c_{22}^{(1)}} + \frac{b_{22}^{(1)}}{c_{22}^{(1)}} \right), \\
\alpha_{52} &= -e^{-R_1^{(1)} kh} \left(1 + \frac{(R_1^{(1)})^2}{c_{22}^{(1)}} + \frac{b_{22}^{(1)}}{c_{22}^{(1)}} \right), \\
\alpha_{53} &= -e^{R_2^{(1)} kh} \left(1 + \frac{(R_2^{(1)})^2}{c_{22}^{(1)}} + \frac{b_{22}^{(1)}}{c_{22}^{(1)}} \right), \\
\alpha_{54} &= -e^{-R_2^{(1)} kh} \left(1 + \frac{(R_2^{(1)})^2}{c_{22}^{(1)}} + \frac{b_{22}^{(1)}}{c_{22}^{(1)}} \right), \\
\alpha_{55} &= 0, \quad \alpha_{56} = 0, \\
\alpha_{61} &= e^{R_1^{(1)} kh} \left(A_{22}^{(1)} R_1^{(1)} - A_{12}^{(1)} \left(\frac{R_1^{(1)}}{c_{22}^{(1)}} + \frac{b_{22}^{(1)}}{R_1^{(1)} c_{22}^{(1)}} \right) \right), \\
\alpha_{62} &= e^{-R_1^{(1)} kh} \left(A_{12}^{(1)} \left(\frac{R_1^{(1)}}{c_{22}^{(1)}} + \frac{b_{22}^{(1)}}{R_1^{(1)} c_{22}^{(1)}} \right) - A_{22}^{(1)} R_1^{(1)} \right), \\
\alpha_{63} &= e^{R_2^{(1)} kh} \left(A_{22}^{(1)} R_2^{(1)} - A_{12}^{(1)} \left(\frac{R_2^{(1)}}{c_{22}^{(1)}} + \frac{b_{22}^{(1)}}{R_2^{(1)} c_{22}^{(1)}} \right) \right), \\
\alpha_{64} &= e^{-R_2^{(1)} kh} \left(A_{12}^{(1)} \left(\frac{R_2^{(1)}}{c_{22}^{(1)}} + \frac{b_{22}^{(1)}}{R_2^{(1)} c_{22}^{(1)}} \right) - A_{22}^{(1)} R_2^{(1)} \right), \\
\alpha_{65} &= 0, \quad \alpha_{66} = 0.
\end{aligned}$$

APPENDIX A.3

The explicit expressions of the α_{ij} in the dispersion equation (5.17)

$$\begin{aligned}
\alpha_{11} &= -\frac{R_1^{(1)}}{c_{22}^{(1)}} - \frac{b_{22}^{(1)}}{R_1^{(1)}c_{22}^{(1)}}, & \alpha_{12} &= \frac{R_1^{(1)}}{c_{22}^{(1)}} + \frac{b_{22}^{(1)}}{R_1^{(1)}c_{22}^{(1)}}, \\
\alpha_{13} &= -\frac{R_2^{(1)}}{c_{22}^{(1)}} - \frac{b_{22}^{(1)}}{R_2^{(1)}c_{22}^{(1)}}, & \alpha_{14} &= \frac{R_2^{(1)}}{c_{22}^{(1)}} + \frac{b_{22}^{(1)}}{R_2^{(1)}c_{22}^{(1)}}, \\
\alpha_{15} &= \frac{R_1^{(2)}}{c_{22}^{(2)}} + \frac{b_{22}^{(2)}}{R_1^{(2)}c_{22}^{(2)}}, & \alpha_{16} &= \frac{R_2^{(2)}}{c_{22}^{(2)}} + \frac{b_{22}^{(2)}}{R_2^{(2)}c_{22}^{(2)}}, \\
\alpha_{21} &= 1, & \alpha_{22} &= 1, & \alpha_{23} &= 1, & \alpha_{24} &= 1, & \alpha_{25} &= -1, & \alpha_{26} &= -1, \\
\alpha_{31} &= -\mu_{12}^{(1)} \left(\frac{(R_1^{(1)})^2 + b_{22}^{(1)}}{c_{22}^{(1)}} + 1 \right), \\
\alpha_{32} &= -\mu_{12}^{(1)} \left(\frac{(R_1^{(1)})^2 + b_{22}^{(1)}}{c_{22}^{(1)}} + 1 \right), \\
\alpha_{33} &= -\mu_{12}^{(1)} \left(\frac{(R_2^{(1)})^2 + b_{22}^{(1)}}{c_{22}^{(1)}} + 1 \right), \\
\alpha_{34} &= -\mu_{12}^{(1)} \left(\frac{(R_2^{(1)})^2 + b_{22}^{(1)}}{c_{22}^{(1)}} + 1 \right), \\
\alpha_{35} &= \mu_{12}^{(2)} \left(\frac{(R_1^{(2)})^2 + b_{22}^{(2)}}{c_{22}^{(2)}} + 1 \right), \\
\alpha_{36} &= \mu_{12}^{(2)} \left(\frac{(R_2^{(2)})^2 + b_{22}^{(2)}}{c_{22}^{(2)}} + 1 \right), \\
\alpha_{41} &= A_{22}^{(1)} R_1^{(1)} - A_{12}^{(1)} \left(\frac{R_1^{(1)}}{c_{22}^{(1)}} + \frac{b_{22}^{(1)}}{R_1^{(1)}c_{22}^{(1)}} \right), \\
\alpha_{42} &= -A_{22}^{(1)} R_1^{(1)} + A_{12}^{(1)} \left(\frac{R_1^{(1)}}{c_{22}^{(1)}} + \frac{b_{22}^{(1)}}{R_1^{(1)}c_{22}^{(1)}} \right), \\
\alpha_{43} &= A_{22}^{(1)} R_2^{(1)} - A_{12}^{(1)} \left(\frac{R_2^{(1)}}{c_{22}^{(1)}} + \frac{b_{22}^{(1)}}{R_2^{(1)}c_{22}^{(1)}} \right), \\
\alpha_{44} &= -A_{22}^{(1)} R_2^{(1)} + A_{12}^{(1)} \left(\frac{R_2^{(1)}}{c_{22}^{(1)}} + \frac{b_{22}^{(1)}}{R_2^{(1)}c_{22}^{(1)}} \right), \\
\alpha_{45} &= -A_{22}^{(2)} R_1^{(2)} + A_{12}^{(2)} \left(\frac{R_1^{(2)}}{c_{22}^{(2)}} + \frac{b_{22}^{(2)}}{R_1^{(2)}c_{22}^{(2)}} \right), \\
\alpha_{46} &= -A_{22}^{(2)} R_2^{(2)} + A_{12}^{(2)} \left(\frac{R_2^{(2)}}{c_{22}^{(2)}} + \frac{b_{22}^{(2)}}{R_2^{(2)}c_{22}^{(2)}} \right), \\
\alpha_{51} &= -e^{R_1^{(1)}kh} \left(1 + \frac{(R_1^{(1)})^2}{c_{22}^{(1)}} + \frac{b_{22}^{(1)}}{c_{22}^{(1)}} \right), \\
\alpha_{52} &= -e^{-R_1^{(1)}kh} \left(1 + \frac{(R_1^{(1)})^2}{c_{22}^{(1)}} + \frac{b_{22}^{(1)}}{c_{22}^{(1)}} \right),
\end{aligned}$$

$$\begin{aligned}
\alpha_{53} &= -e^{R_2^{(1)kh}} \left(1 + \frac{(R_2^{(1)})^2}{c_{22}^{(1)}} + \frac{b_{22}^{(1)}}{c_{22}^{(1)}} \right), \\
\alpha_{54} &= -e^{-R_2^{(1)kh}} \left(1 + \frac{(R_2^{(1)})^2}{c_{22}^{(1)}} + \frac{b_{22}^{(1)}}{c_{22}^{(1)}} \right), \\
\alpha_{55} &= 0, \quad \alpha_{56} = 0, \\
\alpha_{61} &= e^{R_1^{(1)kh}} \left(A_{22}^{(1)} R_1^{(1)} - A_{12}^{(1)} \left(\frac{R_1^{(1)}}{c_{22}^{(1)}} + \frac{b_{22}^{(1)}}{R_1^{(1)} c_{22}^{(1)}} \right) \right), \\
\alpha_{62} &= e^{-R_1^{(1)kh}} \left(A_{12}^{(1)} \left(\frac{R_1^{(1)}}{c_{22}^{(1)}} + \frac{b_{22}^{(1)}}{R_1^{(1)} c_{22}^{(1)}} \right) - A_{22}^{(1)} R_1^{(1)} \right), \\
\alpha_{63} &= e^{R_2^{(1)kh}} \left(A_{22}^{(1)} R_2^{(1)} - A_{12}^{(1)} \left(\frac{R_2^{(1)}}{c_{22}^{(1)}} + \frac{b_{22}^{(1)}}{R_2^{(1)} \times c_{22}^{(1)}} \right) \right), \\
\alpha_{64} &= e^{-R_2^{(1)kh}} \left(A_{12}^{(1)} \left(\frac{R_2^{(1)}}{c_{22}^{(1)}} + \frac{b_{22}^{(1)}}{R_2^{(1)} c_{22}^{(1)}} \right) - A_{22}^{(1)} R_2^{(1)} \right), \\
\alpha_{65} &= 0, \quad \alpha_{66} = 0.
\end{aligned}$$

CURRICULUM VITAE



Name Surname: Masoud NEGIN

Place and Date of Birth: Iran 1977

E-Mail: mesudnegin@gmail.com

B.Sc.: Civil Engineering, 2002, Azad University, Iran

M.Sc.: Structural Engineering, 2006, Azad University, Iran

M.Sc.: Mathematics, 2014, Isik University, Turkey

Professional Experience:

2007-2008 Teaching assistant, Azad University, Tebriz, Iran

2001-2003 Civil engineer, Technical office, South Pars Gaz Field, Assaluyeh, Iran

List of Publications:

- Hasanoglu, E., & **Negin, M.** (2014), Asymptotic Solutions of Love Wave Propagation in a Covered Half Space with Inhomogeneous Initial Stresses, *TWMS Journal of Pure and Applied Mathematics*. (submitted)
- Sheidaii, M.R., & **Negin, M.** (2011), Effect of Random Imperfections on Reliability of Double-Layer Space Structures, *Civil and Environmental Engineering Journal of Tebriz University*, Vol. 4(1), pp 33-40.
- Lotfollahi Yaghin, M.A., & **Negin, M.** (2011), Effect of Random Member Crookedness on Reliability of Steel Frames, *The Modares Journal of Civil Engineering, Modares University, Tehran*, Vol. 10(4), pp. 57-69.
- Lotfollahi Yaghin, M.A., **Negin, M.** & Behraves, A. (2007), Safety Assessment of Steel Frames with Different Bracing Types, *3rd Iranian National Congress of Civil Engineering, Tabriz University, Tebriz, Iran*.
- Armaghani, A., & **Negin, M.** (2008), *Lecture Notes in Engineering Mathematics*, Feyzi Publications, Tebriz, Iran.

PUBLICATIONS/PRESENTATIONS ON THE THESIS

- **Negin, M.**, Akbarov, S.D., & Erguven, M.E. (2014), Generalized Rayleigh Wave Dispersion Analysis in a Pre-stressed Elastic Stratified Half-space with Imperfectly Bonded Interfaces, *Journal of computers, materials & continua*, Vol. 42(1), pp. 25-61.

- Akbarov, S.D., & **Negin, M.** (2014), Near-surface waves in a system consisting of a covering layer and a half-space with imperfect interface under two-axial initial stresses. *Journal of vibration and control*. (accepted)
- Akbarov, S.D., **Negin, M.**, & Ipek, C. (2014), Effect of imperfect contact on the generalized Rayleigh wave dispersion in a system consisting of a pre-stressed layer and a pre-stressed half-plane, *Journal of Mechanics of composite materials, Institute of Polymer Mechanics, University of Latvia*. (accepted)
- **Negin, M.** (2014), Generalized Rayleigh Wave Propagation in a Stratified Half-Space with a Liquid Upper Layer, *Journal of Earthquake Engineering and Engineering Vibration*. (submitted)
- **Negin, M.**, & Ipek, C. (2014), Effect of imperfect contact on the generalized Rayleigh wave dispersion in a system consisting of a pre-stressed layer and a pre-stressed half-plane, *XVIII International conference on mechanics of composite materials*, Riga, Latvia.